UNIVERSITÁ DEGLI STUDI DI PADOVA

CORSO DI LAUREA MAGISTRALE IN MEDICINA E CHIRURGIA

DIPARTIMENTO DI MEDICINA (DIMED)

Direttore: Ch.mo Prof. Roberto Vettor

U.O.C. MEDICINA DELLO SPORT E DELL'ESERCIZIO

Direttore: Prof. Andrea Ermolao

TESI DI LAUREA

EVALUATION OF QTc BEFORE AND AFTER EXERCISE TESTING IN A POPULATION OF PATIENTS WITH SEVERE OBESITY: POSSIBLE ASSOCIATION WITH OBSTRUCTIVE SLEEP APNOEA

RELATORE: Dr.ssa Francesca Battista

LAUREANDO: Martino Casarin

ANNO ACCADEMICO 2022/2023

INDEX

1. ABSTRACT

1.1 Introduction

Obesity is a leading contributor to cardiovascular and all-cause morbidity and mortality, both directly and indirectly through the development of comorbidities, including obstructive sleep apnoea (OSA). Obesity and OSA has been independently associated with QT interval prolongation and a higher occurrence of arrhythmia. Provocative manoeuvres, such as brisk standing and exercise testing (which evaluate the dynamic QT interval adaptation to changes in the autonomic tone), can be used to "unmask" repolarization abnormalities. The literature evaluating QT interval adaptations to provocative manoeuvres in patients with obesity and OSA is scarce; therefore, the primary aim of this study was to evaluate the QT interval and its adaptations to brisk standing and exercise testing in patients with severe obesity and moderate to severe OSA. We also investigated, as secondary outcomes, (1) the cardiopulmonary function in patients with severe obesity and moderate to severe OSA; (2) the influence of CPAP therapy over the QT interval and the cardiopulmonary function in this patient population; and (3) the association between OSA and the number of arrhythmic events during exercise testing.

1.2 Materials and methods

This is an observational cross-sectional study conducted on 126 patients with severe obesity and suspected OSA. All patients underwent cardiorespiratory sleep study, spirometry, brisk standing test, and cardiopulmonary exercise testing (CPET).

1.3 Results

Age and anthropometric parameters were similar in patients with obesity and OSA (Ob OSA) compared to those without OSA (Ob no OSA), while waist circumference was significantly higher in the first group (140.8±14.7 cm vs. 133.0±16.0 cm; p=0.019). Ob OSA compared to Ob no OSA had significantly longer QTc rest (QTc rest D2 427.1±23.3 ms vs. 414.3±24.9 ms; p=0.004), QTc return (QTc return D2 421.8±19.3 ms vs. 410.0±24.4 ms; p=0.035), and QTc 4-min recovery (QTc 4min recovery D2 421.0±21.3 ms vs. 408.1±30.7 ms; p=0.007) despite none of these QT interval parameters were prolonged enough to reach the

cutoff value for the diagnosis of LQTS. Moreover, there was a significant correlation between QTc rest and AHI. CPET parameters indicated a lower cardiorespiratory fitness (CRF) in patients with untreated OSA compared to patients without OSA and those with OSA and CPAP therapy. The difference in the total number of PSVCs and PVCs between patients with and without OSA was not statistically significant. Finally, among patients with OSA, we did not observe any significant difference in QT interval measurements between those with CPAP therapy and those without it.

1.4 Conclusions

(1) We speculate that OSA may not lead to a pathological prolongation of the QT interval *per se* but rather to a reduced repolarization reserve, which is clinically relevant as it increases the susceptibility to QT interval-prolonging agents; (2) patients with severe obesity and moderate to severe OSA showed reduced aerobic capacity, exercise tolerance, and ventilatory response to exercise compared to those without OSA; (3) central adiposity is a better predictor of obesity-related comorbidities than BMI; (4) we found no significant difference in the total number of PSVCs and PVCs between obese patients with and without OSA during exercise testing; and (5) we observed beneficial effects of CPAP therapy on cardiorespiratory fitness but not on QT interval.

2. RIASSUNTO

2.1 Introduzione

L'obesità è una delle principali cause di morbilità e mortalità per cause cardiovascolari e non, a cui contribuisce sia direttamente che indirettamente attraverso lo sviluppo di comorbidità, tra cui le apnee ostruttive del sonno (OSA). Obesità e OSA sono stati indipendentemente associati ad un prolungamento dell'intervallo QT e ad una maggior incidenza di aritmie. Le manovre provocatorie, come un brusco passaggio da clino ad ortostatismo e il test da sforzo (che valutano l'adattamento dinamico dell'intervallo QT a variazioni dell'attività del sistema nervoso autonomo), possono essere utili nello "smascherare" delle anomalie di ripolarizzazione. La letteratura sugli adattamento dell'intervallo QT alle manovre provocatorie in pazienti con obesità e OSA è scarsa; pertanto, lo scopo principale di questo studio era valutare l'intervallo QT e i suoi adattamenti al brusco passaggio da clino ad ortostatismo e al test da sforzo in pazienti con obesità grave e OSA moderata/grave. Abbiamo anche indagato, come obiettivi secondari, (1) la funzionalità cardiorespiratoria in pazienti con obesità grave e OSA; (2) l'influenza della terapia con CPAP sull'intervallo QT e sulla funzionalità cardiorespiratoria in questa popolazione di pazienti; e (3) l'associazione fra l'OSA e il numero di eventi aritmici durante il test da sforzo.

2.2 Materiali e metodi

Si tratta di uno studio osservazionale trasversale condotto su 126 pazienti con obesità grave e sospetta OSA. Tutti i pazienti sono stati sottoposti a studio cardiorespiratorio del sonno, spirometria, test provocativo di passaggio da clino a ortostatismo, e test da sforzo cardiopolmonare (CPET).

2.3 Risultati

Età e parametri antropometrici erano simili nei pazienti con obesità e OSA (Ob OSA) rispetto a quelli senza OSA (Ob no OSA), mentre la circonferenza vita era significativamente più alta nel primo gruppo (140.8±14.7 cm vs. 133.0±16.0 cm; p=0.019). Il gruppo Ob OSA aveva QTc a riposo (QTc rest D2 427.1±23.3 ms vs. 414.3±24.9 ms; p=0.004), QTc return (QTc return D2 421.8±19.3 ms vs. 410.0±24.4 ms; p=0.035) e QTc al 4-min di recupero (QTc 4min recovery D2

421.0±21.3 ms vs. 408.1±30.7 ms; p=0.007) significativamente più lunghi rispetto al gruppo Ob no OSA, nonostante nessuno di questi parametri era abbastanza prolungato da raggiungere il valore soglia per la diagnosi di LQTS. Inoltre, c'era una correlazione significativa tra QTc a riposo e AHI. I parametri CPET indicavano una fitness cardiorespiratoria (CRF) inferiore nei pazienti con OSA non trattati rispetto ai pazienti senza OSA e a quelli con OSA e trattati con CPAP. La differenza nel numero totale di BESV e BEV tra pazienti con e senza OSA non era statisticamente significativa. Infine, tra i pazienti con OSA, non abbiamo osservato alcuna differenza significativa nelle misurazioni dell'intervallo QT tra quelli in terapia con CPAP e quelli senza terapia.

2.4 Conclusioni

(1) Ipotizziamo che l'OSA possa portare non tanto ad un prolungamento patologico dell'intervallo QT, bensì ad una riduzione della riserva di ripolarizzazione, il che è clinicamente rilevante in quanto aumenta la suscettibilità agli agenti che prolungano l'intervallo QT; (2) i pazienti con obesità grave e OSA da moderata a grave hanno mostrato ridotte capacità aerobica, tolleranza all'esercizio, e risposta ventilatoria all'esercizio rispetto ai pazienti senza OSA; (3) l'obesità centrale è un migliore predittore di comorbidità legate all'obesità rispetto al BMI; (4) non abbiamo riscontrato differenze significative nel numero totale di BESV e BEV durante il test da sforzo tra pazienti obesi con e senza OSA; e (5) abbiamo osservato effetti positivi della terapia con CPAP sulla funzionalità cardiorespiratoria ma non sull'intervallo QT.

3. INTRODUCTION

3.1 Molecular mechanisms of cardiac electrical activity in ventricular working cardiomyocytes

3.1.1 The cardiac action potential

The action potential (AP) of a cell is a sequence of events involving the influx and efflux of multiple ions through the cell membrane. In cardiac cells, action potential is initiated by a depolarizing stimulus, generally an electric current coming from an adjacent cell, that abruptly changes the resting membrane potential (E_m) to a critical value (the threshold); as a consequence, the properties of the cell membrane and ion conductance change dramatically, precipitating that sequence of events, involving inward and outward ion currents, that together make up for the action potential. In this fashion, an electrical stimulus is conducted from one cell to all the cells adjacent to it. [1]

From now on, it will be discussed the action potential in working ventricular cardiomyocytes.

Resting membrane potential is approximately -80/-90 mV. Threshold level is around -65 mV. Peak membrane potential is approximately +30 mV. [1]
When an excitatory stimulus depolarizes the cell beyond threshold level, enough Na^+ channels open, and the inward Na^+ current (I_{Na}) is large enough to result in a rapid shift of the E_m to a positive voltage range (the peak membrane potential, around +30 mV, is reached in this phase of the AP). This event triggers a series of successive opening and closure of selectively permeable ion channels, giving rise to a regenerative (i.e., propagated) AP. [1] The threshold is the lowest E_m at which the number of Na^+ channels that are able to open are enough to generate a propagated action potential. Subthreshold stimuli depolarize the membrane in proportion to the strength of the stimulus and cause only local responses, because the Na current that is generated is not large enough to initiate a propagated AP. On the contrary, when the stimulus is sufficient to reach threshold, a propagated AP is initiated, and the extent of subsequent depolarization is independent of the initial depolarizing stimulus (the result is an all-or-nothing response). [1]

Action potential duration and configuration exhibit regional differences, not only between nodal cells, atrial myocardium, Purkinje fibres, and ventricular myocardium, but also within the three layers of ventricular myocardium (endo, mid, and epicardium), see *Figure 1*. This is due to regional (and transmural) differences in ion channels expression and their relative densities.

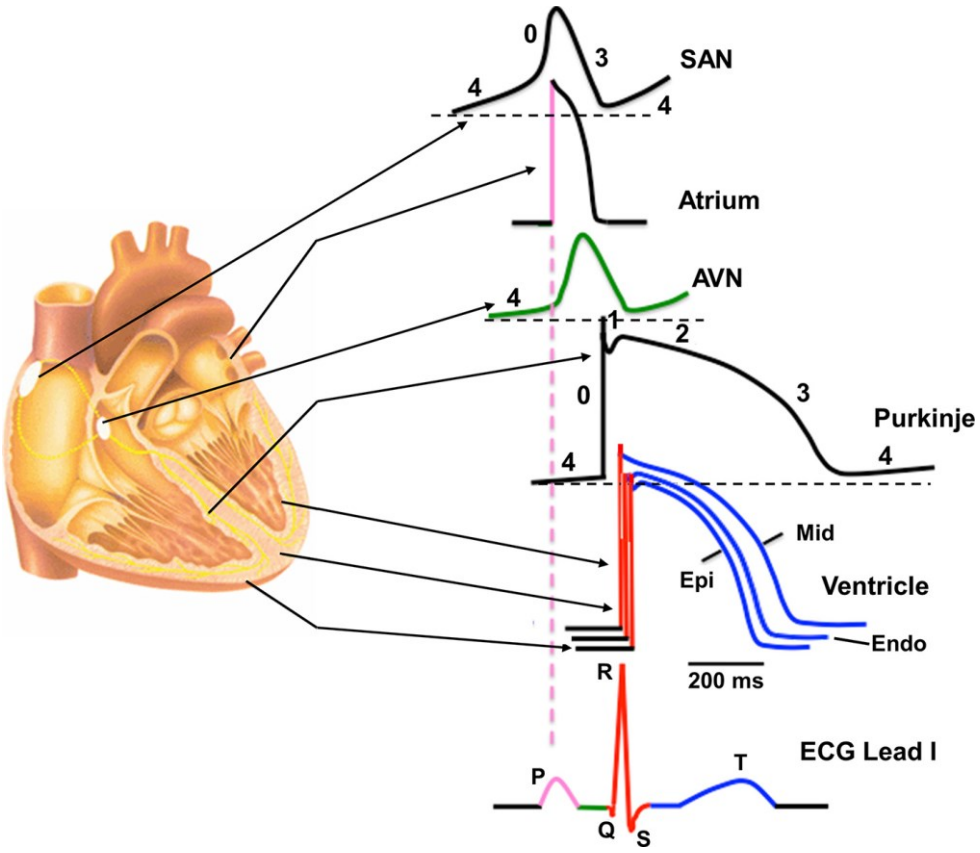

Figure 1 *Regional differences in cardiac action potential configurations. SAN, sinoatrial node; AVN, atrioventricular node; Endo, endocardium; Mid, midmyocardium; Epi, epicardium. From Varró et al. 2021* [2]

3.1.2 Phases of ventricular action potential

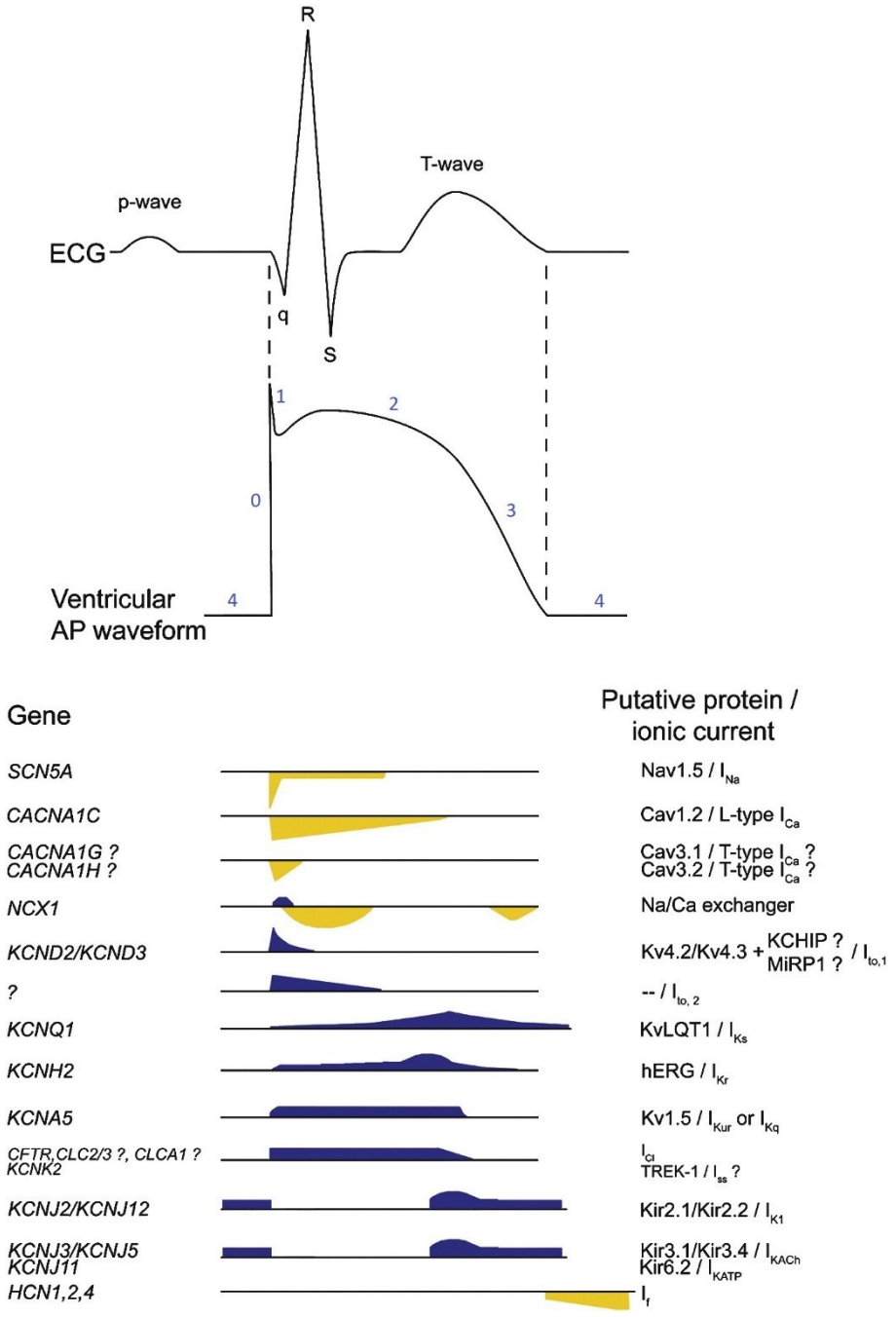

Figure 2 *Standard ECG, the underlying ventricular action potential, and the different ion currents that contribute to it. The numbers in blue indicate the phases of AP. Modified from Saenen et al. 2008* [3]

3.1.2.1 PHASE 4 – RESTING MEMBRANE POTENTIAL

In resting conditions, the membrane is most permeable to K^+ ions and relatively impermeable to other ions (K^+ has the largest transmembrane conductance at rest), therefore resting membrane potential (-80/-90 mV in ventricular myocytes) is mostly influenced by K^+ equilibrium and is close to K^+ Nernst potential (E_k , -94

mV). The resting membrane potential is determined and maintained near E_k mainly by the inward rectifier K^+ (Kir) channels, responsible for an outward K^+ current (I_{K1}). Kir channels exhibit a strong inward rectification property because of a strong voltage-dependent decline of K^+ efflux (i.e., reduction of outward current) on membrane depolarization. As such, I_{K1} passes K^+ ions over a limited range of E_m. At a negative E_m, close to resting values, I_{K1} conductance is much larger than that of any other current, thus it clamps the resting E_m close to the Nernst potential for K^+. On depolarization, I_{K1} channels close almost immediately, remain closed throughout the plateau, and open again at potentials negative to -20 mV. I_{K1} channels conduct a substantial outward current at an E_m between -40 and -90 mV. Thus, I_{K1} also contributes to terminal phase 3 of repolarization (see later). [1]

The Na/K ATPase as well contributes to the resting membrane potential, helping the formation of concentration gradients of Na^+ and K^+ across the membrane. At faster heart rates, Na^+/K^+ pumping increases to maintain the same ionic gradients, thus counteracting the intracellular gain of Na^+ and loss of K^+ with each depolarization. [1]

Reduction of cytosolic Ca^{2+} concentration during phase 4 is achieved by Ca_{2+} reuptake into the sarcoplasmic reticulum via activation of the SERCA pump, and by extrusion across the sarcolemma via the Na^+/Ca^{2+} exchanger (NCX). [1]

3.1.2.2 PHASE 0 – RAPID DEPOLARIZATION (THE UPSTROKE)

When an excitatory stimulus depolarizes the cardiomyocyte beyond threshold level (ca. -65 mV), Na^+ channels pass from the closed to the opened state (they activate), generating a large and rapid influx of Na^+ (inward Na^+ current, I_{Na}) (Na^+ channels start to open at threshold values; the influx of Na^+ further depolarizes the membrane, and this further increases Na^+ conductance, which allows more Na^+ to enter – a regenerative AP is triggered). The activation of Na^+ channels is transient: their inactivation is very fast, and starts with just a little delay after the activation, thus the channels remain open just under 1 ms to conduct I_{Na} and reach peak E_m of ca. +30 mV before they close. The rate and magnitude of Na^+ entry into the cell is a determinant of conduction velocity for the propagated action potential [1].

3.1.2.3 PHASE 1 – EARLY REPOLARIZATION

Phase 0 is followed by a rapid and brief phase of repolarization, during which the membrane rapidly and transiently repolarizes to almost 0 mV, shaping an early notch on the AP curve. Phase 1 (early repolarization) is due to the activation of the transient outward K^+ current (I_{to}) and concomitant inactivation of I_{Na} (inward Na^+ current). [1] I_{to} rapidly activates by depolarization (in less than 10 ms), and then rapidly inactivates (25 to 80 ms for the fast component $I_{to,f}$ and 80 to 200 ms for the slow component $I_{to,s}$). The influx of K^+ ions partially repolarize the membrane, shaping the rapid repolarization of the action potential and setting the height of the initial plateau (phase 2). [1]

3.1.2.4 PHASE 2 – THE PLATEAU

Phase 2 of ventricular AP represents a delicate balance between inward depolarizing currents (I_{CaL} and late I_{Na}) and outward repolarizing currents (rapidly I_{Kr} and slowly I_{Ks} activating components of the delayed rectifier outward K^+ current). Phase 2 is the longest phase of the action potential, lasting hundreds of milliseconds in His-Purkinje system and ventricles. The plateau phase marks Ca^{2+} entry into the cell. [1]

I_{CaL} is largely responsible for the action potential plateau, is a major determinant of the duration of the plateau phase (and hence of AP duration and refractoriness), and it also links membrane depolarization to myocardial contraction ("excitation-contraction coupling" through the mechanism of calcium-induced calcium release, in concert with the ryanodine receptor RyR2). Moreover, L-type Ca^{2+} channels are the main portal of entry of Ca^{2+} into cardiac cells during depolarization, and are the dominant factor in mediating positive inotropy. [1,2]

L-type Ca^{2+} channels activate on membrane depolarization at potentials positive to -40 mV, thus they are normally activated during phase 0 by the regenerative depolarization caused by fast I_{Na}. However, the amplitude of I_{CaL} is not maximal near the action potential peak because of the slow activation of I_{CaL}, and the low driving force ($E_m - E_{Ca}$) for I_{CaL}; therefore, I_{CaL} contributes very little to the action potential until after completion of phase 0 (hence, I_{CaL} affects mainly the plateau of action potentials). [1]

Na^+ channels make a minor contribution to the plateau phase: after phase 0 of the AP, some Na^+ channels occasionally fail to inactivate, or reopen repetitively for hundreds of ms after variable and prolonged latencies, resulting in a small inward I_{Na} (less than 1% of the peak I_{Na} responsible for phase 0). This persistent or "late" Na^+ current (I_{NaL}) gives a little contribution to the plateau phase. [1]
However, in some pathological conditions (such as LQTS3, heart failure, and hypertrophic cardiomyopathy) late I_{Na} is augmented, and therefore its contribution to the plateau phase dramatically increases, prolonging repolarization and increasing repolarization heterogeneity. Moreover, late I_{Na} augmentation also increases intracellular Ca^{2+} concentrations via Na^+/Ca^{2+} exchanger (NCX). This can evoke arrhythmogenic triggered activity, such as early and delayed afterdepolarizations (EADs and DADs). [2]

I_{Kr} and I_{Ks} channels (the rapid and slow components of the delayed rectifier K^+ current, see *Figure 3*) are critical determinants of the duration and morphology of cardiac AP [4]. Both I_{Kr} and I_{Ks} are activated at depolarized potentials, but their dynamics and biochemical properties are different.

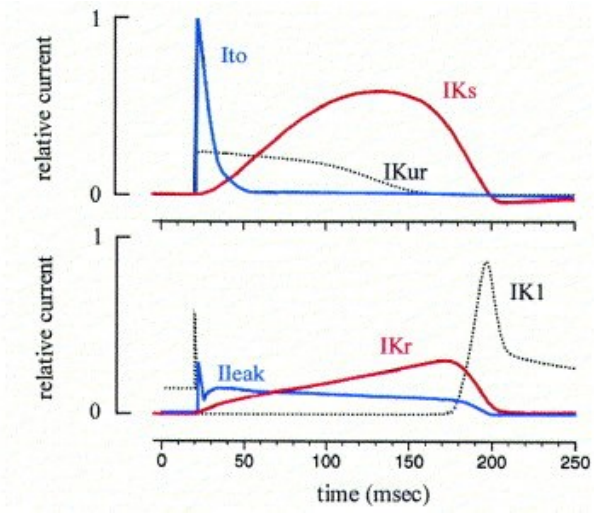

Figure 3 *Delayed rectifier K^+ currents. Modified from Tristani-Firouzi et al. 2001* [5]

I_{Kr} plays the largest role in repolarization under normal conditions, and is characterized by prominent inward rectification caused by a rapid voltage-dependent inactivation [4]. Rectification is the property of an ion channel to allow currents preferentially to flow in one direction, or limit currents from flowing in the other direction [1]; the conductance of rectifying channels usually depends on membrane potential (that is, it varies with changes in membrane potential). In the

case of I_{Kr}, at more positive potentials the inactivation is greater and channels conduct smaller outward current, and, as repolarization progresses, channels recover from inactivation and produce a large outward current, which repolarizes the membrane [4].

I_{Kr} activates relatively fast (in the order of tens of milliseconds) on membrane depolarization, but voltage-dependent inactivation thereafter is very fast. The fast voltage-dependent inactivation limits outward current through the channel at the positive voltages of early phase 2, and thus helps maintain the action potential plateau. However, as the voltage becomes less positive at the end of the plateau phase (as repolarization progresses) the channels recover rapidly from inactivation; this process leads to a progressive increase in I_{Kr} amplitudes during late phase 2 and phase 3, with maximal outward current occurring before the final rapid declining phase of the action potential. Next, I_{Kr} channels deactivate (close) in a slow, voltage-*in*dependent process (in contrast to the inactivation, which is voltage-dependent). [1]

I_{Ks} participates as well to the plateau phase. I_{Ks} is activated on membrane depolarization, and its activation is extremely slow, slower than any other known K^+ current. Hence, the contribution of I_{Ks} to the net repolarizing current is gradual, and greatest late in the plateau phase, particularly during action potentials of long duration. Moreover, I_{Ks} inactivation is as well very slow. [1]

I_{Ks} contribution to repolarization is minimal under normal conditions [2]. I_{Ks} plays an important role in determining the rate-dependent shortening of the cardiac action potential (especially in response to adrenergic stimulation): as heart rate increases, I_{Ks} increases because channel deactivation is slow and incomplete during the shortened diastole; this allows I_{Ks} channels to accumulate in the open state during rapid successive depolarizations and mediate the faster rate of repolarization [1] (which is essential to maintain adequate diastolic filling at high heart rates). Importantly, I_{Ks} is functionally upregulated when other repolarizing currents (especially I_{Kr}) are reduced, becoming the largest contributor to cellular repolarization: I_{Ks} is a critical contributor to the repolarization reserve (which is a safeguard mechanism against the loss of repolarizing power, according to which repolarization is provided by multiple redundant ionic currents that can compensate for each other's loss of function). [1,2,4]

The Na^+/Ca^{2+} exchanger and the Na^+/K^+ ATPase provide minor current components during phase 2 plateau [1].

On note, during the plateau phase, membrane conductance to all ions is rather low; in particular, K^+ conductance falls during the plateau phase because of the strong inward rectification properties of I_{Kr}. Thus, less change in current is required near plateau levels than near resting potential levels to produce the same changes in E_m [1]. This property confers energetic efficiency in the generation of the action potential [1], but at the same time, as written later in the text, makes the cardiomyocyte vulnerable to the development of early afterdepolarizations, EADs.

3.1.2.5 PHASE 3 – FINAL RAPID REPOLARIZATION

Phase 3 of the action potential represents a final rapid repolarization that restores membrane potential to its resting value. Phase 3 is mediated by the increasing conductance of the delayed rectifier K^+ currents (I_{Kr} and I_{Ks}), the inward rectifier K^+ currents (I_{K1} and acetylcholine-activated K^+ current I_{KACh}), and time-dependent inactivation of I_{CaL}. Final repolarization during late phase 3 results from K^+ efflux through the I_{K1} channels, which open at potentials negative to –20 mV. [1]

3.1.3 Transmural dispersion of repolarization

There is substantial heterogeneity in action potential duration and configuration across the ventricular myocardial wall, from endocardium, midmyocardium (putative M cells), to epicardium (see *Figure 1*). This is mainly due to transmural differences in ion channels expression and their relative densities. [1,2]

I_{to} density is higher in the epicardium and midmyocardium than in the endocardium; therefore, in epicardial and midmyocardial cells phase 1 is shorter, the notch is more prominent, and the AP shows a more pronounced spike and dome morphology compared with endocardial cells. These I_{to} related AP differences between epicardium and endocardium produce a transmural voltage gradient during early ventricular repolarization that registers as a J wave or J point elevation on surface ECG. [1]

The midmyocardial (M) cells appear to have the longest action potential duration across the myocardial wall, because of reduced I_{Ks} expression, larger late I_{Na}, and larger Na^+/Ca^{2+} exchanger current [1]. Accordingly, there are prominent differences between M cells and the surrounding myocardial cells in the response to various action potential duration (APD)-prolonging agents: the action potential of M cells tends to prolong disproportionately more relative to the other myocardial layers in response to APD-prolonging agents, such as drugs, genetic channel mutations (congenital LQTS), and other conditions (ex. acquired LQTS), resulting in a dramatic increase of transmural dispersion of repolarization (TDR) [6].

Figure 4 shows that I_{Kr} blockers, such as d-sotalol (B) and erythromycin, produce a much greater prolongation of APD in M cells than in the epicardium or endocardium [7]. Accordingly, these drugs (as the majority of APD-prolonging agents) dramatically increase the transmural dispersion of repolarization.

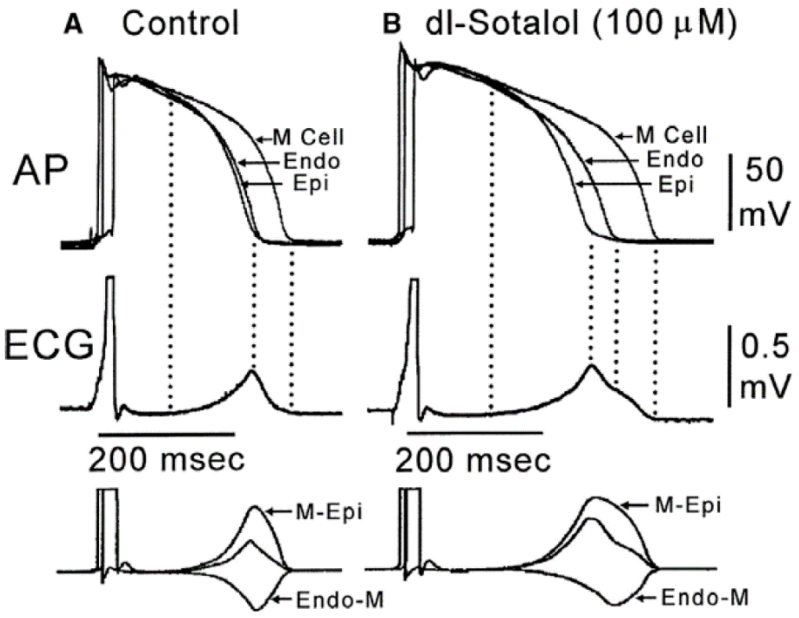

Figure 4 *Transmural dispersion of repolarization. Shown here are the baseline (A) and sotalol-induced changes (B) in APD throughout the different layers of myocardial wall. Note the increased TDR after sotalol-induced I_{Kr} blockade. From Yan, Antzelevitch 1998* [7]

Therefore, M cells have a significant role in arrhythmogenesis under pathological conditions associated with QT interval prolongation (such as LQTS), secondary to exaggeration of transmural repolarization heterogeneity [1].

A large increase in TDR is likely to be arrhythmogenic because is a favourable setup for reentrant and triggered ventricular arrhythmias [6].

As written later in text (*3.4.3 Twave abnormalities in LQTS*), T wave abnormalities mark an increased ventricular TDR, thus they likely represent an increased arrhythmic risk [6].

TpTe, i.e. the time interval between T-wave peak to T-wave end, has been proposed as a measure of repolarization heterogeneity. Increased TpTe has been associated with development of Torsade des Pointes (TdP) in pathological conditions associated with QT prolongation, and is considered a better predictor of TdP (thus, of SCD) than either QTc or QT intervals [6]. This suggests that the arrhythmic risk is not simply mediated by prolonged QTc, but repolarization heterogeneity has an important role as well.[6] The increased duration of the TpTe interval likely reflects the period when the epicardium is completely repolarized but the midmyocardium (M-cells) is still recovering, which is a favourable electrical substrate for reentrant arrhythmia [8].

Thus, studies conducted in patients with either congenital or acquired LQTS suggested that other ECG markers besides QT interval, such as T-wave abnormalities and increased TpTe, are associated with increased arrhythmic risk. [6]

Lastly, repolarization heterogeneity is associated with adverse outcomes (including SCD), also in the general population [9–14], in patients with myocardial infarction [15–23], congenital heart disease such as tetralogy of Fallot or hypertrophic cardiomyopathy [24–26], valvular heart disease [27], end-stage renal disease [28], LV hypertrophy (LVH) [29], hypertension [30], and heart failure [31].

3.1.4 Refractoriness

When an action potential is initiated, the cardiomyocyte becomes unexcitable to further stimulation until a certain level of repolarization is reached. This property is essential for normal cardiac functioning, because it guarantees the relaxation of the heart before subsequent activation, and prevents multiple compounded action

potentials from occurring. Therefore, this property is a determinant of susceptibility to arrhythmias (especially, reentrant arrhythmias). [1]

Refractoriness is determined by the number of Na^+ channels available for activation (i.e., that have recovered from inactivation). Once inactivated, Na^+ channels do not conduct any more current and cannot be reopened until after recovery from inactivation, which is voltage dependent: channel inactivation is removed during phase 3 and 4 of the AP (i.e., with membrane repolarization). Recovery of Na^+ channels is followed by a closed state, allowing the channels to be activated again during the next action potential. The fraction of channels available for opening varies from almost 100% at -90 mV, to 50% at -75 mV, to almost 0% at +40 mV. [1]

There are an absolute, an effective, and a relative refractory periods:

- The absolute refractory period (ARP) lasts over phases 0, 1, 2, and very early phase 3 of the AP, during which the cell is completely unexcitable to a new stimulus (no stimulus whatsoever, regardless of its strength, can reexcite the cell), as all Na^+ channels are inactivated. [1,32]
- After the absolute refractory period, during early phase 3, a new stimulus may cause some cellular depolarization, but without leading to a propagated action potential, as the fraction of Na^+ channels that have recovered from inactivation is so small that a depolarization can be elicited, but cannot be propagated to neighbouring cells. The sum of this brief period and the ARP is called effective refractory period (ERP). [1,32]
- The relative refractory period (RRP) follows the ERP and extends over the middle and late parts of phase 3, during which a new propagated action potential can be elicited but a larger than normal stimulus is required, because the number of Na^+ channels available is not maximal but still sufficient to propagate the depolarization to neighbouring cells. [1,32]

3.1.5 Cardiac ion channels

3.1.5.1 Na^+ channels (I_{Na})

The I_{Na} determines excitability and conduction in atrial, His-Purkinje system, and ventricular myocardium. It determines phase 0 rapid upstroke of the AP, and also makes a contribution to the plateau phase with late I_{Na} (I_{NaL}), which is minimal under normal conditions, but can potentially play an important role in diseased hearts. [1,2]

Moreover, Na^+ channel inactivation determines the refractoriness of cardiac cells, hence Na^+ channels help to regulate the frequency of AP firing. Regulation: β adrenergic stimulation enhances I_{Na} and α adrenergic stimulation reduces I_{Na}, respectively through PKA and PKC mediated phosphorylation of Na^+ channels. [1,2]

3.1.5.2 Transient outward potassium channel (I_{to})

I_{to} is the prominent repolarizing current responsible for the rapid repolarization (phase 1) of the AP, thus I_{to} shapes phase 1 notch and sets the height of the initial plateau (phase 2). Consequently, I_{to} influences activation, inactivation, and kinetics of those transmembrane channels that operate during the plateau phase (mainly I_{CaL} and the delayed rectifier K^+ channels), therefore I_{to} modulates duration and amplitude of phase 2 [1,2]. In particular, I_{to} modulates Ca^{2+} influx through L-type Ca^{2+} channels (LTCC) [33]. Phase 1 notch affects the function of the Na^+/Ca^{2+} exchanger, and subsequently intracellular Ca^{2+} handling and Na^+ channel function. [1]
All of this means that the activity of I_{to} influences the later phases of the action potential through regulation of several other ion channels.

I_{to} participates in creating repolarization heterogeneity across the myocardial wall, being more expressed in the epicardium and midmyocardium than in the epicardium.

I_{to} is strongly rate dependent. I_{to} fails to recover from previous inactivation at very fast heart rates; hence, abrupt changes in heart rate and pauses have important consequences for the early repolarization of the membrane. [1]

I_{to} activity is affected in many pathological conditions (such as heart failure, cardiac hypertrophy, diabetes mellitus, obesity, and some forms of LQTS) and by many drugs (such as quinidine, flecainide, and propafenone) [2]. Changes in I_{to} activity can

have different and opposite effects on AP duration and morphology because the interactions between I_{to} and the other ion channels are both very complex and also reciprocal. [1,2]

- Initial enhancement of I_{to} (thus of phase 1 notch) increases phase 2 dome and delays repolarization, presumably by delaying the peak of I_{CaL} and reducing I_{CaL} inhibition [1]. As a consequence, AP duration is prolongated.
- However, further enhancement of phase 1 notch prevents the rising of phase 2 dome and abbreviates AP duration, presumably by reduction of I_{CaL} through deactivation or voltage modulation. [1]
- Therefore, progressive enhancement of I_{to} activity (hence deepening of phase 1 notch) can cause initial enhancement followed by sudden disappearance of phase 2 dome, and corresponding prolongation followed by abbreviation of action potential duration. [1]
- On the other hand, a reduction of I_{to} results in attenuation of (phase 1) early repolarization, which decreases the driving force of Ca^{2+} through L-type Ca^{2+} channels (LTCC) [2], which in turn prolongates their open state, resulting in increased Ca^{2+} influx [33] and AP prolongation.
- Moreover, I_{to} reduction increases repolarization heterogeneity.

I_{to} is downregulated in heart failure, diabetes mellitus, cardiac hypertrophy, and obesity. I_{to} reduction leads to APD prolongation, enhanced Ca^{2+} influx, asynchronous Ca^{2+} release from the sarcoplasmic reticulum (SR), impaired excitability-contraction coupling, impaired Ca^{2+} handling, and increased repolarization heterogeneity. Hence, I_{to} downregulation contributes to arrhythmia in these pathological settings. [1,2,33,34]

β adrenergic stimulation decreases I_{to} activity via PKA and PKC mediated phosphorylation. Moreover, *chronic* β adrenergic stimulation causes I_{to} downregulation via transcriptional mechanisms. Chronic β adrenergic stimulation is associated with many pathological conditions, such as those mentioned above, and has been demonstrated to be one of the mechanisms causing I_{to} downregulation in those conditions. [2,34]

3.1.5.3 Delayed rectifier K^+ channels (I_{Kr} and I_{Ks})

I_{Kr} and I_{Ks} channels are critical determinants of the duration and morphology of cardiac AP. They both participate in the plateau phase and in the first part of phase 3 repolarization.

I_{Kr} and I_{Ks} are both reduced in many pathological conditions, such as heart failure, myocardial infarction, diabetes, obesity, OSA, and hypokalaemia [1,2,35].

I_{Kr} plays the largest role in repolarization under normal conditions, and is characterized by prominent inward rectification caused by a rapid voltage-dependent inactivation [4]. I_{Kr} likely plays a role in dynamic action potential adaptation to the heart rate, especially at intermediate heart rates during early exercise (a so-called "I_{Kr} zone"). However, the predominant current responsible for dynamic APD adaptation to the heart rate is I_{Ks}, especially during periods of increased sympathetic activity, during which is upregulated (see later) (of note, I_{Kr} channels are not as sympathetically responsive as I_{Ks} channels) [1,2,36]. I_{Kr} channels have unusual susceptibility to blockade by a wide range of drugs (if compared with other cardiac channels), likely because of its unique structural properties. In fact, almost all drugs that cause acquired LQTS target this channels. [1] Proarrhythmia induced by I_{Kr} blockade (in acquired and congenital LQTS) is related to:

- Excessive prolongation of the action potential duration near plateau voltages, especially those favouring the development of EADs [1].
- Increase of repolarization heterogeneity (prolongation of the AP caused by I_{Kr} blockade is more marked in midmyocardial than in epicardial/endocardial cells, because of the relative scarcity of I_{Ks} and hence less “repolarization reserve” in the M cells) [1].

I_{Ks} contribution to repolarization is minimal under normal conditions [2], but becomes increasingly important as heart rate increases (I_{Ks} is important for rate-dependent shortening of the cardiac AP). I_{Ks} is markedly increased by β adrenergic stimulation through PKA and PKC dependent phosphorylation: during periods of increased sympathetic activity (such as exercise) I_{Ks} becomes the predominant repolarization current rather than I_{Kr}. This is why in LQT1, LQT5, and LQT11 (i.e., the forms of congenital LQTS in which I_{Ks} current is affected; see later in text, *Table 3*, *3.3.7 QT interval prolongation and LQTS*) arrhythmia is triggered by adrenergic stimuli

and QT prolongation is especially notable during periods of increased sympathetic activity [1]. Besides, I_{Ks} is also a critical contributor to the repolarization reserve [2].

3.1.5.4 Inward rectifier K^+ channels (Kir)

Kir channels (responsible for I_{K1} current) are the main determinants of resting membrane potential (phase 4) and of the terminal part of phase 3 repolarization [1,2]. Kir channels exhibit a strong inward rectification property because of a strong voltage-dependency of K^+ conductance; Kir rectification property is also modulated by Mg^{2+} and Ca^{2+} concentrations [1] (explaining why an alteration of these ions' concentration affects AP duration).

I_{K1} is reduced by both β and α adrenergic stimulation (respectively via PKA and PKC mediated phosphorylation) [1,2]. Kir is downregulated in heart failure and cardiomyopathy. Kir downregulation leads to APD prolongation, increased spontaneous excitability (because of a less negative resting E_m), and facilitates triggered activity (generation of both EADs and DADs) [1].

3.1.5.5 ATP-sensitive K^+ channels (K_{ATP})

K_{ATP} is a ligand-gated K^+ channel with weak inward rectification, regulated by intracellular ATP and ADP concentrations, linking the cellular metabolic state to the membrane potential (and thus to excitability and contractility). K_{ATP} is inhibited by a high ATP/ADP ratio and activated by a decreased ATP/ADP ratio. [1]

Under normal metabolic conditions, K_{ATP} channels are predominantly closed (inhibited by intracellular ATP) and they do not significantly contribute to cardiac action potential, resting E_m, or cell excitability. However, when exposed to a severe metabolic stress (such as metabolic inhibition or ischemia) K_{ATP} channels become activated (secondary to reduced intracellular ATP levels) and conduct an outward repolarizing K^+ current (I_{KATP}), which results in abbreviation of the action potential duration and reduction of Ca^{2+} influx through L-type Ca^{2+} channels. By reducing Ca^{2+} entry, K_{ATP} channels depress muscle contractility thereby conserving scarce energy resources, and prevent the damaging effects of intracellular Ca^{2+} overload.[1]

Role of K_{ATP} in disease: (1) metabolic dysregulation of I_{KATP} created by disease-induced structural remodelling appears to contribute to the dysfunction of heart failure; (2) K_{ATP} channels have been further implicated in the adaptive cardiac response to chronic pathophysiological hemodynamic load; (3) K_{ATP} channel

deficiency affects structural remodelling, renders the heart vulnerable to calcium-dependent maladaptation, and predisposes to heart failure; (4) reactive oxygen species (ROS) desensitize K_{ATP} to intracellular ATP inhibition; (5) since K_{ATP} channels are unevenly distributed across the myocardial wall, their dysregulation affects differently the myocardial layers, increasing dispersion of repolarization. [1]

3.1.5.6 L-type Ca^{2+} channels (LTCC) (I_{CaL})

I_{CaL} is largely responsible for the action potential plateau, is a major determinant of the duration of the plateau phase (and hence of AP duration and refractoriness), and it also links membrane depolarization to myocardial contraction ("excitation-contraction coupling" through the mechanism of calcium-induced calcium release, in concert with the ryanodine receptor RyR2). Moreover, L-type Ca^{2+} channels are the main portal of entry of Ca^{2+} into cardiac cells during depolarization, and are the dominant factor in mediating positive inotropy. [1,2]

L-type Ca^{2+} channels activate on membrane depolarization at potentials positive to -40 mV, and I_{CaL} peaks between 0 and +10 mV. Although I_{CaL} is normally activated during phase 0 of the AP by the regenerative depolarization caused by fast I_{Na}, its contribution to the action potential is very little until after completion of phase 0, because of their slow activation as well as the low driving force ($E_m - E_{Ca}$) for I_{CaL} near AP peak. Hence, I_{CaL} mainly affects the plateau of the action potential. [1]

LTCC is inactivated by two mechanisms: a slow voltage-dependent inactivation, and a fast Ca^{2+}-dependent inactivation. Fast Ca^{2+}-dependent inactivation serves as a safeguard mechanism (negative feedback) to avoid Ca^{2+} overload (which is harmful causing both arrhythmias and cell death), and to ensure normal contraction and relaxation of the heart. This mechanism depends primarily on the Ca^{2+} released from the sarcoplasmic reticulum (but Ca^{2+} entering through LTCC can contribute as well), and is mediated by both calmodulin and an autoregulatory subunit of the channel itself. Slow voltage-dependent inactivation (induced by membrane depolarization) serves to prevent a premature rise in I_{CaL} during maintained depolarization, when intracellular Ca^{2+} concentration decreases and thus Ca^{2+}-dependent inactivation terminates. Recovery from inactivation follows the same two mechanisms. [1]

During maintained depolarization (ex. in case of repetitive stimulation at a partially depolarized E_m between pulses) SR Ca^{2+} reuptake is accelerated, so intracellular Ca^{2+} concentration decreases, and LTCC can recover from Ca^{2+}-dependent inactivation, enabling the possibility of subsequent premature reactivation of LTCC and a premature rise in I_{CaL}. This leads to instability of the cell membrane potential and may be the basis for the EADs that are capable of initiating torsades de pointes (TdP). [1]

I_{CaL} voltage-dependent recovery from inactivation between action potentials is slow at depolarized E_m, and it becomes very fast as repolarization is nearly complete. As a consequence, I_{CaL} declines in response to repetitive stimulation at a partially depolarized E_m between pulses (because of incomplete recovery of LTCC from inactivation), and a negative staircase of contractility is observed. In contrast, at normal resting potentials, recovery of LTCC from inactivation is fast, and I_{CaL} may increase progressively during repetitive stimulation. This positive staircase (or rate-dependent potentiation) of contractility is Ca^{2+} dependent, and is likely the result of diminished Ca^{2+}-dependent inactivation at frequencies with accelerated SR Ca^{2+} reuptake. [1]

L-type Ca^{2+} channels are regulated mainly by catecholamines (both of neurohumoral and circulating origin). Phosphorylation is the most important pathway for LTCC regulation. β adrenergic stimulation induces LTCC activation through PKA-mediated phosphorylation, increasing probability and duration of the open state of the channels, and consequently I_{CaL} amplitude. PKA-mediated phosphorylation of LTCC determines a shift in activation to a more negative E_m and the reduction of voltage-dependent inactivation. [1]

Voltage steady-state activation and inactivation are sigmoidal: the activation range is between -40 and +10 mV (with a half-activation near –15 mV), and the half-inactivation potential is near –35 mV. The overlap between steady-state voltage-dependent inactivation (SSI) and activation (SSA) curves defines a window current near the action potential plateau (see *Figure 5*), within which transitions from closed to open states can occur, and may play a major role in the initiation of EADs. As the action potential repolarizes into the window region, I_{CaL} increases and, in case of reduced repolarization reserve, can potentially be sufficient to reverse repolarization, thus generating the EAD upstroke (see later in text). For example, a

failure to deactivate I_{CaL} completely may be an essential mechanism underlying EADs caused by suppression of the delayed rectifier K^+ currents (see *Figure 10*, *3.2.2.2 Early afterdepolarizations*). [1]

Dysfunction of Ca^{2+} currents or intracellular Ca^{2+} transients (or both) in acquired diseases may induce both arrhythmia and contractile dysfunction [1].

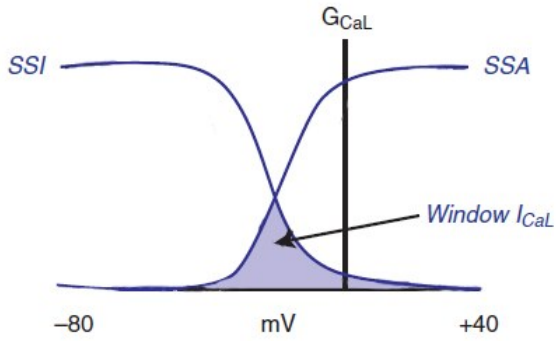

Figure 5 *L-type Ca^{2+} window current (window I_{CaL}). Overlap between steady-state voltage-dependent inactivation (SSI) and activation (SSA) curves of L-type Ca^{2+} channels defines a window current (in blue) near the action potential plateau. G_{CaL}, calcium conductance. Modified from Issa, Miller, Zipes, Clinical Arrhythmology and electrophysiology: a companion to Braunwald's Heart Disease, Third edition* [37]

3.1.5.7 T-type Ca^{2+} channels

T-type Ca^{2+} channels are functionally expressed in embryonic hearts, but they are almost undetectable in postnatal ventricular myocytes. In the adult heart, they are mostly expressed in nodal cells and Purkinje fibres. T-type Ca^{2+} channels activation range overlaps the pacemaker potential; thus, they play a minor role in generating pacemaker depolarizations, and contribute to automaticity. T-type Ca2+ channels are re-expressed in atrial and ventricular myocytes under various pathological conditions such as cardiac hypertrophy, myocardial infarction, and heart failure. These findings reflect a reversion to a fetal or neonatal pattern of gene expression, and I_{CaT} contributes to abnormal electrical activity and excitation-contraction coupling in these pathological conditions. [1]

3.1.5.8 Ryanodine Receptor 2 (RyR2)

RyR2 is a ligand-activated Ca^{2+} channel located on the sarcoplasmic reticulum membrane. RyR2 is activated with high affinity by cytosolic Ca^{2+}, and is the mediator of calcium-induced calcium release (CICR) in cardiac cells: Ca^{2+} entry into the cytosol through L-type Ca^{2+} channels during the plateau phase of AP

triggers RyR2 activation, which causes Ca^{2+} outflow from the sarcoplasmic reticulum, enabling cardiac muscle contraction. [1] RyR2 opening probability increases by elevation of sarcoplasmic reticulum Ca^{2+} concentration: when levels of Ca^{2+} in the sarcoplasmic reticulum reach a critical threshold, RyR2 can spontaneously open and release Ca^{2+} in the cytosol (Ca^{2+} leak), a process known as "store overload-induced Ca^{2+} release" (SOICR). Ca^{2+} concentration in the sarcoplasmic reticulum is physiologically increased as an effect of adrenergic (sympathetic) stimulation. [1,38] RyR2 is deactivated by the decline of Ca^{2+} concentration in the sarcoplasmic reticulum that follows its release during CICR (luminal Ca^{2+}-dependent deactivation); this results in a period of mechanical refractoriness of the heart. [1] RyR2 is finely regulated by PKA, CaMKII (Ca^{2+}/calmodulin-dependent kinase II), calmodulin, calstabin2, and calsequestrin2. β adrenergic stimulation results in PKA phosphorylation of RyR2, which activates the channel both by increasing RyR2 sensitivity to cytosolic Ca^{2+} and by decreasing the binding affinity of calstabin2 to RyR2 (that increases the probability of an open state). This results in an amplified response to Ca^{2+} influx via LTCC (and thus increased SR Ca^{2+} release). Chronic β adrenergic stimulation (associated with many pathologies, such as heart failure) causes PKA hyperphosphorylation of RyR2, which results in incomplete channel closure and Ca^{2+} leak from the SR during diastole. This causes the generation of spontaneous Ca^{2+} waves during diastole, an underlying mechanism to DAD-induced triggered arrhythmia. [1]

3.1.5.9 Cardiac gap junctions

Gap junctions are assemblies of intercellular channels that provide electrical and biochemical coupling between adjacent cells. Gap junction coupling is influenced by some endogenous mediators, likely via phosphorylation-mediated mechanisms. Several agents decrease gap junction coupling, including fatty acids, insulin, and angiotensin. Modification of cell-to-cell coupling occurs in numerous pathological settings (ex. MI, ventricular hypertrophy, cardiomyopathy) as a consequence of acute changes in the average conductance of gap junctions or by changes in the expression or cellular distribution patterns of gap junctions (remodelling). The alteration of gap junctions distribution and function can lead to conduction delay or block, and exaggerate anisotropy, thus providing a substrate for reentrant activity and increased susceptibility to arrhythmias. [1]

3.2 Electrophysiological mechanisms of cardiac arrhythmias

The mechanisms responsible for cardiac arrhythmias are generally divided into categories of disorders of impulse formation (automaticity or triggered activity), disorders of impulse conduction (reentry), or combinations of both. Some arrhythmias can be started by one mechanism and perpetuated by another. Automaticity is the property of cardiac cells to initiate an impulse spontaneously, without need for prior stimulation. Triggered activity is impulse initiation in cardiac fibers caused by depolarizing oscillations in membrane voltage (known as afterdepolarizations) that occur consequent to one or more preceding action potentials. Reentry occurs when a propagating action potential wave fails to extinguish after initial tissue activation; instead, it blocks in circumscribed areas, circulates around the zones of block, reenters and reactivates the site of original excitation after it recovers excitability. Reentry is the likely mechanism of most recurrent clinical arrhythmias. [1]

3.2.1 Automaticity

Automaticity is the property of cardiac cells to generate spontaneous propagated action potentials, in the absence of external electrical stimulation. It is the result of a spontaneous progressive diastolic depolarization caused by a net inward current during phase 4 of the AP, which progressively brings the membrane potential to threshold. [1,39]

The sinoatrial (SA) node is the dominant pacemaker of the heart because it normally displays the highest intrinsic rate of spontaneous depolarization. All other pacemakers are referred to as subsidiary or latent pacemakers because they take over the function of dominant pacemaker of the heart only when the SA node is unable to generate impulses or when these impulses fail to propagate. [39] The sinus node maintains its dominance over subsidiary pacemakers in the AVN and the Purkinje fibers through the mechanism of overdrive suppression, by which the impulse initiated by the sinus node depolarizes all the other pacemakers be fore they can spontaneously reach threshold potential (because the SA node is faster), thus suppressing their automaticity and keeping them under control. The mechanism of

overdrive suppression is mostly mediated by enhanced activity of the Na^+/K^+ pump: depolarization of latent pacemakers at a higher frequency than their intrinsic rate of automaticity leads to intracellular accumulation of Na^+, which enhances the activity of Na^+/K^+ pump, which generates a hyperpolarizing electrogenic current that opposes phase 4 depolarization. [1,39]

Automaticity results from two mechanisms: "voltage clock" and "calcium clock" (see *Figure 6*).

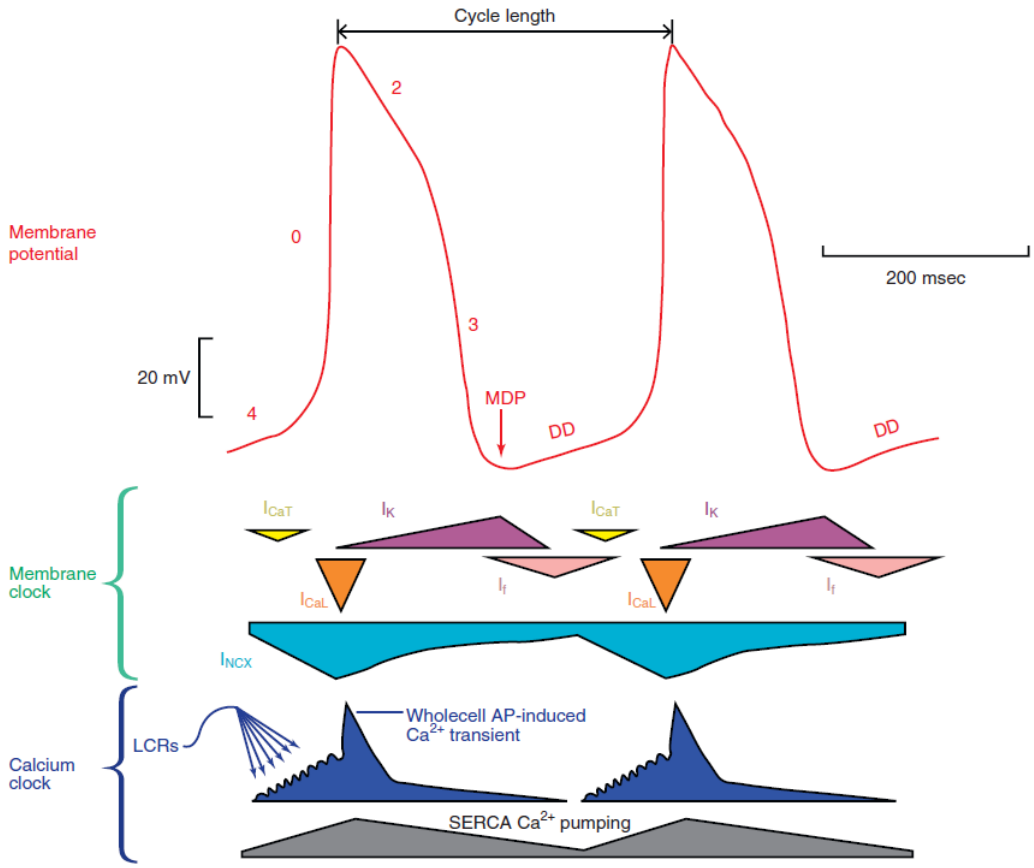

Figure 10 *Ionic currents involved in the sinus node pacemaker activity. DD, diastolic depolarization; LCRs, local Ca^{2+} releases; MDP, maximum diastolic potential. From Murphy et al. 2016* [40]

- Voltage clock refers to the time- and voltage- dependent membrane currents underlying pacemaker activity (I_f, I_{CaL}, I_{CaT}). I_f ("funny" current because, unlike most voltage-sensitive currents, is activated by hyperpolarization rather than depolarization) is the most important pacemaker current, and is carried out by hyperpolarization-activated cyclic nucleotide-gated (HCN) channels. I_f is a mixed Na^+-K^+ inward current modulated by the autonomic nervous system through cAMP. I_f is activated at the end of the action

potential as repolarization (carried by the outward K^+ current) brings membrane potential to resting values. Once activated, I_f depolarizes the membrane to a threshold level where L-type Ca^{2+} channels activate to initiate the action potential. In addition to If, multiple time- and voltage-dependent ionic currents contribute to diastolic depolarization in pacemaker cells (such as I_{CaL}, I_{CaT} and various types of delayed rectifier K^+ currents); many of these currents respond to β-adrenergic stimulation. [1,39,41]

- Calcium clock involves spontaneous calcium release from the sarcoplasm reticulum which activates I_{NCX}. In nodal cells, during late phase 3 and phase 4 of the AP, spontaneous rhythmic Ca^{2+} release from the SR via RyR2 receptors activates the Na^+/Ca^{2+} exchanger, which exchanges 3 extracellular Na^+ with 1 intracellular Ca^{2+} operating in its forward mode. This generates a net inward current (I_{NCX}) that causes exponential increase of the late diastolic depolarization (thus driving the membrane potential to the threshold for LTCC opening). The activation of local oscillatory Ca^{2+} release is independent of membrane depolarization, and is driven by a high level of basal state phosphorylation of Ca^{2+} handling proteins, L-type Ca^{2+} channels, and RyR2, provided by the autonomic nervous system. Phosphorylation-dependent regulation of calcium clock is the essential regulatory mechanism of pacemaker rate and rhythm. [1,39]

Altered automaticity can be caused by enhanced normal automaticity or by abnormal automaticity. The discharge rate of normal or abnormal pacemakers can be influenced by drugs, various forms of cardiac disease, reduction in extracellular potassium (K^+), or alterations of autonomic nervous system tone. [1]

3.2.1.1 Enhanced normal automaticity

Enhanced normal automaticity refers to the accelerated generation of an action potential by normal pacemaker tissue (SA node and other subsidiary or latent pacemakers): impulse initiation is a normal property of the primary and latent pacemakers [1].

Once the enhanced rate exceeds that of the sinus node, the enhanced ectopic pacemaker prevails and overdrives the sinus node and other subsidiary pacemakers.

A premature impulse caused by enhanced automaticity of latent pacemakers comes *early* in the normal rhythm. Enhanced automaticity is usually caused by increased sympathetic tone, which increases the rate of diastolic depolarization of latent pacemaker cells and diminishes the inhibitory effects of overdrive. Other causes of enhanced normal automaticity include periods of hypoxemia, ischemia, electrolyte disturbances, and certain drug toxicities. [1,39]

3.2.1.2 Abnormal automaticity

In the normal heart, automaticity is confined to the sinus node and other specialized conducting tissues (subsidiary pacemakers). Working atrial and ventricular myocardial cells do not normally exhibit spontaneous diastolic depolarization and do not initiate spontaneous impulses. However, abnormal automaticity occurs in these cells when there are major abnormalities in their transmembrane potentials, and in particular when their diastolic resting potential is reduced (i.e. is shifted to less negative values): when the resting E_m of these cells is depolarized sufficiently, to approximately -70 to -30 mV, spontaneous diastolic depolarization can occur and cause repetitive impulse initiation, a phenomenon called “depolarization-induced automaticity” or “abnormal automaticity”. [1,41]

Depolarization of membrane potential associated with disease states is most commonly a result of reduced I_{K1} current (the outward K^+ current that largely determines the resting membrane or maximum diastolic potential) that can be caused by (1) hypokalaemia, which reduces I_{K1}; (2) a reduced number of Kir channels; (3) a reduced K^+ conductance across Kir channels; or (4) electrotonic influence of neighbouring cells in the depolarized zone. Similar to normal automaticity, abnormal automaticity is enhanced by β-adrenergic agonists and by reduction of external potassium (both of which, among other things, decrease I_{K1}).[39] Catecholamines can increase the rate of discharge caused by abnormal automaticity and therefore can contribute to a shift in the pacemaker site from the sinus node to a region with abnormal automaticity [1].

Abnormal automaticity is not caused by the normal pacemaker mechanism (membrane and calcium clocks), but other different mechanisms lead to the generation of Na^+ and Ca^{2+} inward currents. [1]

Abnormally automatic cells and tissues at reduced levels of membrane potential are less sensitive to overdrive suppression. As a result, even transient sinus pauses can permit an ectopic focus to capture the heart for one or more beats. [1]

Although automaticity is not responsible for most clinical tachyarrhythmias, which are usually caused by reentry or triggered activity, abnormal automaticity can lead to arrhythmias caused by nonautomatic mechanisms; for example, premature beats caused by automaticity can initiate reentry. [1]

3.2.1.3 Parasystole

Parasystole is a form of arrhythmia caused by the presence of a subsidiary pacemaker working in parallel with the SA node. This happens because the parasystolic pacemaker (or focus) is protected from overdrive suppression by the dominant pacemaker by an entrance block, thus it can spontaneously generate impulses at its own intrinsic rate. The entrance block can be constant or intermittent, and must be unidirectional, so that activity from the ectopic pacemaker can exit and produce depolarization whenever the surrounding myocardium is excitable. [1]
A region of entrance block arises when the ectopic pacemaker is surrounded by ischemic, infarcted, or otherwise compromised cardiac tissue [39].

A pacemaker region exhibiting entrance block and exit conduction is referred to as a “parasystolic focus”. The ectopic activity generated by a parasystolic focus is characterized by premature ventricular complexes (PVCs) with variable coupling intervals, fusion beats, and inter-ectopic intervals that are multiples of a common denominator. This rhythm is relatively rare and is usually considered benign, although a premature ventricular activation of parasystolic origin can induce malignant ventricular arrhythmias in the ischemic myocardium or in the presence of a suitable myocardial substrate. [39]

“Modulated parasystole” is a variant of the classical parasystole (also called “fixed parasystole”). In this variant, the entrance block is incomplete, thus the dominant pacemaker can modulate the activity of the parasystolic focus, forcing it to discharge at periods that may be faster or slower than its own intrinsic cycle. In modulated parasystole coupling intervals are fixed. [1,41]

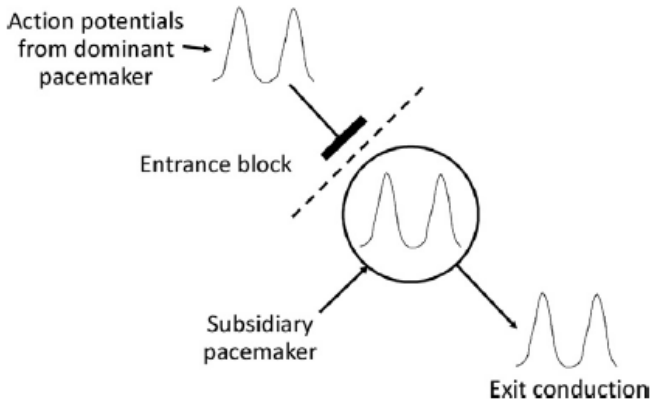

Figure 7 *Protected pacemaker (parasystolic focus). From Tse 2016* [41]

3.2.2 Triggered activity

Triggered activity is premature impulse initiation in cardiac fibres caused by afterdepolarizations. Afterdepolarizations are depolarizing oscillations in membrane potential that occur consequent to one or more preceding action potentials. Afterdepolarizations can occur early during the repolarization phase of the action potential (early afterdepolarizations, EAD) or late, after completion of the repolarization phase (delayed afterdepolarizations, DAD). When either type of afterdepolarization is large enough to reach the threshold potential for activation of a regenerative

inward current, a new action potential is generated, which is referred to as *triggered*. Unlike automaticity, triggered activity is not a self-generating rhythm: it occurs in response to a preceding impulse (the trigger). [1] These triggered events give rise to extrasystoles, which can precipitate tachyarrhythmias [39].

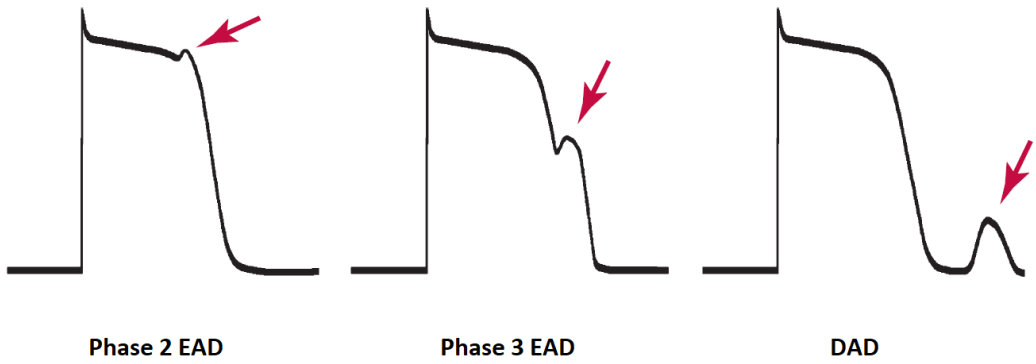

Figure 8 *Afterdepolarizations. EAD, early afterdepolarization; DAD, delayed afterdepolarization. From from Issa, Miller, Zipes, Clinical Arrhythmology and electrophysiology: a companion to Braunwald's Heart Disease, Second edition* [1].

3.2.2.1 Delayed afterdepolarizations (DADs)

DADs are depolarizing oscillations in membrane potential that occur after the completion of repolarization (i.e., during phase 4 of the AP). [1]

DADs are usually observed under conditions of intracellular calcium overload, which can result from exposure to toxic levels of digitalis, catecholamines, hypokalaemia, and hypercalcemia; pathological conditions such as cardiac hypertrophy, heart failure, and myocardial infarction; and genetic mutations affecting RyR2 or calcium handling proteins (familial CPVT). [1,39,41]

Ca^{2+} overload of the sarcoplasmic reticulum may cause spontaneous Ca^{2+} release after repolarization, which induces the generation of Ca^{2+}-dependent depolarizing currents. The most important calcium-sensitive current implicated in DAD formation is that induced by activation of the Na^{+}/Ca^{2+} exchanger (NCX): spontaneous Ca^{2+} release from the SR activates the NCX operating in forward mode, which exchanges three Na^{+} in for one Ca^{2+} out, thus generating a net inward Na^{+} influx (I_{NCX}), causing transient oscillations of the membrane potential (DADs). [1,2,39,41] See *Figure 9* for schematic representation of this process.

DADs are more likely to occur at fast heart rates or with increased premature beats [1,39]. Beta-adrenergic stimulation promotes the development of DADs by increasing intracellular Ca^{2+} overload via several mechanisms (see *Figure 9*), including (1) increasing L-type Ca^{2+} channels activity (thus I_{CaL}); (2) enhancing NCX activity; (3) enhancing Ca^{2+} uptake by the SR, leading to increased Ca^{2+} stored in the SR and subsequent release of more Ca^{2+}; (4) increasing RyR2 activity; (5) increasing the heart rate. Therefore, DADs development is often exercise-induced [1]. Premature impulses increase intracellular Ca^{2+} because of repeated activation of I_{CaL}. [1]

If the depolarization produced by the DAD is sufficiently large to reach threshold (suprathreshold DAD), it activates I_{Na}, triggering a new action potential [2,41]. The triggered action potential can cause focal non-reentrant arrhythmias (for ex., ventricular ectopic beats, or ventricular tachycardia) or initiate reentry if a vulnerable tissue substrate is encountered. The first triggered action potential is often followed by a short or long train of additional triggered action potentials, each arising from the DAD caused by the previous action potential. [1]

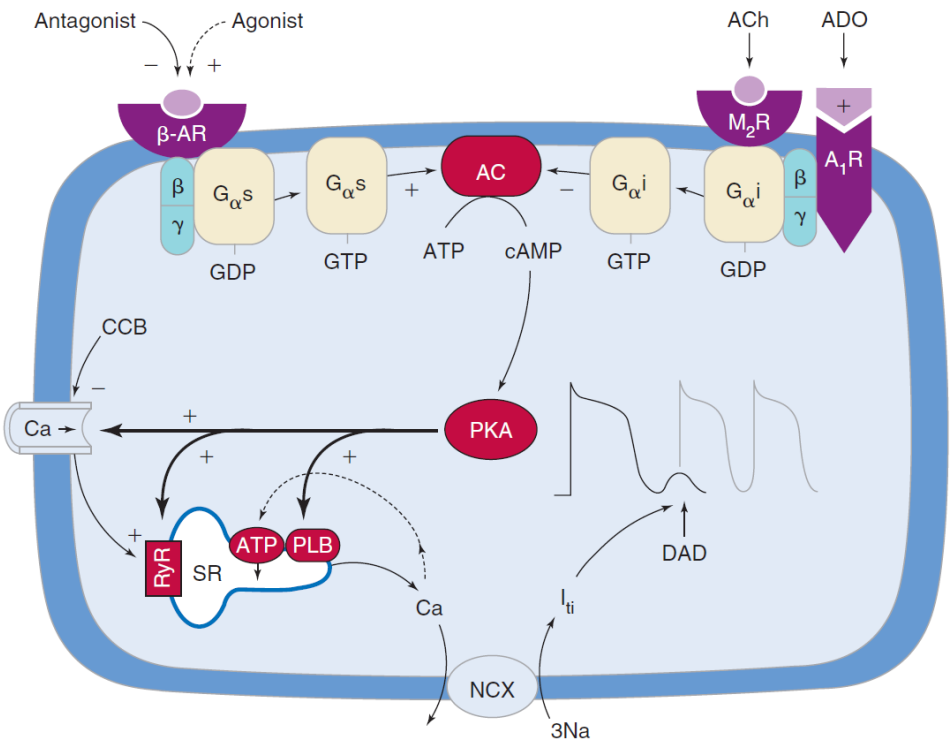

Figure 9 *Signal Transduction Scheme for Initiation and Termination of Cyclic Adenosine Monophosphate* (cAMP)*-Mediated Triggered Activity* [1]*. A1R, α1-adenosine receptor; AC, adenylyl cyclase; ACh, acetylcholine; ADO, adenosine; ATP, adenosine triphosphate; Ca, calcium; CCB, calcium channel blocker; DAD, delayed afterdepolarization; GDP, guanosine diphosphate; GTP, guanosine triphosphate; Gαi, inhibitory G protein; Gαs, stimulatory G protein; Iti, transient inward current; M2R, muscarinic receptor; Na, sodium; NCX, sodium (Na+)-calcium (Ca2+) exchanger; PKA, protein kinase A; PLB, phospholamban; RyR, ryanodine receptor; SR, sarcoplasmic reticulum; β-AR, β-adrenergic receptor. From Lerman 2007* [42]

Probably, the most important influence that causes subthreshold DADs to reach threshold is a decrease in cycle length, because it increases both the amplitude and the rate of DADs. Hence, initiation of arrhythmias triggered by DADs can be facilitated by an increase in the heart rate. [1]

Subthreshold DADs can play a role in arrhythmogenesis by creating a region of unidirectional conduction block: they cause partial depolarization of the cell membrane, hence inactivating a portion of Na^+ channels, reducing their availability during the subsequent (triggered or non-triggered) action potential. The resultant regional dispersion of excitability and refractoriness generates a tissue substrate vulnerable to reentry. [1]

DADs can generate both the vulnerable substrate and the trigger to reentry. When both suprathreshold and subthreshold DADs coexist in the same tissue, the combination of triggers and a vulnerable substrate can lead directly to reentry: in

some regions, subthreshold DADs promote regional conduction block, whereas in other regions, suprathreshold DADs trigger an action potential; once the triggered action potential propagates to the region of conduction block, it can initiate reentry.[1]

DAD-related triggered activity is thought to be a mechanism for tachyarrhythmia in various diseases, such as heart failure, myocardial infarction, atrial fibrillation, digitalis toxicity, some idiopathic VTs, and CPVT [1,2,41,42].

3.2.2.2 Early afterdepolarizations (EADs)

EADs are depolarizing oscillations in membrane potential that occur during the plateau (phase 2 EAD) or terminal repolarization (phase 3 EAD) of the action potential, and interrupt the orderly repolarization of the cardiomyocyte [1]. They are usually, but not exclusively, associated with prolonged action potential duration (APD) (i.e., prolongated QT interval) [41].

EADs are typically observed in LQTS [1,2,41] and in cardiac tissues exposed to injury, altered electrolytes, hypoxia, acidosis, catecholamines, and pharmacologic agents, including antiarrhythmic drugs. Ventricular hypertrophy and heart failure also predispose to the development of EADs. [39]

EADs develop more commonly in midmyocardial M cells than in epicardial or endocardial cells when exposed to action potential duration (APD)-prolonging agents, because of a weaker I_{Ks} and stronger late I_{Na} in M cells [39] (see *3.1.3 Transmural dispersion of repolarization*). Therefore, EADs can increase the dispersion of repolarization [1], creating a vulnerable substrate to reentry.

Normally, during phase 2 and 3, the net membrane current is outward. Any factor that transiently shifts the net current in the inward direction can potentially overcome and reverse repolarization, and lead to EADs and EAD-related arrhythmias. Such a shift can arise from decreased outward repolarizing currents (I_{Kr}, I_{Ks}, I_{K1}), increased inward depolarizing currents (late I_{Na}, I_{CaL}, or I_{NCX}), or both. [1,41] Moreover, EADs can also be promoted by intracellular Ca^{2+} oscillations or by prolonged Ca^{2+} transients via Na^{+}/Ca^{2+} exchanger current (I_{NCX}). [1] Combinations of these interventions (for ex., calcium loading and I_{Kr} or I_{Ks} reduction) or pathophysiological states can act synergistically to facilitate the development of EADs. [39]

Several mechanisms have been proposed to underlie EAD generation:

1. As a consequence of the prolongated action potential, some L-type Ca^{2+} channels can recover from inactivation and reopen, causing positive voltage oscillations during the plateau (phase 2 EAD) or terminal repolarization (phase 3 EAD). [2]

2. The overlap between steady-state voltage-dependent inactivation (SSI) and activation (SSA) curves of L-type Ca^{2+} channels defines a window current near the action potential plateau, within which transitions from closed to open states can occur. As the action potential repolarizes into the window region, I_{CaL} increases and, in case of reduced repolarization reserve (ex. in case of reduced delayed rectifier I_K current), it can potentially be sufficient to reverse repolarization, thus generating the EAD upstroke (*Figure 10*). [1]

3. The increase in Ca^{2+} influx through L-type Ca^{2+} channels (I_{CaL}) increases the activity of NCX in the forward mode, resulting in a net inward Na^+ current (I_{NCX}), thus facilitating EAD formation and increasing the probability of an EAD-triggered action potential [1].

4. Late Na^+ current (I_{NaL}) gives little contribution to the plateau phase under normal conditions. However, under pathophysiological conditions (such as LQTS3, heart failure, cardiomyopathy, ischemia, drugs) Na^+ channel inactivation may be either delayed or reversed to allow channel reopening before repolarization, and the result is an increased late I_{Na} current that persists throughout the action potential plateau. The increased late I_{Na} prolongates the repolarization phase and the action potential duration. The resulting delay in the repolarization process triggers EADs by favouring the reactivation of L-type Ca^{2+} channel during phase 2 or 3 of the action potential. [1]

5. APD prolongation and/or intracellular Ca^{2+} loading promote spontaneous calcium release from the sarcoplasmic reticulum during phase 3 of the AP, at membrane potentials negative to the threshold of I_{CaL} activation, but before full repolarization. Spontaneous Ca^{2+} release form the SR activates I_{NCX}, resulting in membrane depolarization (phase 3 EADs). This type of EADs strongly resemble DADs in their mechanism, but differ in the timing

of the Ca^{2+} release from the SR (during the repolarizing phase of the action potential in phase 3 EADs, and at the resting membrane potential for DADs, i.e. during AP vs. after AP). [2,41] This interrelationship among intracellular Ca^{2+}, DADs, and EADs can be one explanation for the susceptibility to arrhythmias in heart failure (which is featured by Ca^{2+} overload, prolongated AP, and increased sympathetic tone), where both EADs and DADs have been implicated as the mechanisms of arrhythmogenesis, particularly on exposure to action potential-prolonging drugs. [1,2,41]

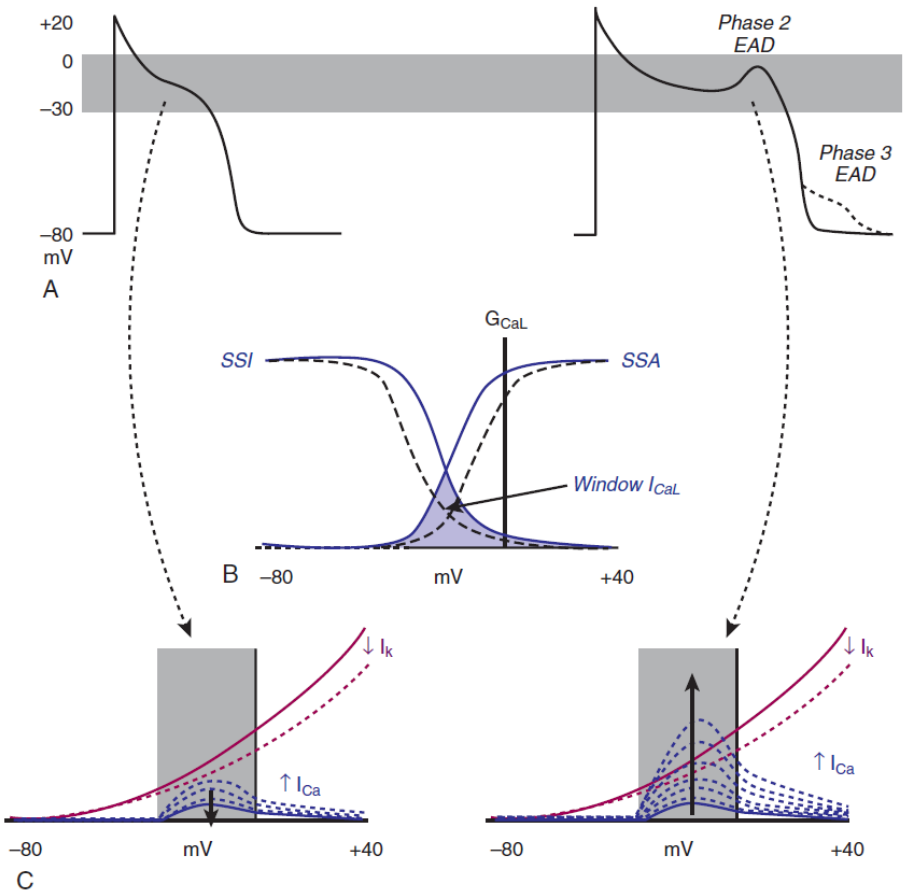

Figure 10 *Role of the window I_{CaL} in the generation of EADs. (A) On the left, normal action potential (left), and on the right, an action potential with phase 2 EAD (solid line) or phase 3 EAD (dashed line). (B) Overlap between steady-state voltage-dependent inactivation (SSI) and activation (SSA) curves of L-type Ca^{2+} channels defines a window current (in blue) near the action potential plateau. Dashed lines show a potential therapeutic intervention that shifts the SSA and SSI curves of LTCC to reduce the overlapping window current region. (C) Schematic diagram illustrating the interaction between time-dependent I_{CaL} reactivation (dashed blue lines) and time-dependent deactivation of repolarizing currents (I_K) (dashed red lines) in the window voltage range during action potential repolarization. For the normal action potential (left), the repolarization rate is too fast for I_{CaL} to grow larger than I_K. However, if the repolarization rate is too slow (right), I_{CaL} can grow larger than I_K, thereby reversing repolarization to cause an EAD (right). LTCC, L-type Ca^{2+} channels; G_{CaL}, calcium conductance. Text from [37]; image from Weiss et al. 2010 [43].*

6. EADs have also been associated with APD shortening. These EADs occur during *late* phase 3; here, an abbreviated APD permits *normal* Ca^{2+} release from the SR to induce membrane depolarization by activating I_{NCX} [39,41]. In contrast to DADs or previously described calcium-dependent EADs, it is *normal*, not *spontaneous* SR calcium release that is responsible for their generation. Two principal conditions are required for the appearance of late phase 3 EADs: APD abbreviation and strong SR calcium release. Such conditions may occur when both parasympathetic and sympathetic influences are combined. [39]

Both types of EADs are rate dependent, with the reactivation-driven mechanism appearing predominantly at slow pacing, and the release-driven EADs occur at fast pacing [2]. However, EADs are usually associated with slow heart rates because action potentials are longer in duration [1].

Whatever be the underlying mechanism, if the change in membrane potential brought about by the EAD is sufficiently large, it will activate I_{Na}, resulting in triggered activity [41].

The upstrokes of the action potentials elicited by phase 2 and phase 3 EADs are different. Phase 2 EAD-triggered action potential upstrokes are exclusively mediated by Ca^{2+} currents. Even when these triggered action potentials do not propagate, they can substantially exaggerate repolarization heterogeneity (a key substrate for reentry) because EADs occur more readily in some regions (Purkinje fibers, midmyocardial M cells) than others (epicardium, endocardium). Action potentials triggered by phase 3 EADs arise from more negative membrane voltages; therefore, the upstrokes can be caused by Na^+ and Ca^{2+} currents and are more likely to propagate. [1] Both suprathreshold and subthreshold EADs can create dispersion of refractoriness and a tissue substrate vulnerable to reentry. When EADs reach the threshold to propagate, they generate triggers that initiate reentry in the vulnerable substrate. Therefore, depending on the cellular and tissue properties, EADs can result in purely reentrant arrhythmias, multiple shifting foci, and a mixture of multiple shifting foci and reentry. EAD-mediated triggered activity likely underlies initiation of the characteristic polymorphic VT, torsades de pointes (TdP), seen in patients with congenital and acquired forms of LQTS [1].

3.2.3 Reentry

Reentry occurs when a propagating action potential wave fails to extinguish after initial tissue activation, but reenters and reactivates the site of original excitation after it has recovered from refractoriness. It can be divided in two types: reentry that occurs in the presence of an obstacle, around which an action potential can travel (circus-type reentry); and reentry that occurs without an obstacle (reflection and phase 2 reentry). Reentry is the likely mechanism of most recurrent clinical arrhythmias. [1,41]

3.2.3.1 Reflection

Reflection is a special subclass of reentry in which the excitation wavefront does not require a circuit but appears to travel back and forth in a linear segment of tissue (ex. trabeculae or Purkinje fibers) containing an area of conduction block. Reflection may be responsible for premature cardiac contractions and may initiate fatal cardiac arrhythmias such as VT and VF. [1]

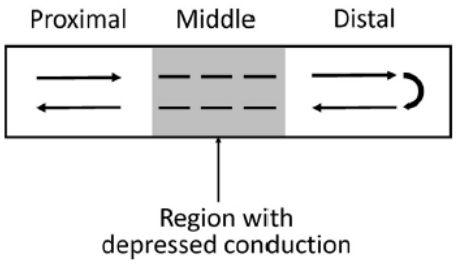

Figure 11 *Reflection reentry. From Tse 2016* [41]

3.2.3.2 Phase 2 reentry

Exaggeration of transmural voltage gradients and dispersion of repolarization can cause the generation of electronic currents during phase 2 of the AP, flowing from sites with longer APDs to sites with shorter APDs, causing local reexcitation when the latter sites have recovered from refractoriness. This local reexcitation can generate a closely coupled extrasystole that, in turn, can initiate VT or VF via circus-type reentry. [1,41]

3.2.3.3 Circus-type reentry

This occurs when an action potential travels around an anatomical or functional obstacle and reexcites its site of origin [41].

Requisites for circus-type reentry:

- Substrate, given by the presence of adjacent regions or pathways in the myocardial tissue with different electrophysiological properties (conduction and refractoriness) and joined both proximally and distally (forming a circuit). These circuits can be anatomical, functional, or both, and they can either be stationary or move within the myocardial tissue. [1]
- Central obstacle (central area of block), which is a core of unexcitable tissue around which the wavefront can circulate to sustain reentry. The nature of this central obstacle can be anatomical, functional, or both. When functional, it is sustained by centripetal activation from the circulating wavefront that, by repeatedly bombarding the central area of block, maintains the state of refractoriness of this region. [1]
- Unidirectional conduction block, which usually results from the spatial dispersion (heterogeneity) of conduction and refractoriness in the myocardial substrate. [1,41]
- Area of slow conduction, so that the tissue initially activated by the excitation wavefront has sufficient time to recover its excitability by the time the reentrant wavefront returns (i.e., the length of the reentrant pathway must equal or exceed the reentrant wavelength). [1]
- Initiating trigger (usually, a premature impulse). Changes in heart rate or autonomic tone, ischemia, electrolyte or pH abnormalities, or the occurrence of a premature depolarization can be sufficient to initiate reentrant tachycardia. The trigger is usually required because it elicits or brings to a critical state one or more of the conditions necessary to achieve reentrant excitation. In fact, premature depolarizations frequently initiate these tachyarrhythmias because they can cause slow conduction and unidirectional block. The premature impulse can be caused by automaticity or triggered activity. [1]

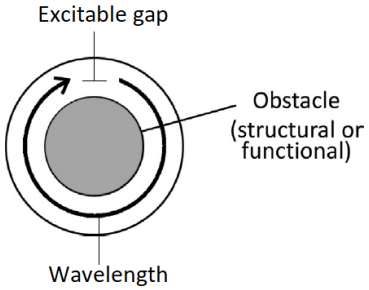

Figure 12 *Circus-type reentry. Modified from Tse 2016* [41]

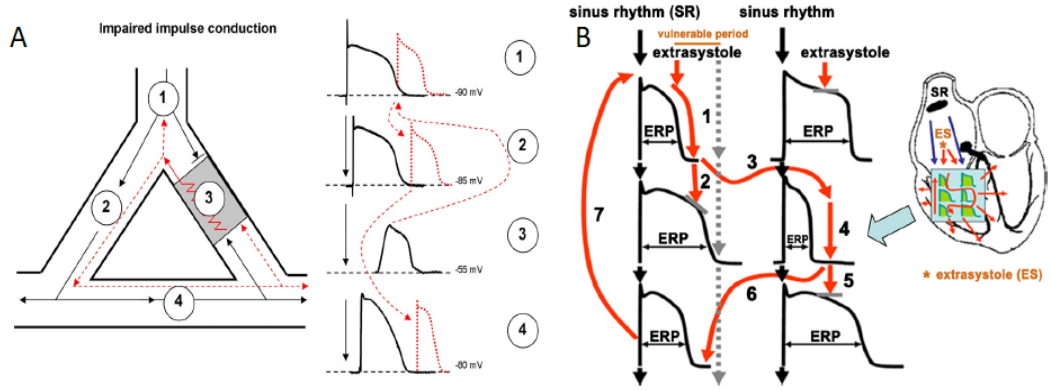

Figure 13 *(A) Schematic illustration of anatomical reentry. An area of branching cardiac tissue, providing separate paths for impulse propagation from proximal (1) to distal (2-4) directions. The separate paths for impulse conduction can be variable, for example they can be ventricular muscle segments with nonconducting fibrosis, scar, or infarcted tissue in the core; an area of depolarized myocardium at site 3 (due to asymmetric severe local myocardial damage) provides unidirectional conduction block. In case the impulse travels from site 4 in the retrograde direction, it can propagate back very slowly through this damaged area (site 3), and if conduction velocity in this area is slow enough to outlast the effective refractory period of the tissue in front of the impulse, it can reexcite the proximal tissue, establishing a circus movement and reentry arrhythmia. (B) Schematic illustration of functional reentry. The arrhythmia substrate is represented by enhanced dispersion of refractoriness and action potential duration. An early ectopic impulse (trigger, red arrow) can only propagate via pathways where the tissue is not depolarized, and consequently its refractoriness is over, whereas the conduction is blocked in directions where the tissue is not fully repolarized and cells are still in the refractory state. Thus the abnormal impulse can travel in a zig-zag direction through reentry paths created by heterogeneous repolarization and conduction. The dispersion of repolarization creates a time window called the vulnerable period, where extra stimuli could elicit the reentry arrhythmia. However, outside this window extra stimuli would only cause a single or multiple relatively harmless extrasystoles. CV, conduction velocity; ES, extrasystole; SR, sinus rhythm.* [2] *Modified from Varró, Baczkó 2010* [44]

3.2.3.4 Functional circus-type reentry

Electrical activation initiated by regular stimuli spreads normally throughout the tissue. In contrast, an impulse initiated by premature stimuli only propagates in the direction of shortened refractory periods and does so at a reduced conduction velocity. The unidirectional block of the premature impulse is caused by spatial dispersion in the refractory periods. [41]

To explain the properties of a single functional re-entrant circuit, Allessie and colleagues formulated the “leading circle” concept. The leading circle was defined as the smallest possible pathway in which the impulse can continue to circulate, in which the stimulating efficacy of the wavefront is just enough to excite the tissue ahead which is still in its relative refractory phase; thus the head of the circulating wavefront is continuously biting its tail of refractoriness, and the length of the reentrant pathway equals the wavelength of the impulse. [1]

3.2.3.5 Spiral wave activity

The leading circle concept was based on properties of impulse propagation in a one-dimensional tissue that forms a closed pathway (e.g., a ring). Spiral waves typically describe reentry in two dimensions, [1] and the three-dimensional equivalent of a spiral wave is a "scroll wave". A spiral wave is a two-dimensional wave of excitation emitted by a self-organizing source of functional reentrant activity, termed "rotor". [41]

Propagation of two- and three-dimensional waves depends on wavefront curvature, a property that is not present in one-dimensional preparations. The curvature of an activation wavefront influences the source-sink balance: flat wavefronts have source-sink balance (each cell activates one cell downstream), whereas convex wavefronts have a smaller source and a larger sink (each cell activates more than one cell downstream). Therefore, this source-sink mismatch decreases the depolarizing current available for each downstream cell, resulting in a smaller rate of voltage rise, hence a smaller conduction velocity than that of a planar wave. [1,41] As curvature of a wavefront increases, conduction velocity decreases; with sufficient curvature, propagation fails. Because the maximal velocity of a convex rotating wavefront can never exceed the velocity of a planar wavefront and the period of rotation remains constant in a stable rotating wave, the velocity has to decrease from the periphery (where the highest value corresponds to linear velocity) to the centre of a rotating wave. As a consequence, any freely rotating wave has to assume a spiral shape. The curvature of the rotating spiral waves progressively increases (and the conduction velocity progressively decreases) toward the tip near the spiral centre (the core). At the tip the convex curvature reaches a critical value, forming a singularity point (rotor) that organizes the reentrant spiral wave activity. At the singularity point the curvature is so extreme that makes it impossible for the activity to invade the core. Therefore, instead of moving farther into the centre, the rotor spins in the myocardium at high speed around a core of unexcited tissue, organizing the electrical activity around it in the form of spiral waves. [1]

Spiral waves are not fixed in space but can drift through the tissue away from their origin [41]. This depends on the electrical (ex. wavelength) and structural (ex. fibrosis) properties of the tissue in which they occur. Monomorphic VT results when the spiral wave is anchored within the ventricular myocardium and cannot

drift away from its origin. In contrast, a polymorphic VT, such as the torsades de pointes (TdP) encountered with LQTS, caused by a drifting spiral wave. VF seems to be the most complex representation of rotating spiral waves in the heart: VF occurs when the single spiral wave responsible for VT breaks up (ex. after meeting an anatomical or functional obstacle), leading to the development of multiple meandering daughter spiral waves that are continuously extinguished and recreated, resulting in disordered electrical activity. [1]

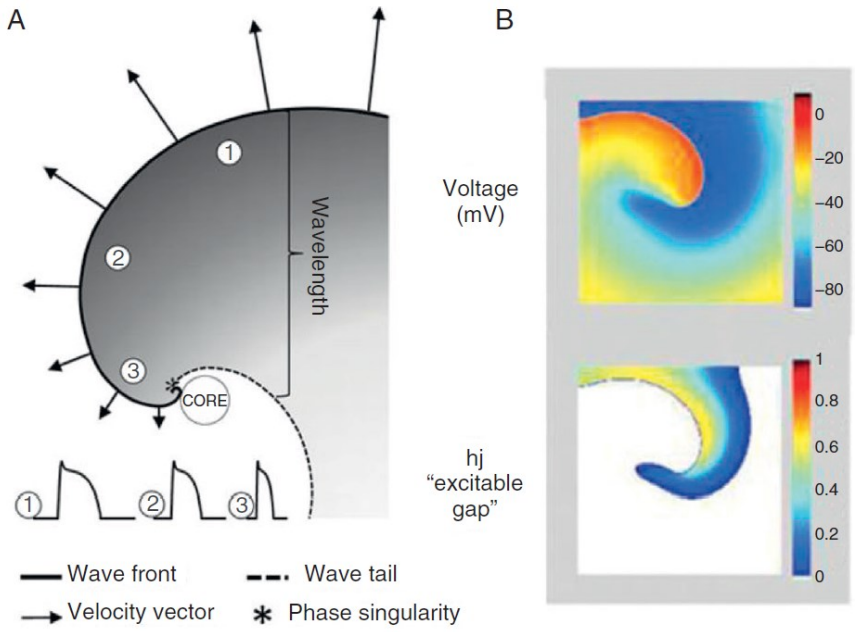

Figure 14 *(A) Snapshot of the spiral wave: electrotonic effects of the core decrease conduction velocity (arrows), action potential duration (representative examples shown from positions 1, 2, and 3), and wavelength (the distance from the wavefront [black line] to the wave tail [dashed line]). Conduction velocity decreases and wavefront curvature becomes more pronounced, near the rotor, which is a phase singularity at the point where the wavefront and the wave tail meet (asterisk). (B) Computer simulation of reentry. Top, Snapshot of the transmembrane voltage distribution during simulated reentry in chronic atrial fibrillation conditions in a two-dimensional sheet incorporating human atrial ionic math models. Bottom, Snapshot of inactivation variables of sodium current (hj) during reentry. Text from* [1]*. Image: modified from Pandit et al. 2013*[45]

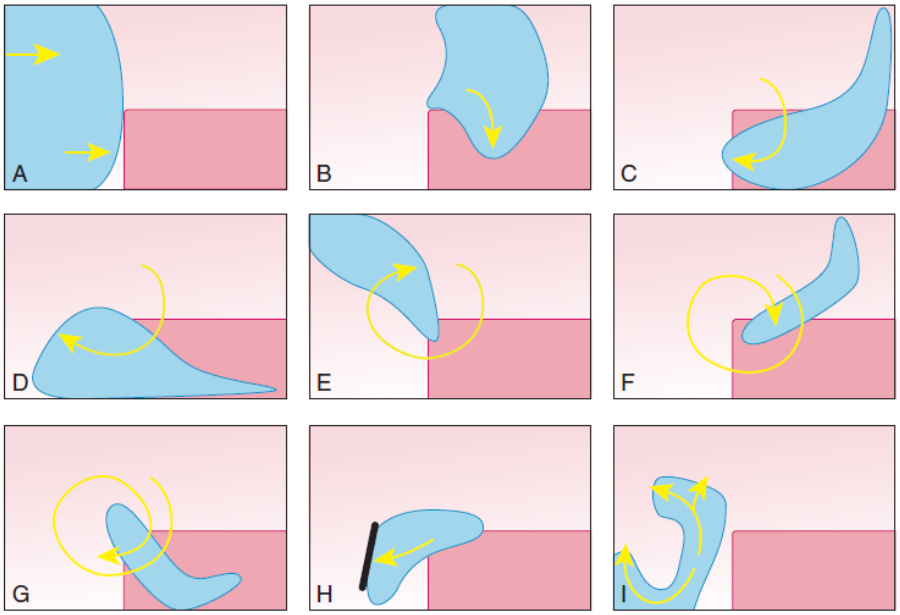

Figure 15 *Spiral wave reentry. The area of blue represents an excitation wave of depolarization. (A) A wave front propagates from left to right and encounters a region of incompletely recovered tissue (dark red region). (B) The wave front propagates along the margin of refractory tissue until it reaches recovered tissue and propagates inferiorly (C). (D) to (G) The wave front continues re-entering and establishing a circuit that continues to spiral through the tissue (yellow arrow). (H) The spiral wave encounters a region of block (black line), which splits the wave front (I). Multiple potential wave fronts can be generated, thereby leading to fibrillation. From Stevenson, 65 - Ventricular Arrhythmias, Goldman's Cecil Medicine (24th edition), W.B. Saunders, 2012* [46].

3.3 QT Interval

3.3.1 Definition

On a standard ECG, the QT interval is the time from the start of the Q wave to the end of the T wave, and it represents the period of electrical depolarization and subsequent repolarization of the ventricles [8,47].

3.3.2 Measurement

The QT interval is typically measured in leads II and V5, as they usually have the largest T-wave amplitude or longest QT interval (which is well known to vary in the different leads of the same ECG) interval [48]; in alternative, leads I and V6 can be used. The QT interval can be measured either manually or automatically, and the manual measurement is the most used. The measurement of the QT interval is subjective because the end of the T wave can be difficult to identify accurately (since it usually merges gradually with the isoelectric line), and is affected by its morphology and by the eventual presence of the U wave. [8,49] The end of the T wave is usually measured with the tangent method (according to which, the end of the T wave is determined by the intersection between the isoelectric line and the tangent to the T wave at the point of maximum downward slope) or the threshold method (according to which the end of the T wave is determined as the point where the T wave merges with the isoelectric line) (see *Figure 16*) [8]. When the U wave is present, most studies suggest including it in the measurement of the QT interval when large, and to exclude it when small [48]. The exact significance of the U wave is not clearly understood, but is thought to represent repolarization of Purkinje fibres [50].

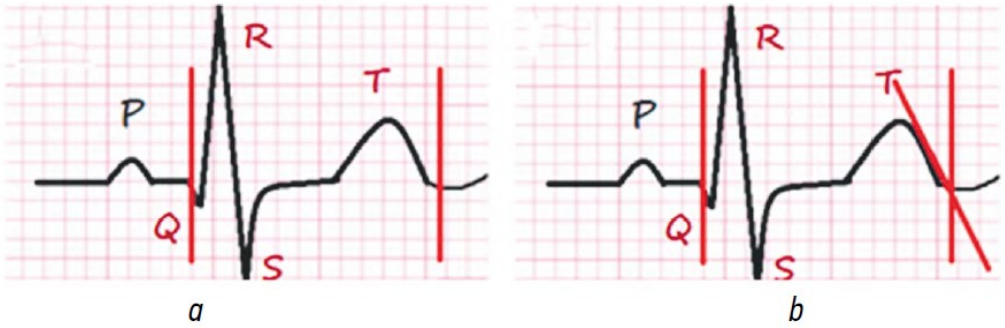

Figure 16 *Measurement of the QT interval - a) threshold method - b) tangent method. From Ardashev et al. 2022* [8]

3.3.3 Correction for Heart Rate

QT interval duration is influenced by the heart rate (RR interval): the QT interval shortens as the heart rate increases and vice versa, because the duration of the repolarization phase is affected by the preceding diastolic interval (a concept known as "action potential duration restitution"). [51] The ion channel mechanism of APD restitution is thought to be the incomplete recovery and/or deactivation of different inward (I_{Na}, I_{CaL}) or outward (I_{to}, I_{Ks}, I_{Kr}) currents [2]. Therefore, the QT interval can be corrected for heart rate (QTc) in order to increase the reliability of the measurements and to facilitate the comparison of QT intervals measured at different heart rates [8,52]. The corrected QT interval (QTc) corresponds to the predicted value of the measured QT interval at a reference HR of 60 bpm (RR interval of 1 s) [52].

The first correction formula was proposed in 1920 by H. Bazett ($QTc = QT/\sqrt{RR}$) (QTc equals QT interval in seconds divided by the square root of the preceding RR interval in seconds) [8,52]. The reference is the *preceding* RR interval because the action potential duration depends on the *previous* diastolic interval (APD restitution). Bazett's formula works more precisely in the heart rate range 60-100 bpm, while it gives inaccurate results both at slow heart rates (< 60 bpm, excessive correction) and at fast heart rates (> 100 bpm, insufficient correction) [8,52].

Fridericia proposed and alternative correction formula using the cube-root of RR ($QTc = QT/\sqrt[3]{RR}$); this formula as well overcorrects below 60 bpm, but is more accurate at fast heart rates (> 100 bpm) [52].

Over the years, various correction formulas were developed to overcome these inaccuracies, such as Sagie, Hodges, Rautaharju, Dmitrienko, Ashman, etc. (see *Table 1*).

Correction formulae are exponential (Bazett, Fridericia), logarithmic (Ashman), linear (Sagie, Hodges, Rautaharju), or mixed (Dmitrienko).

Table 1 QT correction formulas

Formula		Comment
Bazett	$QTcB = QT/\sqrt[2]{RR}$	Exponential
Fridericia	$QTcF = QT/\sqrt[3]{RR}$	
Sagie (Framingham)	$QTcFra = QT + 0.154\,(1 - RR)$	Linear
Hodges	$QTcH = QT + 1.75\,(HR - 60)$	
Ashman	$QT = K1 \times \log(10 \times [RR + K2])$	Logarithmic
Dmitrienko	Mixed effects modelling formula	Mixed

QTc, corrected QT interval; RR, R-R interval; HR, heart rate; K1 and K2 are constants correcting for age and sex.

However, there is no general consensus on which is the best correction formula for clinical practice. Of note, most formulas provide comparable results in resting conditions, with heart rates between 60 and 90 bpm [8,52]. At the present day, Bazett formula is still the most commonly used both in clinical practice and in research (due to its simplicity and reliability), and Fridericia is widely used in subjects with tachycardia (above 100 bpm) [8,52].

3.3.4 Gender differences

The QT interval shortens during puberty in boys because testosterone enhances I_{Ks}, while in girls the QT interval is prolonged by estradiol-mediated reduction of K^+ currents [8,53]. This difference goes from 12-15 ms in the young, decreases to 6-10 ms in middle age, and practically levels out in old age (because of the fall of estradiol levels with menopause, and the fact that the age-related increase in QT interval duration is more pronounced in men than in women). Thus, in young and middle-aged women QT interval is longer than in men of the same age. [8,53]

3.3.5 QT interval and aging

The QT interval increases with age because of age-related myocardial changes, including the development of fibrosis, and age-related changes in sympathovagal balance; moreover, older patients usually take more drugs that can cause QT prolongation compared to younger subjects [8].

3.3.6 QT interval and bundle branch block

The QRS interval can be modified by several factors (such as bundle branch blocks). These changes in depolarization propagation can alter repolarization, both by delaying cycle initiation for certain areas, and by a direct effect on ion movement (affecting stretch-activated channels); thus, in this case, the QT interval may not be an accurate reflection of repolarization duration [52,53].

3.3.7 Normal and abnormal intervals

Reference values for QTc are presented in *Table 2* [52]. Bazett's formula has been used more frequently in medical publications than Fridericia's formula. Therefore, most reported criteria for normal and abnormal values for QTc are derived from Bazett's formula [52].

Table 2 QTc value by Age and Gender (Bazett Formula) [52]

QTc value	1-15 years	Males	Females
Normal	< 440 ms	< 430 ms	< 450 ms
Borderline	440-460 ms	430-450 ms	450-470 ms
Prolonged	> 460 ms	> 450 ms	> 470 ms

QTc, corrected QT interval (Bazett's formula)

3.3.8 QT interval prolongation and Long QT Syndrome (LQTS)

Abnormal prolongation of the QT interval is reflective of delayed ventricular repolarization [1]. Prolongation of the QT interval is caused by a decrease in outward positive (repolarizing) currents (I_{Ks}, I_{Kr}, I_{K1}, I_{KACh}), or an increase in inward positive (depolarizing) currents (I_{Na}, I_{CaL}) during phase 2 and 3 of the cardiac AP, which can

be the result of genetic mutations (affecting cardiac ion channels or proteins modulating their function, or their intracellular trafficking) – congenital LQTS, or the effects of acquired conditions [1,53,54].

QT interval prolongation is a known risk factor and independent predictor of ventricular tachyarrhythmias, syncope, and sudden cardiac death (SCD) [55,56]. Excessive QT interval prolongation predisposed to arrhythmogenesis due to asynchronous repolarization of different areas of the ventricular myocardium and increase in the general length of repolarization, which induce early afterdepolarizations and spatial dispersion of refractoriness (i.e., trigger and substrate for reentry, respectively). [8]

In *Tables 3* and *4* are presented the congenital/genetic syndromes as well as some acquired conditions associated with QT prolongation.

Table 3 Congenital LQTS and related genetic mutations [53,57]

Syndrome	Gene	Function/Comments
LQTS1*	KCNQ1	Kv7.1 Alpha subunit of the slow delayed rectifier K^+ channel – I_{Ks} potassium current
LQTS2*	KCNH2/hERG	Kv11.1 Alpha subunit of the rapid delayed rectifier K^+ channel – I_{Kr} potassium current
LQTS3*	SCN5A	Nav1.5 Alpha subunit of the cardiac Na^+ channel – I_{Na} late sodium current
LQTS4	ANKB	Ankyrin beta anchors the ion channels to the cytoskeleton; mutations increase Ca^{2+} and Na^+ currents
LQTS5	KCNE1	MinK (beta – regulatory – subunit of I_{Ks})
LQTS6	KCNE2	MiRP1 (beta – regulatory – subunit of I_{Kr})
LQTS7	KCNJ2	Kir2.1 Alpha subunit of inward rectifier K^+ channel – I_{K1} potassium current
LQTS8	CACNA1	Cav1.2 Alpha subunit of the long-type Ca^{2+} channels – I_{CaL} calcium current
LQTS9	CAV3	Caveolin 3 (scaffold protein, important for assembly of membrane proteins). Mutations lead to increased Nav1.5 function (I_{Na} current)
LQTS10	SCN4B	Beta subunit of cardiac sodium channels (I_{Na} current)

LQTS11	AKAP9	A-kinase anchor protein 9 (binds to the regulatory subunit of protein kinase A, which is involved in adrenergic receptor signal transduction, and interacts directly with Kv7.1 (I_{Ks} current)
LQTS12	SNTA1	Alpha-1-syntrophin (cytoskeletal protein, which interacts with Nav1.5) (increased I_{Na} current)
LQTS13	KCNJ5	GIRK4, G protein-sensitive inwardly rectifying potassium channels (Kir3.4), which carry the potassium current I_{KACh}
LQTS14-16	CALM1/2/3	Calmodulin-1/2/3, Ca-binding messenger, interacts with I_{CaL} current

LQTS, long QT syndrome; * LQT1, LQT2, and LQT3 account for more than 90% of all inherited LQTS cases.

Table 4 Acquired causes of QT prolongation

Cause	Comments
Drugs	Various antimicrobial, psychoactive, antiarrhythmics, diuretics, antihistamines, antitumoral drugs, through various mechanisms such as a direct action on cardiac ion channels, electrolyte imbalances, etc. [53]
Inflammatory conditions	Inflammatory cytokines influence the expression of cardiac ion channels; hence, inflammatory conditions change cardiac ion channels expression, leading to action potential prolongation. Also production of ROS cause QT prolongation [53]
Obesity	Cardiac structural and electrical remodelling, autonomic nervous system imbalance with chronic sympathetic overactivity, and additive effect of obesity-related comorbidities. [58,59]
Diabetes	Metabolic abnormalities such as hyperglycaemia, hyperlipidemia, and decreased GLP-1 levels cause: activation of RAAS, cardiac autonomic neuropathy, alterations of calcium homeostasis, myocardial hypertrophy and fibrosis, and oxidative stress (which causes disfunction of hERG channel – I_{Kr} potassium current). Insulin resistance is associated with defective inactivation of I_{CaL} (through decreased expression of Cav 1.2 and calmodulin). Hyperinsulinemia causes I_{Ks} current suppression. [60]
Hypertension	Anatomical remodelling of the heart (LV hypertrophy, fibrosis), alterations of the cardiac autonomic nervous system tone. [61]
Elevated lipid profile	Modulation of cardiac ion channels function and expression, modulation of ANS activity, lipotoxicity. [58,59]
Heart Failure	Reduced I_{Kr} and increased late I_{Na} currents, intramyocardial Ca^{2+} overload [53]

Renal failure	Electrolyte disturbance, metabolism disorders, cardiac autonomic neuropathy, uremic toxin accumulation, hemodialysis, hypertension, and myocardial hypertrophy. [60]
Liver failure	Cardiac autonomic neuropathy (CAN) - enhanced sympathetic activity; cardiac remodelling (cirrhotic cardiomyopathy); cardiac calcium channel dysfunction. [62]
Female sex	Effects of sex hormones on ionic currents. Estradiol inhibits cardiac potassium currents (whereas testosterone enhances I_{Ks} and inhibits I_{CaL})
Age	Changes in sympathovagal balance, development of myocardial fibrosis, other mechanisms affecting various organs [8]
Hypokalaemia	Mimics effects of potassium channel mutations
Hypocalcaemia	Reduces the negative feedback of intracellular Ca^{2+} on long-type calcium channels (I_{CaL}), prolonging their open state
Hypomagnesemia	Reduced magnesium inhibition of calcium release from the sarcoplasmic reticulum, reduced activity of NA/K ATPase (Mg^{2+} is a cofactor), and reduced potassium efflux via I_{K1} channels
Ischaemia	Activation of sodium/hydrogen exchangers, other effects on various ion channels
Hypothyroidism	Decreased expression and activity of calcium ATPase and phopholamban, thus increasing intramyocardial Ca concentration during the repolarization phase
Bradycardia	Explained by the normal APD restitution curve. Relevant if concomitant use of torsadogenic medications or LQTS3 (congenital bradycardia-associated LQTS)
Hypothermia	Calcium ion channel aberrations
Starvation	Electrolyte imbalances

ROS, reactive oxygen species; GLP-1, glucagon-like peptide-1; RAAS, renin-angiotensin-aldosterone system; LV, left ventricle; ANS, autonomic nervous system; APD, action potential duration; LQTS, long QT syndrome.

3.4 Long QT syndrome

Long QT syndrome (LQTS) is a condition characterized by abnormally prolongated QT interval *and* increased propensity to life-threatening ventricular arrhythmias, leading to syncope and sudden cardiac death [1,54]. In LQTS there is an excessive and *heterogeneous* prolongation of the repolarization phase of the ventricular AP [1,63]. LQTS is the major cause of sudden cardiac death (SCD) among subject without structural heart disease, and accounts for 10-20 % of all SCDs [1,53]. LQTS can be congenital or acquired; the prevalence of congenital LQTS is estimated to be 1 in 2500 live births [64], and that of acquired LQTS is estimated to be 25-30% in hospitalized populations [65].

3.4.1 Diagnosis of LQTS

Diagnosing LQTS can be difficult for various reasons. Firstly, the QT interval is highly variable in both healthy subjects and LQTS patients, with significant overlap between: about one third of patients with proven LQTS genetic defect have resting QTc intervals < 440 ms, and approximately 10-15% of healthy people have QTc values ≥ 440 ms [8,66]. Moreover, up to 50% of patients with LQTS have a nondiagnostic QTc at rest (either normal or borderline) [67]. This is due to a combination of variable penetrance of LQTS and individual variability in QT interval duration [63]. Secondly, arrhythmia-related symptoms almost invariably occur in unmonitored settings, and up to one third of patients remain asymptomatic [1,68]. Lastly, genetic testing has the greatest value for a definitive diagnosis, but it still has some limitations: it cannot be applied routinely to every patient, and it can often be incomprehensive, costly, or unavailable) [1,68].

Therefore, the diagnosis of LQTS relies on resting QTc, some other ECG parameters (such as the presence of T wave abnormalities or T wave alternans), clinical history (symptoms such as palpitations, presyncope, syncope, or cardiac arrest), family history, and in some cases also genetic testing; furthermore, provocative manoeuvres (such as brisk standing, exercise testing, and adrenaline infusion) are widely used in clinical practice to unmask "concealed" forms of LQTS with undiagnostic (normal or borderline) QTc interval at rest [1,54,69].

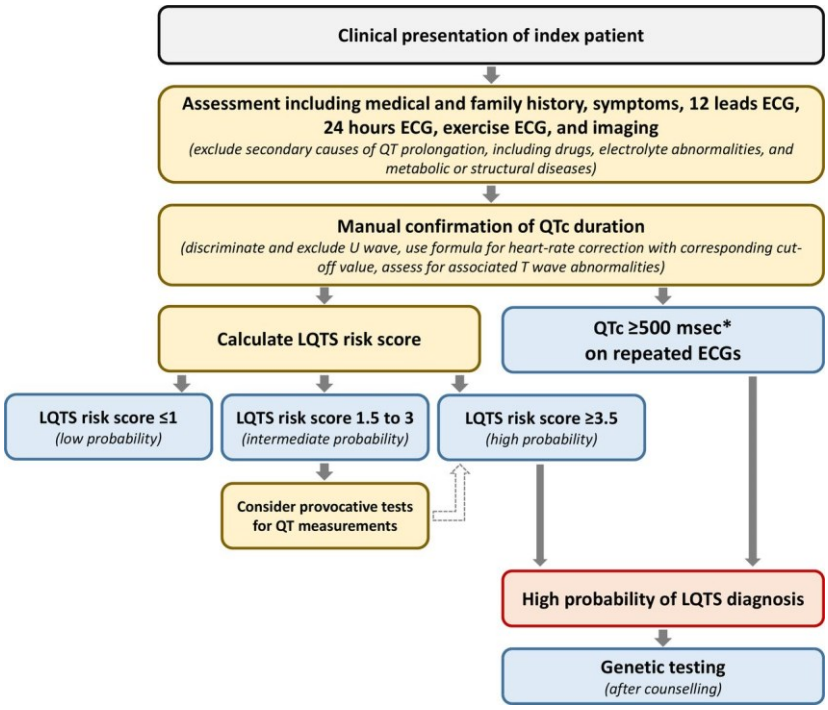

Figure 17 *Schematic flow chart for the diagnosis LQTS, following the Heart Rhythm Society consensus document from 2013* [70]*. * In the ESC 2015 guidelines a QTc ≥ 480 ms is sufficient, for HRS is required QTc ≥ 500 ms. Image taken from Wilde et al. 2022* [54]*.*

According to the European Society of Cardiology (ESC) 2015 guidelines [71], LQTS is diagnosed if one of the following criteria is satisfied:

- QTc ≥ 480 ms (at rest) and asymptomatic
- QTc ≥ 460 ms (at rest) in presence of unexplained syncope
- Schwartz score > 3
- Positive genetic testing (regardless of QT interval)

According to the Heart Rhythm Society (HRS) 2013 guidelines [70], LQTS is diagnosed if one of the following criteria is satisfied:

- QTc ≥ 500 ms (at rest) and asymptomatic
- QTc ≥ 480 ms (at rest) in presence of unexplained syncope
- Schwartz score > 3
- Positive genetic testing (regardless of QT interval)

Schwartz criteria are given in *Table 5* [72].

A diagnosis of LQTS is given with a Schwartz score of ≥ 3.5 points, intermediate probability of LQTS by a Schwartz score between 1-3.5 points, and a low probability of LQTS by a Schwartz score of ≤ 1 point.

Table 5 Schwartz score (diagnostic criteria for LQTS) [72]

		Points
Electrocardiographic findings		
QTc at rest (calculated by Bazett's formula)	≥ 480 ms	3
	460-479 ms	2
	450-459 ms *and* male sex	1
QTc 4th min of recovery from exercise test	≥ 480 ms	1
Torsade de Pointes*		2
T-wave alternans		1
Notched T wave in 3 leads		1
Low resting heart rate	Below 2nd percentile for age	0.5
Clinical history		
Syncope*	With stress	2
	Without stress	1
Congenital deafness		0.5
Family history		
Family members with definite LQTS		1
Unexplained SCD before age 30 among immediate family members		0.5

Diagnostic criteria for long QT syndrome (LQTS) (the 'Schwartz-score'). In the family history rows, the same family member cannot be counted in both categories. * Torsade de Pointes and syncope are mutually exclusive.

3.4.2 Pathophysiology of arrhythmia in LQTS

The following *Figure 18* gives an overview over the pathophysiology underlying arrhythmia in LQTS.

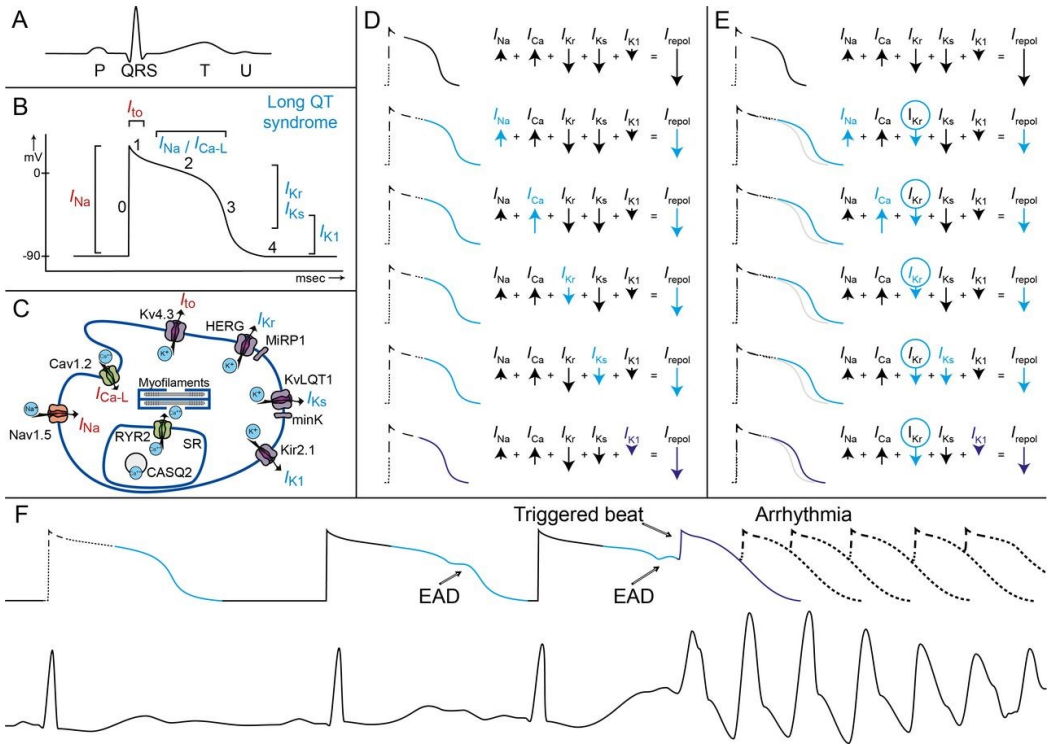

Figure 18 *Pathophysiological mechanisms underlying LQTS and the associated arrhythmia. From Wilde et al. 2022* [54].

(Figure 18A) shows a standard ECG. (*Figure 18B)* shows the corresponding ventricular action potential (AP) and cardiac ion currents (I) responsible for its different parts [54]. (*Figure 18C)* shows a cardiomyocyte with the different ion channels and their currents; the ion channels involved in most forms of LQTS are phase 2 late sodium inward current (I_{Na}) and calcium inward current (I_{CaL}), or phase 3 and 4 potassium rectifier currents (I_{Kr}, I_{Ks}, I_{K1}) [54]. (*Figure 18D)* shows how changes in one of the repolarizing currents (in blue), by a decrease in the net repolarising current (I_{repol}), cause prolongation of the AP: if any of the repolarizing currents is altered (ex. by a mutation) the ventricular AP (and the corresponding QT interval) will lengthen [54]. (*Figure 18E)* shows how a second hit on the net repolarising current (for example, a further decrease of I_{Kr} or I_{Ks} current due to the use of certain drugs) further lengthens the ventricular AP and the QT interval [54]. In (*Figure 18F)* the prolongated ventricular AP (and the corresponding QT interval) is further challenged (ex. by changes in heart rate induced by an adrenergic trigger),

resulting in early afterdepolarizations (EADs); when EADs reach threshold for Na^+ channels opening they trigger a beat, which initiates reentry, and degenerates into malignant ventricular arrhythmia (Torsade de Pointes, TdP) [54]. Furthermore, excessive transmural heterogeneity of repolarization provides the substrate for unidirectional block and functional reentry circuits to propagate TdP [1].

QT prolongation *per se* is not sufficient for the occurrence of arrhythmia in LQTS, but other factors are needed; indeed, there is no identifiable QT prolongation cutoff associated with the occurrence of TdP [53]. Prolonged repolarization, transmural dispersion of repolarization, and early afterdepolarizations (EADs) are the three electrophysiological components thought to be at the basis of TdP in LQTS [1]. The excessive increase in the action potential duration (APD) favours the generation of EADs because of reactivation of L-type Ca^{2+} channels and increased activity of the Na^+/Ca^{2+} exchanger; EADs can cause PVCs that can potentially trigger the initiation of ventricular arrhythmias [1]. Furthermore, excessive repolarization heterogeneity provides the substrate for unidirectional block and functional reentry circuits to propagate TdP. [1]

Adrenergic triggers, particularly exercise and swimming, are the most important triggers for arrhythmic events in LQT1, whereas in LQT2 sudden arousal (ex. auditory stimuli) is predominant; events in LQT3 occur most frequently at rest (at lower heart rates). [54]
(Anyway, induction of arrhythmias during exercise is rare in LQTS patients: exercise-induced ventricular ectopy beyond isolated PVCs is observed in less than 10% of patients [1]).

These genotype-specific characteristics explain why β-blockers efficacy is not the same in all LQTS genotypes: β-blockers are highly effective in preventing arrhythmic events in LQT1 patients, but are less effective in LQT2 compared to LQT1, and even less effective in LQT3. LQT3 patients are most sensitive to (late) sodium channel current blockers. [1,54]
Because genotype-specific features have an impact on prognosis and therapy, genetic testing is an important part of the diagnosis and management of LQTS patients. [54]

3.4.3 T wave abnormalities in LQTS

The transmural dispersion of repolarization (TDR) across the ventricular wall is largely responsible for both morphology and duration of the T wave on the ECG [6]. Epicardial cells are the first to repolarize, and M cells are the last; thus, T-wave-peak corresponds to the end of epicardial cells repolarization, and T-wave-end corresponds to the end of M cells repolarization [1,6]. Moreover, the opposing currents flowing adjacent to M cells play a role in determining duration and amplitude (height) of the T wave, and also the degree to which either the ascending or descending limb of the T wave is interrupted, causing a bifurcated or notched appearance [6]. This, together with the fact that APD-prolonging agents increase the degree of repolarization heterogeneity (having a disproportionately larger effect on M cells), explains the T wave abnormalities found in LQTS.

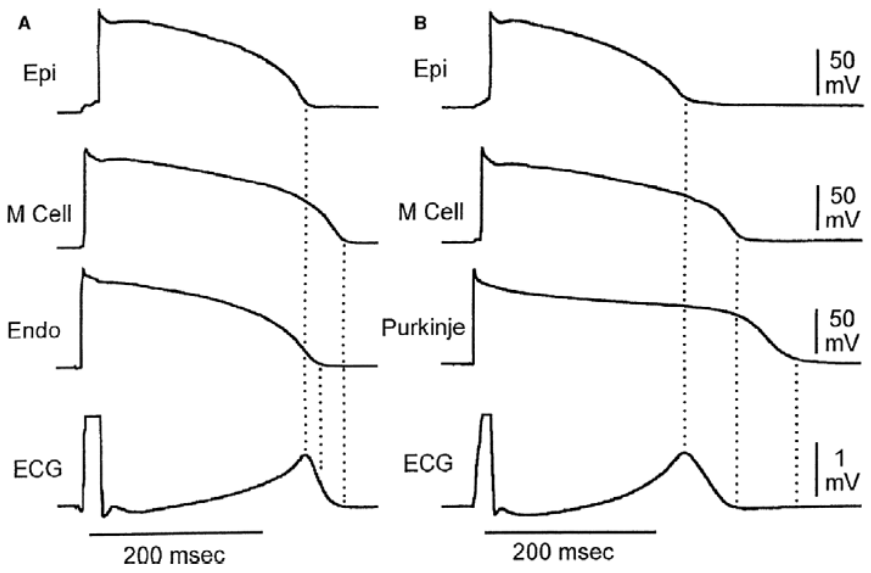

Figure 19 *Cellular basis of T wave inscription. Here is shown the temporal relationship between AP recorded from epicardial, midmyocardial M cells, and endocardial (A) or subendocardial Purkinje fibres (B); note that M cells repolarization is aligned with the end of the T wave, and epicardial cells repolarization is aligned with the peak of the T wave [6]. From Yan et al. 1998 [7].*

T wave abnormalities are frequent in patients with LQTS, and some are genotype-specific (see *Figure 20)*. LQT1 patients commonly present smooth broad-based T waves, particularly in the precordial leads; LQT2 patients often have low-amplitude, notched or bifid T waves; and LQT3 patients commonly display late-onset, narrow, peaked, and/or biphasic T waves with a prolongated isoelectric ST segment [1].

Abnormal T-wave morphology is augmented in LQTS patients during exercise testing or abrupt postural changes [63] (see later, *3.5 Provocative manoeuvres*).

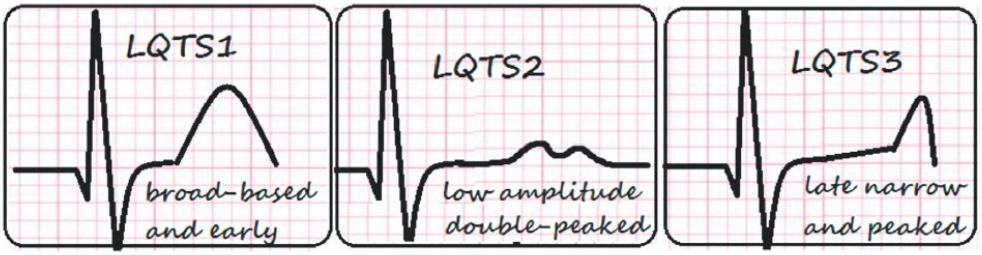

Figure 20 *T wave abnormalities in LQTS1, LQTS2, and LQTS3.. From Ardashev et al 2022* [8].

T wave abnormalities can also be observed in other patient populations without congenital LQTS, in which LQTS-like T-wave abnormalities likely seem to represent increased arrhythmic risk (because T wave abnormalities underlie an increased ventricular repolarization heterogeneity) [6].

Furthermore, recent studies reported an association of prolonged Tpeak-Tend duration with a high risk for developing TdP in patients with both acquired and congenital long QT syndromes [8] (see *3.1.3 Transmural dispersion of repolarization*).

3.4.4 Torsades de Pointes

Torsades de pointes (TdP) is a polymorphic VT occurring in the setting of pathological QT interval prolongation (acquired or congenital LQTS) [1]. TdP is characterized by a progressive change of the electrical axis, typically rotating 180 degrees in 10 to 12 cycles; this results in the characteristic sinusoidal "twisting of the peaks" of QRS complexes around the isoelectric line, hence the name "torsade de pointes" [1]. The heart rate is usually 150 to 300 beats/min. In many cases, TdP is a self-limiting arrhythmia; nevertheless, most patients experience multiple episodes in rapid succession [1]. Only in a minority of cases TdP degenerates in ventricular fibrillation (VF) which, almost without exception, leads to SCD if immediate intervention is unavailable [1]. See *3.2.3.5 Spiral wave activity* for the mechanism.

3.4.5 Principles of management of LQTS

The main therapeutic modalities for the prevention of life-threatening cardiac events in LQTS patients include β blockers (in particular propranolol and nadolol), left stellate gangliectomy, ICD implantation, lifestyle modifications (avoidance of arrhythmic triggers) and avoidance of QT-prolonging drugs. Beta blockers are the mainstay therapy in non-genotyped patients and patients with LQT1 or LQT2 genotype, whereas left stellate gangliectomy and ICD implantation are therapeutic options for high-risk patients who remain symptomatic or have recurrent cardiac events despite beta blocker therapy. [1,69]

3.5 Provocative manoeuvres

Provocative manoeuvres (such as brisk standing and exercise testing) can be used to unmask "concealed" forms of LQTS with undiagnostic QTc interval at rest, or to rule out persons with borderline QTc at rest but normal QT interval adaptation to exercise or sudden heart rate changes (ex. athletes); thus they are widely used in the evaluation of patients with suspected LQTS [1,48,67,68,73–75] .

3.5.1 Brisk standing test

Patients with LQTS have inadequate QT interval shortening in response to the sudden heart rate accelerations provoked by abrupt standing (exaggerated "QT stretching"), and abnormal persistence of QTc prolongation as the heart rate slows back to baseline ("QT stunning"); these two phenomena are of diagnostic value in LQTS and reflect an impaired QT interval adaptation in response to changes in the autonomic tone [48,63,68,73,74,76,77].

The brisk standing test protocol proposed by Adler, Viskin, and colleagues [68] is the following: "*Subjects rested for 10 minutes in the supine position as a baseline ECG was recorded. They were then asked to stand up quickly and remain standing still for 5 minutes during continuous ECG recording. QT measurements were performed at 4 points in time: (1) baseline (QT_{base}), (2) maximal heart rate (QT_{maxHR}), (3) point of maximal "QT stretching" ($QT_{stretch}$) (defined as the time when the end of the T*

wave gets nearest to the next P wave due to R-R–interval shortening without sufficient QT-interval shortening), and (4) upon return of the heart rate to its baseline value (QT_{return}) (defined as the first R-R interval within 40 ms of the baseline R-R interval) [*(Figure 21)*]. *At all points, the QT interval was corrected using the Bazett and Fridericia formulas*" [68,73].

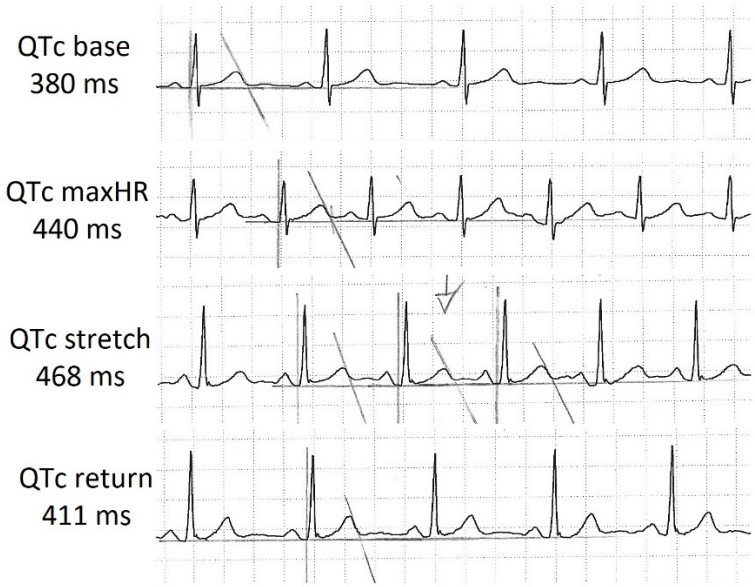

Figure 21 *ECG highlighting QT stretching and QT return to baseline in response to brisk standing.*

In response to brisk standing, the heart rate acceleration is abrupt but the associated QT interval shortening is only gradual: as the R-R interval shortens faster than does the QT interval, the QT appears to "stretch" toward the next P wave, and the corrected QT interval (QTc) for heart rate actually increases [68]. This phenomenon (called "QT stretching") is universal but is exaggerated in patients with LQTS. The heart rate acceleration in response to abrupt standing is similar between LQTS patients and healthy subjects, but their QT interval response is significantly different: on average, as the heart rate increases, the uncorrected QT interval shortens in healthy subjects, whereas it fails to shorten or even increases in LQTS patients [68,73]. Consequently, since the RR interval shortens more than does the QT interval (in either groups), the QTc increases both in healthy subjects and LQTS patients, but is significantly more pronounced in LQTS patients [68,73]. Indeed, the QTc measured at the point of maximal QT stretching ($QTc_{stretch}$) has a high discriminative power for diagnosing LQTS: a $QTc_{stretch}$ cutoff of 490 ms yields high sensitivity and specificity (90% and 86%, respectively) [68,73]. Viskin and colleagues (2010) proposed the measurement of the QTc at maximal stretching after standing

as a tool to "unmask" latent QT interval prolongation in LQTS patients without overt QTc prolongation at baseline [73].

A similar sequence of events takes place as the heart rate returns to baseline: the heart rate deceleration is faster than the associated QT interval lengthening [68]. The heart rate deceleration is similar between LQTS patients and healthy subjects, but their QT interval response is significantly different: on average, as the heart rate returns upon baseline values, QT_{return} is slightly shortened in healthy subjects in comparison with QT_{base}, while it is increased in LQTS patients [68]. Healthy patients may have a QT_{return} longer than QT_{base}, but the magnitude of this difference is significantly smaller than that in LQTS patients [68]. The abnormal persistence of QTc prolongation as the heart rate slows back to baseline after brisk standing is called "QT stunning"; Adler and colleagues found that QTc_{return} differentiates between LQTS patients and healthy controls as reliably as $QTc_{stretch}$ (a QTc_{return} cutoff of 435 ms yielded 90% sensitivity and 84% specificity) [68].

Table 6 Response to standing and return to baseline [68]

	Healthy subjects	LQTS patients
ΔHR during maximal HR (ms)	26 ± 10	-25 ± 10
ΔQT during maximal HR (ms)	-19 ± 26	-2 ± 37
ΔQTc during maximal HR (ms)	62 ± 39	92 ± 48
ΔQT during maximal QT interval stretching (ms)	-14 ± 35	8 ± 51
ΔQTc during maximal QT interval stretching (ms)	66 ± 40	103 ± 80
ΔQT upon return to baseline (ms)	-5 ± 28	22 ± 42
ΔQTc upon return to baseline (ms)	-3 ± 32	28 ± 48

ΔHR, ΔQT, and ΔQTc values (i.e., the variation of heart rate, uncorrected QT, and QTc from baseline) in response to brisk standing and upon return to baseline of the subjects studied in by Adler and colleagues in [68]. Data are presented as mean ± SD.

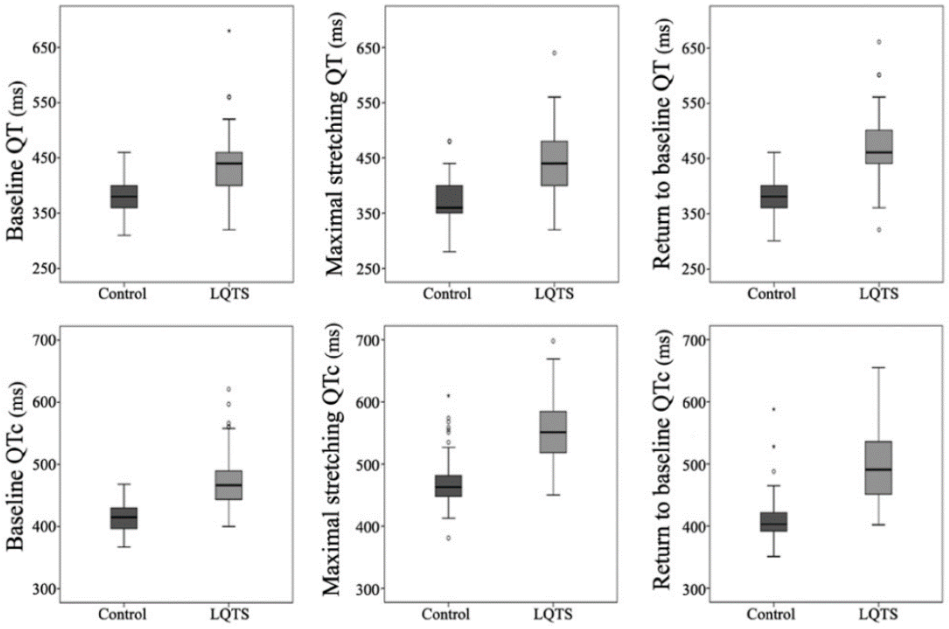

Figure 22 *Box plots of the results obtained in patients with long QT syndrome and controls. Dark boxes represent the interquartile range, the thick black line in the box is the 50th percentile, and the bars represent the range of results excluding outliers. Black dots are "outliers" and asterisks are "extreme outliers". Note that although there is a statistically significant difference between the QTc of patients and controls already at baseline, the magnitude of the difference increases and the overlapping between the groups decreases during the 2 stages of the test. Text and image from Adler et al 2012* [68].

On note, along with abnormal QTc prolongation at maximal stretching and upon return to baseline, LQTS patients often develop abnormal T waves (notched, biphasic, and flat) in response to brisk standing, with added diagnostic value [63,76].

QT prolongation after postural changes is greater in LQT2 than in LQT1: patients with LQT2 develop more QT prolongation than do patients with LQT1 both during maximal tachycardia after standing and when the heart rate slows back to baseline [48,68,73]. Indeed, in LQT2 patients the QT fails to shorten at these intermediate heart rates (the so-called "I_{Kr} zone", where I_{Kr} likely plays a role in dynamic action potential adaptation to the heart rate) because of attenuated I_{Kr} [1].

Interestingly, a few control subjects in the studies by Adler et al. 2012 [68] and Viskin et al. 2010 [73] demonstrated an exaggerated QT interval stretching and a QT stunning that were of the magnitude observed in the LQTS group; "rather than simply representing false positives, it is possible that these are persons with normal QT interval but impaired repolarization reserve" [73].

3.5.2 Exercise stress test

Exercise testing can be useful to assess QT interval adaptation to gradual heart rate acceleration, a measure of the integrity of the I_{Ks} channels [1], and thus it can be used to unmask patients with concealed LQTS, particularly LQT1, with good diagnostic accuracy [75].

The Bruce protocol, modified Bruce protocol, and gradual bicycle protocol are all recommended in exercise test guidelines [48]. Treadmill exercise testing was the most used in the studies under review.

In healthy subjects there is an initial decrease in their QTc at peak exercise with a gradual return to baseline with recovery [75].

Patients with LQT1 typically display attenuated QT shortening and exaggerated QTc prolongation during both early and peak exercise, and this maladaptive/paradoxical QTc prolongation persists during the recovery phase [1,75]. Genetic mutations in LQT1 result in reduction of I_{Ks} amplitude; I_{Ks} is the predominant repolarization current during periods of increased sympathetic activity (such as exercise), and thus has a major role in determining the rate-dependent shortening of the cardiac action potential at faster heart rates; attenuation of I_{Ks} in LQT1 results in failure of the QT interval to adapt (i.e., shorten) in response to increasing heart rate during exercise, and this paradoxical QTc prolongation persists during the recovery phase [1,75]. Unlike LQT1 patients, normal subjects, LQT2 patients, and LQT3 patients decrease their respective QTc intervals from rest at peak exercise, with a gradual return to baseline during recovery [1,75].

In contrast, patients with LQT2 have normal QT shortening and QTc decrease at peak exercise, but they characteristically present an exaggerated QT hysteresis [1,77]. Genetic mutations in LQT2 result in impairment of I_{Kr} channels; I_{Kr} channels are not as sympathetically responsive as I_{Ks}, and they likely contribute to the rate-dependent shortening of the cardiac action potential at intermediate heart rates (a so-called "I_{Kr} zone"), as during early exercise; because of attenuated I_{Kr}, in LQT2 patients the QT fails to shorten at the intermediate heart rates of early exercise; this is followed by recruitment of the unimpaired, sympathetically responsive I_{Ks},

resulting in appropriate QT shortening at faster heart rates through to peak exercise, which persists into the recovery phase [1,77]. This consequently leads to an exaggerated QT difference between exercise and recovery at comparable heart rates, which is manifested as increased QT hysteresis [1,77] . Interestingly, in LQT2 patients the QTc significantly increases towards the end of the recovery phase with a latency of about 3-4 minutes, after the initial drop at the beginning [48,75].

QT hysteresis is calculated as the difference between the QT intervals during exercise and 1 to 2 minutes into recovery at comparable heart rates (ex., when the heart rate accelerates to approximately 100 beats/min during early exercise, and 1 to 2 minutes into the recovery phase, when the heart rate typically decelerates to approximately 100 beats/min) [1,77]. QT hysteresis of ≥ 25 ms has a sensitivity and specificity of 73% and 68%, respectively, at identifying patients with LQT2 over LQT1. [1,77]

The LQT3 phenotype is characterized by supernormal QT shortening with exercise because of stimulation of the intact I_{Ks} channel and augmentation of late inward Na^+ current [1]; this QTc shortening during exercise is then followed by a gradual increase during recovery, approaching resting QTc values [75].

The following *Figure 23, 24* and *25*, show the results of the study by Horner et al. 2011 [75], where the authors compared the responses to treadmill exercise testing of LQTS patients with overt QTc prolongation at baseline vs patients with concealed LQTS vs healthy controls, also differentiating the responses of LQTS patients depending on their genotype.

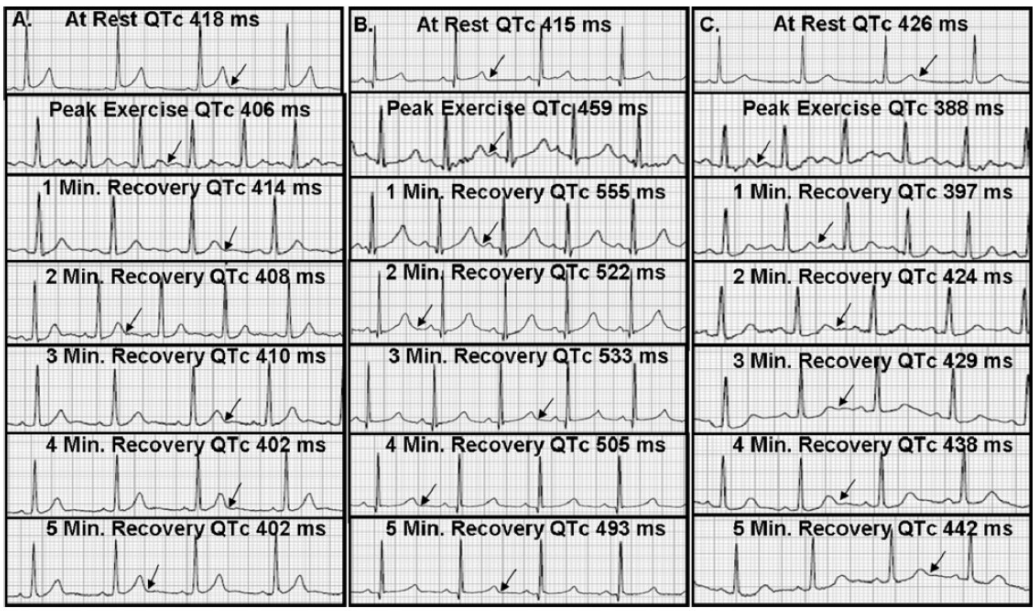

Figure 23 *Examples of the treadmill stress test profiles ECG tracings for controls (A), concealed LQT1 (B), and concealed LQT2 patients (C). Note that in the control patient there is an initial decrease in their QTc at peak exercise with a gradual return to baseline with recovery. In contrast, the concealed LQT1 patient initially lengthens during peak exercise and continues with maladaptive/paradoxical lengthening of QTc during recovering. Finally, the concealed LQT2 patient also displays an initial decrease in QTc at peak exercise; however, the patient continues to increase QTc during recovery beyond baseline. Text and image from Horner et al. 2011* [75].

QTc at peak exercise decreased in controls as well as in LQT2 and LQT3 patients compared to their baseline QTc; in LQT2 and LQT3 patients the QTc decreased more than in controls because of a higher resting QTc; in contrast, LQT1 patients displayed abnormal QTc prolongation (especially in those with concealed LQT1, due to lower resting QTc than that in overt LQT1) [75]. See *Figure 24*.

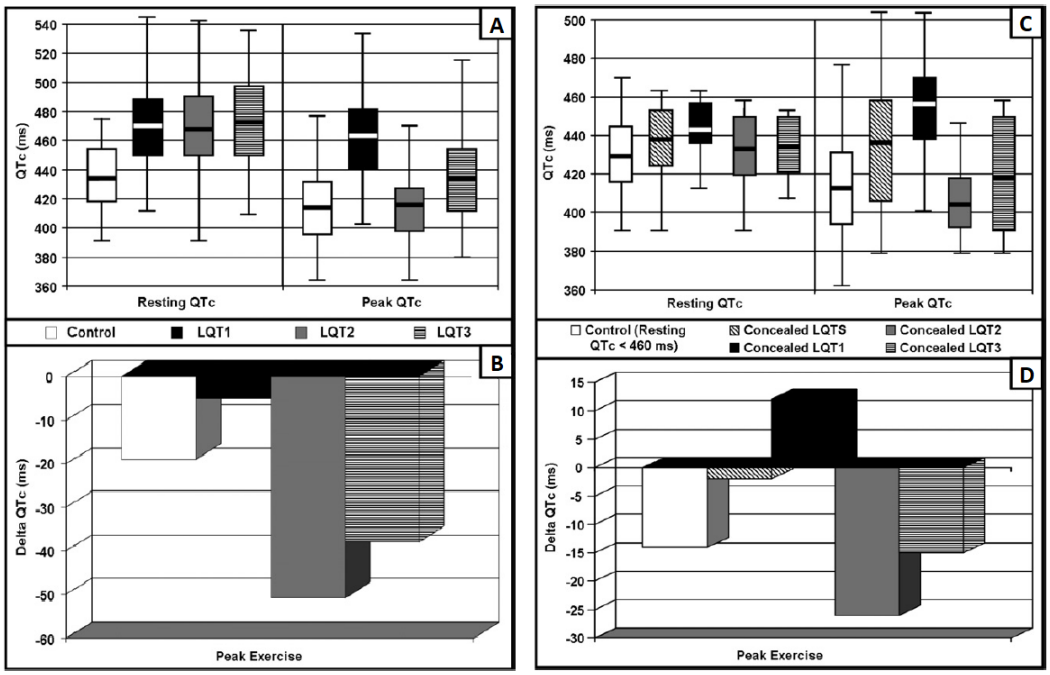

Figure 14 *Effect of peak exercise on QTc and ΔQTc in patients with overt LQTS (A and B) and concealed LQTS (C and D). (A) QTc distribution at rest and peak exercise for control, LQT1, LQT2, and LQT3 patients. (B) Their respective peak ΔQTc, or change from resting QTc. Note that the LQT1 patients' QTc values remained relatively unchanged compared with the observed shortening of the QTc values in the rest of the cohort. (C) QTc distribution at rest and peak exercise for controls, all concealed LQTS patients, and concealed LQT1, LQT2, and LQT3 patients (concealed LQTS: QTc <460 ms at rest like the controls). (D) Their respective peak ΔQTc. Note that while QTc values for the overall concealed LQTS cohort remained relatively unchanged, the QTc values increased at peak exercise in concealed LQT1 but shortened in concealed LQT2/3. The boxes represent the interquartile range (25th to 75th percentiles), with the thick black or white line within the box representing the mean, and the bars represent the range of results excluding extreme outliers. Text and image from Horner et al. 2011* [75].

A maladaptive paradoxical QTc prolongation during the recovery phase was evident among the LQT1 patients, and was most dramatic in concealed LQT1 due to lower baseline QTc; the highest QTc occurred in the first minutes of recovery, and then gradually decreased from minute 4 [75]. On the contrary, controls, LQT2, and LQT3 patients displayed a QTc that was the same or less than their respective baseline resting QTc; their ΔQTc remained negative throughout the whole recovery phase, with gradual return towards baseline; interestingly, patients with concealed LQT2 responded similarly at peak exercise and early stages recovery (1 and 2 minutes), but at 3 minutes of recovery and beyond their QTc lengthened significantly, and their ΔQTc became positive [75] . See *Figure 25*.

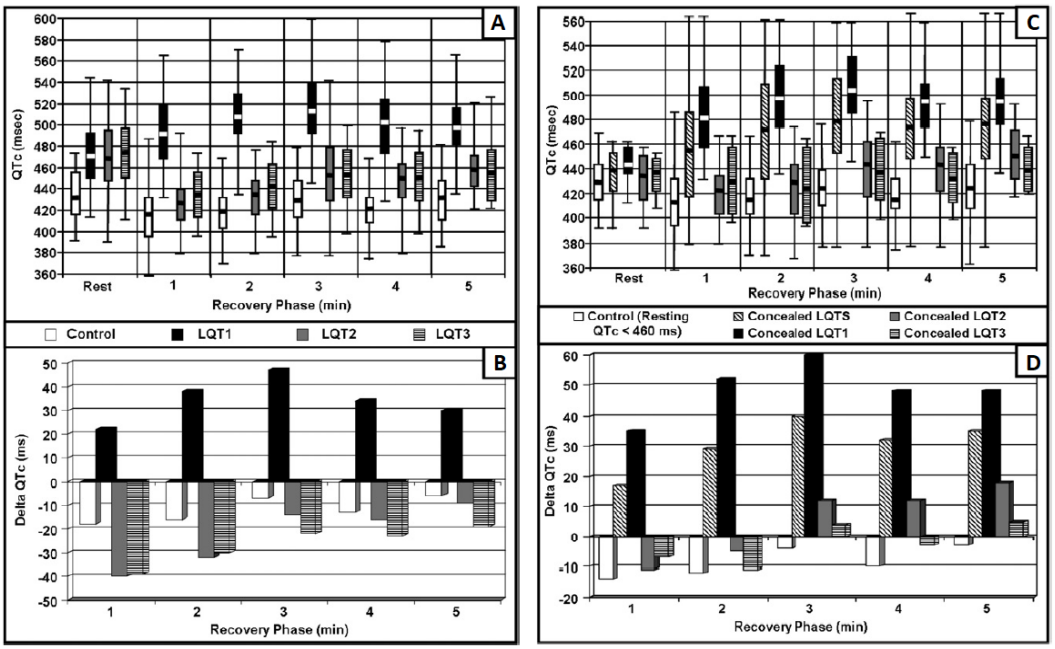

Figure 25 *QTc and ΔQTc during the recovery phase in patients with overt LQTS (A and B) and concealed LQTS (C and D). (A) QTc distribution at rest and at 1, 2, 3, 4, and 5 minutes of recovery for control, LQT1, LQT2, and LQT3 patients. (B) Their respective recovery phase ΔQTc values (QTc recovery minus QTc baseline) are also displayed. Note the significant difference in the recovery QTc and ΔQTc values of the LQT1 patients compared with the rest of the cohort. (C) QTc distribution at rest and at 1, 2, 3, 4, and 5 minutes of recovery for control, all concealed LQTS patients, and concealed LQT1, LQT2, and LQT3 patients (concealed LQTS: QTc <460 ms at rest like the controls). (D) Their respective peak ΔQTc values. Note that the concealed LQT1 patients separate from controls in recovery. The boxes represent the interquartile range (25th to 75th percentiles), with the thick black or white line within the box representing the mean, and the bars represent the range of results excluding extreme outliers. From Horner et al. 2011* [75].

A maladaptive paradoxical QTc prolongation during the recovery phase is of diagnostic value, and various parameters and cut-offs have been proposed:

- Either an absolute QTc ≥ 460 milliseconds during the recovery phase or ΔQTc (QTc during recovery - QTc at baseline) ≥ 30 ms at 3 min of recovery were found to distinguish patients with either manifest or concealed LQT1 from normal subjects and those with LQT2 and LQT3 genotypes [75].
- The updated Schwartz criteria for LQTS use as cutoff a QTc ≥ 480 ms at 4-min recovery in order to reach 100% of specificity, as to identify those patients who almost certainly have LQTS and reserve genetic testing for those patients with a residual normal or borderline result [67].
- Sy and colleagues [67] proposed two exercise ECG parameters for detecting LQTS and predicting genotype *among patients with borderline or normal resting supine QTc*: a QTc ≥ 445 ms at 4-min recovery can be used for detecting LQTS carriers with sensitivity and specificity of 90%, and a QTc interval ≥ 460 ms at 1 minute recovery favours LQT1 [67].

As in postural changes, LQTS patients often develop abnormal T waves (notched, biphasic, and flat) in response to exercise testing, with added diagnostic value [63,76].

3.5.3 Genotype-specific response to brisk standing and exercise testing

The different responses of LQT1 and LQT2 patients to brisk standing and exercise testing are consistent with the known fact that changes in action potential duration to heart rate acceleration differ significantly in response to sudden vs gradual changes in HR [68].

QT prolongation after postural changes is greater in LQT2 than in LQT1: patients with LQT2 develop more QT prolongation than do patients with LQT1 both during maximal tachycardia after standing and when the heart rate slows back to baseline [48,68,73]. On the contrary, QT changes in response to exercise testing are greater in LQT1 patients: they show exaggerated QT prolongation during both early and peak exercise, and also during the recovery phase, whereas LQT2 patients have normal QT shortening and minimal QTc prolongation during peak exercise, but characteristically demonstrate an exaggerated QT hysteresis [1] . This explains why clinical arrhythmias in LQT2 patients are characteristically triggered by situations involving sudden (as opposed to gradual) heart rate acceleration, like sudden startling by noise [73], whereas clinical arrhythmias in LQT1 patients are characteristically triggered by exercise (where the heart rate acceleration is more gradual and the sympathetic activation is more pronounced) [1,74].

On note, LQT3 patients show a more pronounced QT prolongation at rest but demonstrate normal QT interval adaptation during exercise, recovery, and brisk standing [74].

3.6 Obesity

3.6.1 Definition of obesity

Obesity is a medical condition in which excessive fat accumulation and adipose tissue dysfunction pose a risk to the health of affected individuals. According to the current guidelines from the WHO and the US Centers for Disease Control and Prevention, overweight is defined as a BMI between 25 and 30 kg/m^2, and obesity as a BMI of ≥ 30 kg/m^2 [58]. Obesity is further classified in 3 classes: class 1 – moderate obesity (BMI between 30 and 35 kg/m^2), class 2 – severe obesity (BMI between 35 and 40 kg/m^2), and class 3 – morbid obesity (BMI ≥ 40 kg/m^2) [58].

However, these definitions are flawed because body mass index is an imprecise measure of adiposity [78]: BMI does not take into account the distribution of body fat (subcutaneous vs visceral) and the contribution of fat-free mass (FFM) to body weight [79]. This is very relevant, because (1) central obesity has been demonstrated as being a better predictor of morbidity and mortality than general (overall) obesity; (2) even though there is a strong correlation between overall obesity and central obesity, there is considerable (2- to 3- fold) individual variation in the amount of subcutaneous versus visceral adipose tissue at any BMI (total adiposity) level; (3) therefore, based on the BMI definition of obesity, some individuals may be classified as having overall obesity but not abdominal obesity, or as having central obesity but not overall obesity (the so-called "normal-weight obese", i.e., patients who have excess fat but not obesity as classified by BMI); (4) as a consequence, the use of BMI alone as a measure of obesity leads to misclassification and underdiagnosis of adiposity-related morbidity/mortality risk in those with "normal-weight obesity". [80]

This is why various guidelines suggest the use of other anthropometric measures, such as waist circumference (WC) and waist-to-hip-ratio (WHR), which are better indices of central (visceral) obesity than BMI, in addition to BMI to assess the health risk in overweight/obese subjects. [78]

According to the WHO, central obesity is defined as WC ≥ 102 cm in males and ≥ 88 cm in females or WHR ≥ 0.90 in males and 0.85 in females [81], but many studies have shown that a lower waist circumference (WC ≥ 94 cm in males and ≥ 80 cm) is sufficient to confer a high cardiometabolic risk [82–84].

3.6.2 Epidemiology of obesity

The prevalence of overweight and obesity has drastically increased worldwide over the past two decades, primarily as a result of socioeconomical and lifestyle changes including lower energy expenditure (physical inactivity and sedentary lifestyle) and higher calorie intake (increased consumption of energy-rich food) [58]. According to the WHO, the overall prevalence of obesity has doubled in most Westernized countries since 1980 and nearly tripled globally between 1975 and 2016 [58,85]. In 2016, 1.9 billion people were classified as overweight and 650 million adults lived with obesity, accounting for, respectively, 39% and 13% of the global population [58,86]. In Europe, the prevalence of overweight increased from 48% in 1980 to 59.6% in 2015, and that of obesity from 14.5% in 1980 to 22.9% in 2015 [86].

Even more concerning is the vivid rise in the prevalence of childhood obesity during the last decades, with more obese and overweight children growing into overweight and obese adolescents and adults [58,85]. According to WHO data, about 40 million children under the age of 5 were overweight or obese in 2018, more than 340 million children and adolescents between the ages of 5 and 19 were classified as overweight or obese in 2016, and the prevalence of childhood obesity increased from 0.7% to 5.6% in boys and 0.9% to 7.8% in girls between 1975 and 2016 [58,85]. It is worth to consider that being obese during childhood or adolescence contributes to CVD risk into adulthood [80].

3.6.3 Disease burden of obesity

Uncorrected obesity has a negative impact on all physiological functions, affects quality of life, and increases the risk of illness and healthcare burden. Untreated obesity is associated with increased morbidity and mortality, especially due to cardiovascular disease (CVD), musculoskeletal disorders, and certain forms of cancers (breast, ovaries, prostate, liver, kidney, and colon cancers). [58,87,88] Notably, the World Obesity Federation stated that obesity not only acts as a risk factor for other comorbidities, but is *per se* a chronic disease [58]. Worldwide, 120 million disability adjusted life years (DALYs) and 4.0 million deaths (more than two-thirds of which were related to cardiovascular disease) were attributed to excess weight in 2015 [58,87]. Individuals who develop overweight or obesity from young and middle age have a 22% and 49% increased risk of all-cause and CVD mortality,

respectively [58]. Obesity increases the risk of developing various diseases and poor mental health, all of which might reduce the life quality, lower productivity, lead to unemployment and social problems, and increase healthcare expenses. The direct and indirect costs associated with overweight and obesity in Europe were equivalent to 0.47–0.61% of the gross domestic product (GDP). [58,88] According to a systematic review, medical costs of people with obesity were 32% higher than those of lean individuals [58,89].

Obesity often co-exists with modifiable cardiovascular risk factors, such as insulin resistance, hypertension, and dyslipidemia, the combination of which is referred to as metabolic syndrome [90].

3.6.4 Etiology of obesity

Obesity is a multifactorial disease with a complex pathogenesis related to biological, psychosocial, socioeconomic, environmental, and developmental factors, and heterogeneity in the pathways and mechanisms by which it results in adverse health outcomes [58,59,80,91]. Apart from other influencing factors, a positive energy balance caused by a high energy intake and a low energy expenditure is primary cause of weight gain [91].

3.7 Obesity and SCD

The most widely accepted definition of sudden cardiac death (SCD) is: "unexpected death attributable to cardiovascular causes occurring within 1 hour of the onset of acute symptoms, in an individual with or without known pre-existing heart diseases" [92]. SCD is responsible for up to 20% of all-cause deaths and up to 50% of all cardiovascular deaths worldwide [92]. About 75% of SCD cases are due to ischemic heart disease [93], and obesity-related cardiomyopathy has been identified as the most common non-ischemic cause of SCD [80,92,94], with data suggesting that every 5-unit increment in BMI confers a 16% higher risk of SCD [80].

The association between obesity and SCD has been acknowledged for long time. The first to observe this relationship was Hippocrates in the 4th century BC. Hippocrates wrote: "sudden death is more common in those who are naturally fat than in the lean" [95]. Over the last century, numerous epidemiologic and clinical studies have demonstrated a close relationships between obesity and sudden cardiac death (SCD); however, the underlying mechanisms remain incompletely understood [92] . Obesity and sudden cardiac death (SCD) share common risk factors (such as hypertension, diabetes mellitus, obstructive sleep apnea (OSA), NAFLD, coronary heart disease (CHD), cardiac hypertrophy, and heart failure), and obesity in and of itself can result in the development of SCD, independently of associated comorbidities [78,92,96]: patients with obesity have a higher incidence of arrhythmia and SCD, even in the absence of overt cardiac dysfunction [56,90,92,96]. Various evidence supports the role of excess adiposity in determining the risk of SCD, including anatomical and electrical remodelling of the heart, metabolic dysfunction, and autonomic imbalance [59,78,80,92,96]. Hence, obesity (and in particular *central* obesity) is considered as an independent risk factor for arrhythmia and sudden cardiac death [78,92,96,97]. Moreover, obesity-related comorbidities have an additive effect on the development of arrhythmia and SCD [90,92].
Therefore, to sum up, the risks of ventricular arrhythmias and SCD in obesity are likely to be mediated by increasing adiposity as well as cardiometabolic comorbidity that independently cause structural and electrophysiological remodelling of the heart [78].

On note, the set of cardiac structural, electrical, and metabolic abnormalities originating from obesity alone, and the resulting cardiac dysfunction, have collectively been termed as "obesity cardiomyopathy" [58,92].

Here following are presented the main mechanisms through which obesity directly (i.e., independently of associated comorbidities) leads to increased risk of ventricular arrhythmia and SCD.

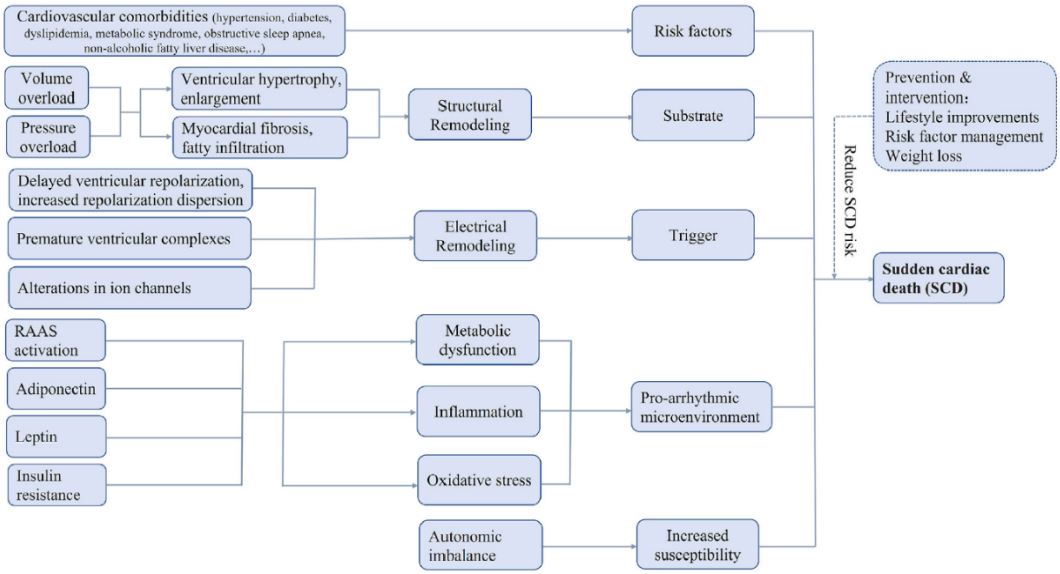

Figure 26 *Possible pathophysiologic mechanisms of sudden cardiac death in obesity. RAAS, renin-angiotensin-aldosterone system, SCD, sudden cardiac death. From Yao, Xue, Li, 2022* [92].

3.7.1 Structural remodelling

In the setting of obesity, a series of hemodynamic and metabolic disorders, systemic and local inflammation, endothelial dysfunction, and abnormal neuroendocrine activation eventually result in cardiac structural remodelling, including cardiac hypertrophy and dilatation (affecting mainly the left ventricle, but also, to a lesser extent, the right ventricle), systolic and diastolic dysfunction, myocardial fibrosis, focal myocardial disarray, fatty infiltration (at the level of the endocardium, pericardium, and perivascular tissues), and myocardial steatosis [58,80,92]. All of these changes, by creating a favourable arrhythmic substrate, may contribute to the increased propensity to ventricular arrhythmias and SCD in obese individuals [92].

Pathophysiological mechanisms of obesity-mediated cardiac structural remodelling are listed below:

- **Hemodynamic changes**: increased blood volume, increased left ventricle (LV) filling pressure, increased cardiac output (CO), pulmonary arterial hypertension (PAH). [58,78,92]

- **Metabolic disorders**: insulin resistance, abnormal glucose transport, free fatty acids spill-over, and amino acid derangement. Insulin resistance likely

plays a pivotal role in cardiac remodelling and dysfunction. Sustained metabolic derangements in obesity promote oxidative stress, inflammation, lipotoxicity, and metabolic inflexibility. [58,78,92]

- **Abnormal neuroendocrine activation**: chronic activation of sympathetic nervous system and renin-angiotensin-aldosterone system (RAAS) [58,78,92]. They play an important role in cardiac hypertrophy and fibrosis (see the 2022 review by Yao, Xue, and Li [92] for more details).

- **Adipose tissue dysfunction** has a central role in the development of chronic systemic inflammation, insulin resistance, and cardiac remodelling. In obesity, various immune cells are recruited to adipose tissue, where they are converted into an active inflammatory phenotype to produce and release proinflammatory cytokines [58]. Dysfunctional adipose tissue releases an abundance of proinflammatory factors, such as leptin, resistin, TNF-α, IL-6, IL-1. Elevated levels of leptin directly contribute to cardiac hypertrophy, and sympathetic nervous system and RAAS activation. [58]Moreover, plasma levels of adiponectin (one of the principal adipokines with insulin-sensitizing and anti-inflammatory properties) are reduced in obesity. [58,78,92]

- **Fatty acid infiltration and lipotoxicity**: pathological expansion of adipose tissue in obesity is accompanied by a decline in adipogenesis, leading to a pathological fat accumulation in peripheral organs such as liver, heart, and muscles [58]. Systemic inflammation and lipotoxicity (caused by ectopic fat accumulation) lead to insulin resistance and functional deficits in peripheral organs. Some ectopic fat depots, such as vascular adipose tissue, intrahepatic fat, and intramuscular fat, mostly generate systemic effects, while pathological accumulation of adipose tissue surrounding the heart (epicardial and pericardial adipose tissue) and most of the blood vessels (PVAT) mainly cause local CV effects via paracrine and autocrine secretion of inflammatory cytokines. [58] Epicardial adipose tissue (EAT) directly exerts local effects on cardiac structure and function, including structural and electrical remodelling and metabolic dysfunction, through paracrine secretion of proinflammatory and profibrotic adipocytokines [58,78,92,98,99]. For more details on the different role of epicardial vs pericardial adipose tissue in CVD risk determination, see the article by Iacobellis (2009) [98].

- **Other factors**: oxidative stress, mitochondrial dysfunction, dysregulation of autophagy and mitophagy, altered intracellular Ca^{2+} homeostasis, ER stress, endothelial dysfunction, and microangiopathy play as well an important role in cardiac hypertrophy, cell death, and fibrosis [92].

- For more details, refer to the 2021 review by Ren and colleagues [58].

3.7.2 Electrical remodelling

Obesity-induced alterations of cardiac cellular electrophysiology are complex and include ion channels modulation, delayed ventricular repolarization, increased repolarization heterogeneity, altered intracellular Ca^{2+} homeostasis, and increased generation of premature ventricular complexes [58,59,92]. Cardiac structural remodelling provides the arrhythmogenic substrate for obesity-related SCD, while electrical remodelling acts as a direct contributor to SCD [92].

- **Cardiac ion channels modulation**: obesity-related changes in cardiac ion channels expression and function are the key mediators between obesity, abnormal repolarization, and SCD [92], and they are at the basis of ventricular repolarization abnormalities seen in obesity. Various obesity-related factors modulate cardiac ion channels, such as proinflammatory cytokines (IL-1, IL-6, TNF-α), free fatty acids (FFAs), hyperinsulinemia, chronic sympathetic overactivity, leptin, ROS (reactive oxygen species), mitochondrial dysfunction, and structural remodelling (especially left ventricular hypertrophy; structural abnormalities always bring in electrophysiological changes because of mechanoelectrical feedback) [59,92,100].

- **Delayed ventricular repolarization and increased repolarization heterogeneity** are characteristic of obesity-associated electrophysiological abnormalities. Numerous studies reported a close association of obesity, and in particular *central* obesity, with QT/QTc interval prolongation (i.e., BMI, WC, and WHR are positively and significantly correlated with QTc prolongation) [56,58,59,78,80,90,92,96,101–104], and this association is independent of comorbidity and lifestyle factors [90]. Indeed, obesity was demonstrated as a direct cause of QT/QTc prolongation and BMI/WC/WHR are independent

predictors of delayed ventricular repolarization [96,102]. Moreover, cardiac hypertrophy showed an additive effect on QT interval prolongation [92], and obesity-related comorbidities (such as hypertension, T2DM, metabolic syndrome, NAFLD, and OSA) showed as well an additive effect on ventricular repolarization abnormalities [80,90,92,96,104] . However, obesity cardiomyopathy was taken as the key culprit to the delayed ventricular repolarization and increased repolarization heterogeneity [58,92].

- **Higher burden of premature ventricular complexes (PVCs)**. Obese patients have a higher frequency of premature ventricular beats [92,97], which is associated with overall adiposity (BMI) and central adiposity (WC, WHR) [105], epicardial adipose tissue expansion [80], sympathovagal imbalance [106], and left ventricular hypertrophy [78,92,97]. Moreover, OSA is associated as well with an increased frequency of PVCs [106]. PVCs are usually unharmful; however, in a context of delayed ventricular repolarization and increased repolarization heterogeneity, they may trigger reentrant arrhythmia [1,92]. PVCs may arise from either abnormal automaticity, triggered activity, reentry, or a combination of the former mechanisms [105]. As for triggered activity, it may arise in the setting of prolonged repolarization (EADs) or intracellular calcium overload (DADs and late EADs), both of which may occur in the setting of obesity [100,105,107]. As for reentry, although it is usually considered most pertinent to sustained arrhythmias, it can play a role in single PVCs generation [105], particularly phase 2 reentry and reflection [100,107]. Lastly, obesity-related sympathetic overactivity and cardiac structural remodelling can lead to PVC generation by abnormal or enhanced normal automaticity [1,105].

- **Altered intracellular Ca^{2+} homeostasis**:
    - Obesity causes altered functional expression of intracellular calcium-handling proteins, such as RyR2, SERCA2, CaMKII PLB, NCX, and IP_3R; altered Ca^{2+} regulation and Ca^{2+} overload likely contribute to the pathogenesis of arrhythmia in obesity [59]. Obesity is associated with hyperphosphorylation of RyR2 [59], which results in incomplete channel closure and spontaneous Ca^{2+} leak from the SR during diastole [1]. Reduced SERCA2a activity and increased NCX

activity have been associated with obesity in a number of studies [58,59]. Increased activity of CaMKII plays an important role in obesity-associated defective calcium-handling and arrhythmia [92]. As for PLB and IP_3R altered functional expression, there are major inconsistencies between studies in regards to the mechanism through which they contribute to arrhythmia in the setting of obesity [59].

- Mitochondrial dysfunction in obesity, among other things, results in aberrant Ca^{2+} homeostasis and mitochondrial Ca^{2+} overload, leading to functional cardiac abnormalities, cell death, and arrhythmia [92].

3.7.2.1 Molecular changes of cardiac ion channels by obesity

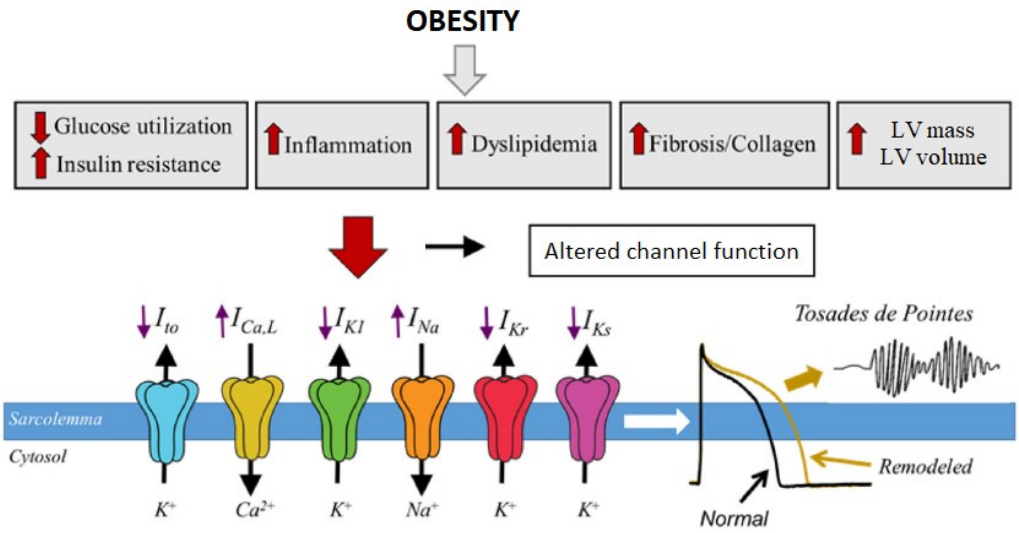

Figure 27 *Molecular changes of cardiac ion channels by obesity. From Aromolaran et al. 2017* [59]

- **I_{Na}**: elevated leptin levels and proinflammatory cytokines increase peak I_{Na} density, while late I_{Na} is increased by the elevated level of FFAs, leading to QT interval prolongation (similarly to the gain-of-function mutation of I_{Na} channels seen in LQT3). [59]
- **I_{CaL}**: various studies have demonstrated that dysfunction of L-type Ca^{2+} channels contributes to QT interval prolongation in the setting of obesity. The precise mechanism is not clear because of contrasting evidence; however, it seems that, overall, obesity leads to a defective inactivation of LTCC and thus an increase in I_{CaL} current, with consequent QT interval prolongation. Leading candidates for obesity-related modulation of LTCC are the proinflammatory cytokines IL-1β and IL-6, FFAs, hyperinsulinemia, and sympathetic overactivation. [1,2,59,100]

- **I_{to}**: a number of studies have demonstrated I_{to} downregulation in obesity [59]. I_{to} reduction leads to APD prolongation, enhanced Ca^{2+} influx through LTCC, asynchronous Ca^{2+} release from the sarcoplasmic reticulum (SR), impaired excitability-contraction coupling, impaired Ca^{2+} handling, and increased repolarization heterogeneity, hence I_{to} downregulation contributes to arrhythmia in the setting of obesity [1,2,33,34]. Obesity-related decrease of I_{to} channel function in ventricular myocytes has been demonstrated to be caused by the pro-inflammatory cytokines IL-1β and TNF-α [59,90], chronic β adrenergic stimulation (which causes I_{to} downregulation both via transcriptional mechanisms and via PKA and PKC mediated phosphorylation [2,34]), and cardiac hypertrophy [1].
- **I_{Kr} and I_{Ks}**: both I_{Kr} and I_{Ks} functional expression is reduced in obesity, leading not only to delayed repolarization and APD prolongation, but also to a higher susceptibility to drug-induced QT prolongation. Pro-inflammatory cytokines (especially IL-6 and TNF-α), hyperglycemia, ROS, and left ventricular hypertrophy have been shown to decrease I_K channel density in the setting of obesity. [59,90,108]

3.7.2.2 Autonomic imbalance

Autonomic imbalance with sympathetic overactivity has been associated with an increased risk of SCD in patients with obesity. Cardiac autonomic dysfunction in obesity is thought to be caused by chronic inflammation, oxidative stress, insulin resistance, dysregulated lipid metabolism, expansion and dysfunction of epicardial adipose tissue, increased leptin levels, and the effect of obesity-related comorbidities such as T2DM, OSA, CHD, and NAFLD. [58,91,92]

On note, the QT interval is influenced by the autonomic tone. Cardiac autonomic dysfunction with sympathetic overactivity has been associated with QT interval prolongation [103,109] and increased repolarization heterogeneity in obese individuals [103]. Thus, cardiac autonomic dysfunction might be responsible for an increased risk of ventricular electrical instability, malignant arrhythmia, and SCD in patients with obesity [103].

3.7.2.3 ECG changes associated with obesity

Obesity is associated with a variety of electrocardiographic (ECG) abnormalities, such as QT/QTc interval prolongation [56,80,92], QRS fragmentation (marker of conduction heterogeneity, likely associated with myocardial fibrosis) [80,92], increased QT/QTc dispersion (marker of spatial heterogeneity of ventricular repolarization) [8,59,78,80,92,96,101,102], wider QRS intervals (conduction delay), increased QRS voltage, longer P waves, ST segment abnormalities, flattening of the T wave, left axis deviation, and late potentials [80].

On note, QT/QTc interval prolongation, increased QT/QTc dispersion, and QRS fragmentation are considered independent predictors of arrhythmia and SCD [1,8,55,80,92].

3.7.3 Effect of weight loss on SCD risk

Weight reduction has been demonstrated to improve obesity-related comorbidities, reverse abnormal cardiac structural and electrical remodelling, bring about favourable hemodynamic and electrocardiographic changes (including a decrease in QT/QTc interval duration and QT/QTc dispersion), and restore physiological metabolic profile and inflammatory status; hence, one might expect that significant weight loss should be protective for SCD [56,58,78,80,92,96,104,110]. However, it is still controversial whether weight loss decreases the risk of SCD, and the underlying reasons are likely to be (1) the presence of "obesity paradox"; (2) the practical challenges in anticipating terminal events and contribution of morbidity; and (3) the limited duration of the follow up period in clinical trials investigating the effect of weight loss on SCD risk [80,92].

Therefore, it may still be appropriate to infer that weight loss, at least partly, mitigates SCD risk in obesity [78,110]. High-quality, prospective studies are needed to address these controversies [92].

In addition to weight reduction, other strategies should be adopted in patients with obesity in order to decrease the risk of SCD:

- Regular aerobic exercise is known to improve cardiorespiratory fitness (CRF), which is a measure of how well the lungs and the cardiovascular system perform during physical activity [58]. Greater CRF (as achieved with

regular aerobic exercise) has been associated with reduced total and CVD mortality and SCD in obese and overweight subjects [58,96].

- Treatment of obesity-related comorbidities (and in particular diabetes, hypertension, and OSA) has been shown to confer additional antiarrhythmic effects and to reduce SCD risk in obese patients [78,92].

3.7.3.1 Obesity paradox

"Obesity paradox" refers to clinical evidence which suggested that, despite overweight and obesity increase the risk of developing cardiovascular diseases, a higher BMI appeared to be associated with improved survival once an individual had developed a heart condition (i.e., a BMI ≥ 30 kg/m^2 appeared to be a protective factor) [79]. The rationale behind this phenomenon is likely that the associations between obesity and CVD outcome have generally been based on BMI alone, which has many limitations as a measure of adiposity and as a prognostic factor; indeed, after adjustment for other prognostic variables there was no longer evidence of a BMI-related "obesity-survival paradox", and alternative anthropometric measurements (such as WC and WHR, which are better reflective of central obesity and CVD risk than BMI) showed no evidence at all for an "obesity-survival paradox" [79].

3.8 Obstructive sleep apnea (OSA)

3.8.1 Definition of OSA

OSA is characterized by repetitive upper airway collapses during sleep leading to intermittent episodes of hypopnea and/or apnea; this results in intermittent hypoxia and hypercapnia, and repetitive intrathoracic pressure swings due to increased respiratory efforts against occluded upper airways [106,111–116]. Apneic episodes are terminated by brief microarousals that result in sleep fragmentation and sleep deprivation [117]. These acute changes result over time in chronic conditions that affect the cardiovascular, pulmonary, and neurocognitive systems [111,114].

3.8.2 Diagnosis of OSA

Clinical symptoms play a key role in identifying patients with OSA; however, none is pathognomonic of the condition, and OSA patients may even not refer any daytime symptom [111]. Polysomnography (PSG) is the standard procedure for the diagnosis of OSA [106,111,117].

Patients usually complain of loud snoring, excessive daytime sleepiness, fatigue, non-restorative sleep, nocturnal gasping or choking, morning headaches, insomnia, and/or falling asleep while driving [106,111,112,117].

The diagnosis of OSA is based on the Apnea-Hypopnea Index (AHI), calculated as the number of obstructive events per hour of sleep. Apnea is defined as a complete cessation of airflow for ≥ 10 seconds, while hypopnea is defined as a clear reduction (but not complete cessation) of the airflow to < 50% of baseline values associated with oxygen desaturation of ≥ 3% or an arousal. The diagnosis of OSA is made with an AHI ≥ 5 events/h, and its severity is classified as follows: mild (5 ≤ AHI < 15), moderate (15 ≤ AHI < 30), and severe (AHI ≥ 30) OSA. [106,111,113,117,118]

3.8.3 Epidemiology of OSA

Obesity, age, and male gender are the main risk factors for OSA [93,119]. OSA is more prevalent in men than women (approximately 2:1 ratio) [93,106,119]. Because of the aging population and the global epidemics of obesity, OSA is a growing public health issue [93,106], affecting 9-38% of the global adult population, and is by far the most common form of sleep-disordered breathing (SDB) [93,106,111,113,117,120]. Despite the high prevalence, OSA is still frequently unrecognized and underdiagnosed, mostly because patients often consider their symptoms as normal variants and/or manifestation of poor lifestyle [117].

Patients affected by OSA are frequently overweight or obese [113]; according to a number of studies, 60-90% of patients with OSA are overweight or obese [121]. There is compelling evidence suggesting excess weight as a causal factor of OSA, as exemplified by the linear increase in the prevalence of OSA with increasing BMI, WC, WHR, and neck circumference [114]. In a longitudinal cohort study [122] it was

observed that a 10% increase in body weight was associated with a 6-fold increased risk of developing OSA. [114]

Moreover, OSA and obesity are tied in a vicious circle: obesity is a causal factor for OSA, and in turn, downstream effects of OSA include physical inactivity, poor dietary habits, insulin resistance, hyperleptinemia, and systemic inflammation [111].

Other risk factors include menopause, neuropathy or myopathy affecting the upper airway muscles, macroglossia, craniofacial abnormalities, family history, smoking, alcohol consumption, and nasal congestion [111,114,117].

3.8.4 Disease burden of OSA

OSA is associated with an increased rate of cardiovascular morbidity and mortality [118], and is well recognized as a major contributor to CVD [111]. OSA is known to be associated with numerous diseases including hypertension, ischemic heart disease, heart failure, atrial fibrillation, ventricular arrhythmias, sick sinus syndrome, pulmonary hypertension, pulmonary thromboembolism, T2DM, stroke, cognitive dysfunction, and mood disorders [93,106,111–114,123]. There is also a strong association between OSA and SCD [93,112,119,121], as patients with untreated moderate-to-severe OSA have a 2-to-3-fold higher risk of nighttime SCD than individuals without OSA, independently of other risk factors such as obesity and CVD [106,112,123]. This relative risk of SCD increases in direct proportion to AHI and the severity of oxygen desaturation during sleep [106,123].

OSA and hypertension

(1) patients with moderate to severe OSA have a 3-fold risk of developing new hypertension compared to those without OSA [114]; (2) OSA is associated with a non-dipping pattern of hypertension [111], which is linked to a worse prognosis; (3) OSA is particularly frequent in patients with resistant hypertension (some studies described the presence of OSA in up to 80% of patients with resistant hypertension) [114]; and (4) the pathophysiology linking OSA and HTN is multifactorial (ANS derangements with sympathetic overactivity, RAAS activation, and sleep inefficiency) [111].

OSA and pulmonary hypertension

OSA is frequently associated with pulmonary hypertension (PH), which is often a direct consequence of this disorder: between 17 to 53% of OSA patients have PH. The increase in the pulmonary arterial pressure (PAP) in patients with obstructive sleep apnea is mainly attributed to five key factors: (1) repetitive hypoxia, causing pulmonary vasoconstriction, vascular remodelling, and endothelial dysfunction; (2) increased inspiratory effort against occluded upper airways, resulting in increased negative intrathoracic pressure, and increased left heart filling pressures; (3) sympathetic overactivity; (4) inflammation; (5) pulmonary thromboembolism resulting from a hypercoagulative state. [111]

3.9 OSA and arrhythmia

Several studies have shown a substantial correlation between OSA and ventricular arrhythmias (VA). VA, mainly premature ventricular contractions (PVCs), have been documented in up to two-thirds of patients affected with OSA, which is significantly higher than the rates reported in individuals without OSA (0 to 12%) [106,121,124–126]. OSA was shown to be an independent predictor of VA: after adjustment for demographic parameters, cardiovascular risk factors, and comorbidities, patients with OSA had around a 2-fold increased probability of experiencing any cardiac arrhythmia [125]. The VA that are more frequently observed in patients with OSA include isolated and non-isolated (bi/tri/quadrigeminism) PVCs, non-sustained ventricular tachycardia (NSVT), sustained ventricular tachycardia (VT), and even sudden cardiac death (SCD) [106,125].

The prevalence of arrhythmia in patients with OSA has been correlated to the severity and duration of hypoxia (i.e., the degree of oxygen desaturation and the amount of time spent with $SpO_2 < 90\%$), higher AHI, lower total sleep time and sleep efficiency [106,124–126].

OSA is considered a predictor of arrhythmia during sleep [125]: indeed, in patients with OSA, VA is most likely to occur during night-time sleep, with the greatest frequency around apneic episodes [106,125]. Furthermore, OSA patients have a

significantly increased risk of SCD at night (between midnight and 06.00 h), a period of relative cardioprotection for individuals without OSA [116,121,124]. Hence, the circadian pattern of VA and SCD distribution in patients with OSA is opposed to that in healthy individuals [106].

3.9.1 Mechanisms of OSA-induced arrhythmia

Recent research have identified a variety of pathophysiological mechanisms thought to increase the propensity of cardiac arrhythmogenesis in patients with OSA. May and colleagues (2017) [116] proposed a conceptual model for OSA-related arrhythmogenesis in which repeated acute pathophysiological stressors (intermittent hypoxia, repetitive intrathoracic pressure swings, and autonomic nervous system fluctuations with sympathovagal imbalance) operate to produce both an arrhythmogenic substrate and arrhythmic triggers through an immediate pathway (i.e., the direct and immediate arrhythmogenic effects of the aforementioned stressors), an intermediate pathway (characterized by systemic inflammation, oxidative stress, and vascular dysfunction), and a chronic pathway (characterized by structural and electrical cardiac remodelling) [106,116,121]. These mechanisms contribute to delayed ventricular repolarization (marked by QT interval prolongation on the ECG) and increased repolarization heterogeneity (marked by increased TpTe interval on the ECG), which appear to be at the basis of OSA-related propensity for ventricular arrhythmias [93,116,126]. In addition, the QT interval further prolongs in sleep during apnea/hypopnea events because of increased vagal activity [112,126]; this is in line with the higher frequency of VA and SCD during sleep, especially around apneic episodes, that has been reported in patients with OSA compared to controls [93]. Moreover, (1) the cardiac structural remodelling associated with OSA creates a favourable substrate for reentrant arrhythmias; (2) hypoxia, hypercapnia, acidosis, sympathetic overactivity, and ventricular hypertrophy, all of which are intrinsic to OSA, are known to precipitate triggered activity via EADs; and (3) the increased levels of catecholamines can precipitate abnormal automaticity or triggered activity via DADs [116].

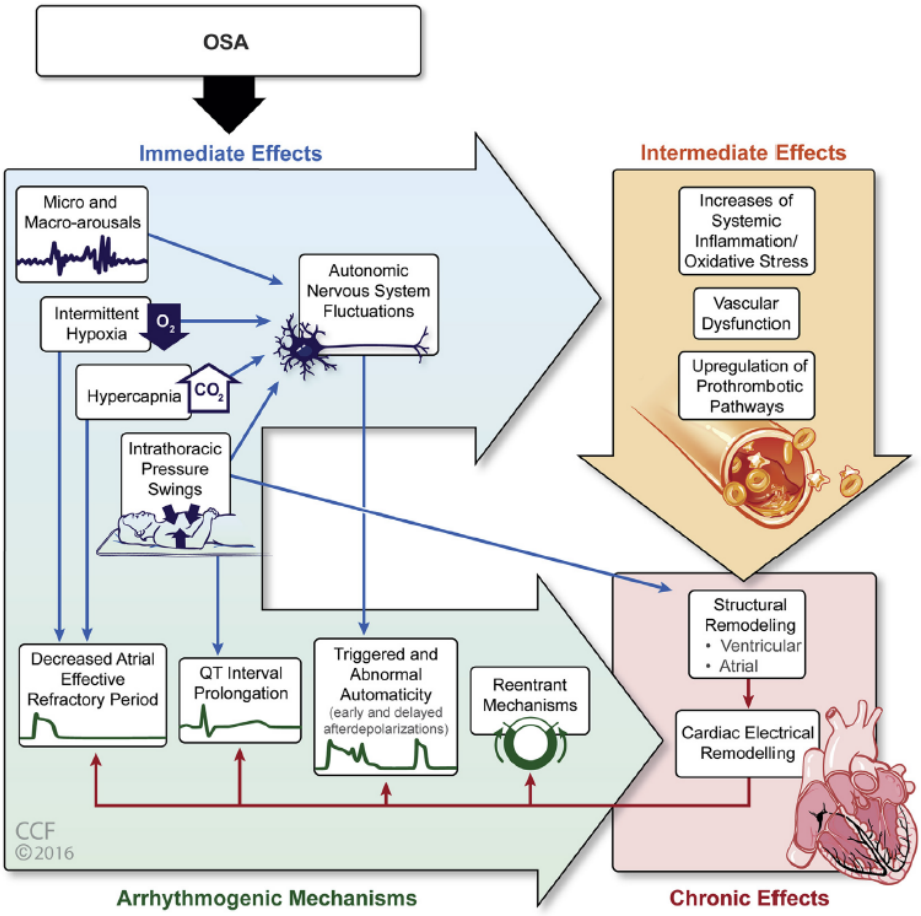

Figure 28 *Proposed mechanisms for OSA-related arrhythmogenesis. From May et al. 2017* [116]

3.9.2 Immediate pathway

3.9.2.1 Hypoxia

Apnea ad hypopnea cause oxygen desaturation and hypoxia. Hypoxia: (1) directly stimulates carotid body chemoreceptors, resulting in sympathetic discharges; (2) directly affects cardiac ion channels, resulting in increased calcium current I_{CaL} and late sodium current I_{NaL} and decreased potassium delayed rectifier currents I_{Kr} and I_{Ks}, hence delayed ventricular repolarization and increased repolarization heterogeneity; (3) directly causes peripheral vasoconstriction, which increases both preload and afterload, thereby increasing cardiac workload; and (4) re-oxygenation after the apneic event results in the formation of dangerous reactive oxygen species (ROS) (oxidative stress), which promote subendocardial ischemia and increase cardiac Ca^{2+} channels activity (thus causing APD prolongation) [35,106,116,118,124].

3.9.2.2 Intrathoracic pressure swings

The increasing respiratory effort against occluded upper airways during apneic episodes results in negative intrathoracic pressure shifts, leading to an increase of (1) cardiac transmural pressure and wall stress; (2) LV afterload; (3) LV preload and venous return to the right heart; and (4) myocardial oxygen demand. Delayed ventricular repolarization (by mechano-electrical feedback) and sympathetic activation are results of these mechanical effect on the heart. [93,106,116,124]

3.9.2.3 Autonomic nervous system (ANS) fluctuations

Increased parasympathetic activation during and unopposed sympathetic surges after respiratory events are features of OSA-related autonomic nervous system oscillations. These autonomic changes are thought to cause electrical instability in the myocardium, and are considered the primary trigger of cardiac arrhythmia in patients with OSA. [106,116,118,124–126]

- Enhanced vagal outflow to the heart during apneic episodes leads to bradycardia (i.e., diving reflex) and QT interval prolongation, creating an electrical substrate responsible for increased susceptibility to arrhythmia [93,106,116].
- Strong sympathetic surges unopposed by vagal activity are elicited with arousal and restoration of the airway patency, favouring triggered activity and abnormal automaticity [106,116,124].

3.9.3 Intermediate pathway

Intermittent hypoxia, repetitive intrathoracic pressure swings, and ANS fluctuations lead to systemic inflammation, oxidative stress, vascular dysfunction, and hypercoagulative state [116].

3.9.3.1 Systemic inflammation

A cardinal feature of OSA is a low-grade systemic inflammatory state (independent of obesity) mainly caused by repetitive hypoxia, oxidative stress, sleep fragmentation/deprivation, and increased catecholamine levels [111,116]. In particular,

hypoxia has been demonstrated to directly activate the inflammatory cascade through upregulation of NF-kB in the white adipose tissue [111].

3.9.4 Chronic pathway

Repetitive intermittent hypoxia, large intrathoracic pressure shifts, systemic inflammation, oxidative stress, and chronic sympathetic overactivity are the main responsible for cardiac structural and electrical remodelling.

- Repeated nocturnal apneic events in result in sustained daytime activation of the sympathetic nervous system, with chronically elevated sympathetic tone even in daytime normoxic conditions [119,126].
- Hypertension, caused by repetitive hypoxia (leading to vasoconstriction and vascular remodelling), oxidative stress (leading to endothelial dysfunction), and chronic activation of RAAS and sympathetic NS [106,111,116,119].
- Myocardial ischemia, caused by (1) hypoxia, responsible for increased preload and afterload (thus increased myocardial workload) despite reduced oxygen supply; (2) oxidative stress, which causes endothelial dysfunction and microangiopathy; and (3) repetitive intrathoracic pressure swings, increased sympathetic activity, and cardiac hypertrophy further increase cardiac workload [116].
- Cardiac structural remodelling characterized by cardiac hypertrophy, chamber dilation, and fibrosis. Its pathophysiology is multifactorial and include hypoxemia, repetitive shifts in transmural pressure, systemic inflammation, oxidative stress, chronic activation of RAAS and sympathetic NS, systemic and pulmonary hypertension, and repetitive ischemic insults. [106,111,116,125]
- Cardiac electrical remodelling characterized by delayed ventricular repolarization, increased repolarization heterogeneity, and increased intracellular Ca^{2+} concentrations. Its pathophysiology includes cardiac hypertrophy and chamber dilation (via mechano-electrical feedback), intermittent hypoxia (which upregulates the expression of cardiac LTCC and downregulates the expression of delayed rectifier K^+ channels), chronic sympathetic activation, systemic inflammation, and oxidative stress. [35,93,116]

3.9.5 ECG predictors of ventricular arrhythmias and SCD in OSA patients

Parameters that can be used to evaluate ventricular repolarization abnormalities in patients with OSA are QT/QTc interval, QT dispersion (QTd), and TpTe interval (which evaluates transmural dispersion of repolarization), and these parameters have been extensively associated with VA and SCD. Thus, delayed ventricular repolarization and increased repolarization heterogeneity provide a mechanistic basis for OSA as a predisposing factor for VA and SCD. [106]

3.9.5.1 QT interval prolongation

OSA has been independently associated with a significant increase in resting daytime QTc [112,126], and the QTc interval further prolongs in sleep during apnoeic events. Moreover, patients with OSA are usually affected by other comorbidities (such as obesity, HTN, and T2DM) or are prescribed with QT-prolonging medications, thus increasing their risk of pathological QTc prolongation [112].

OSA may cause APD (thus QT interval) prolongation by several mechanisms, including repeated nighttime hypoxia, chronically increased sympathetic tone, intrathoracic pressure swings, hypercapnia, and acidosis [106,126].

The extent of QTc prolongation in patients with OSA has been correlated with the severity of hypoxia [93], in particular with the degree of nocturnal oxygen desaturation and the amount of time spent with $SpO_2 < 90\%$ during sleep [126].

3.9.5.2 QT dispersion

QTd is the difference between the maximum and minimum QT intervals on a 12-lead ECG. An increased QTc dispersion (QTcd > 60 ms), reflective of ventricular repolarization inhomogeneity and electrical instability of the myocardium, is an independent risk factor for CVD mortality. Patients with severe OSA have been found to have elevated QTcd, which further increases during sleep, and is correlated with AHI and the severity of oxygen desaturation during sleep. [106,113]

3.5.9.3 TpTe interval

Several studies have demonstrated an increased TpTe interval in patients with OSA compared to healthy controls [106,116]. Suggested mechanisms include hypoxia, enhanced sympathetic tone, and intrathoracic pressure swings [106].

3.5.9.4 QRS fragmentation

QRS fragmentation (fQRS) is a marker of depolarization abnormalities, and reflects disordered electrical conduction through an inhomogeneous substrate and/or myocardial fibrosis; abnormal impulse conduction creates a milieu for re-entrant arrhythmia, thus fQRS is a predictor of VA and SCD in patients with structural heart disease [106]. Recent studies described fQRS in patients with OSA, independently of obesity; proposed mechanisms are cell death and interstitial fibrosis, which may be secondary to chronic hypoxia, metabolic abnormalities, and oxidative stress. [106]

3.9.6 Influence of normal sleep on arrhythmogenesis

Physiologic sleep influences arrhythmogenesis at the molecular level: circadian variations in gene expression contribute to cardiac electrophysiological changes, which may promote arrhythmia in a circadian-fashion in the setting of an underlying cardiac disease; this may contribute to the nocturnal prevalence of VA and SCD observed in patients with OSA [93,127].

3.10 CPAP

Continuous Positive Airway Pressure (CPAP) is a treatment that delivers mild positive air pressure through a mask to maintain the upper airways open during sleep [78,106,120]. CPAP is the treatment of choice for moderate to severe OSA because it has shown the best efficacy in reducing daytime symptoms and all-cause mortality, and in improving the quality of life of the affected patients [106,111].

Patients' compliance and long-term adherence, which are difficult to obtain and are the main issues faced by physicians, are crucial for obtaining the beneficial effects of CPAP on symptoms, quality of life, morbidity, and mortality [106,120].

Other treatment options include lifestyle changes, such as weight loss (achieved by a healthier and hypocaloric diet, regular exercise, and bariatric surgery in extreme cases), avoidance of alcohol, tobacco, and sedatives [106,111]. Weight loss is likely to

be an effective measure because it affects not only OSA, but also the cardiovascular comorbidities that are frequently present alongside OSA [106]. Another alternative is the use of mandibular advancement devices (MAD), aiming to expand and stabilize the airways in order to mitigate or prevent their collapse during sleep; oral appliances can be used in patients with mild to moderate OSA in certain circumstances, such as when there is poor compliance and adherence to CPAP [111].

3.10.1 Effect of CPAP on cardiovascular outcomes

Numerous studies reported that treatment with CPAP was associated with a significantly lower risk of adverse cardiovascular outcomes [93,111,123]. However, an adequate adherence (defined by ≥ 4 h CPAP use per night) is critical for achieving these benefits, as demonstrated by some studies in which CPAP use was not associated with reduced risk of CV morbidity and mortality in the general study population of OSA patients, but only in the subgroup of patients who used CPAP for more than 4 hours per night. [93]

CPAP therapy has been demonstrated to significantly reduce nocturnal arousals, hypoxia, sympathetic surges, exaggerated negative intrathoracic pressure swings, systemic blood pressure, pulmonary pressure, ventricular ectopy [93,111,120,121], and biomarkers of inflammation and of oxidative stress [111,121] in patients with OSA. Furthermore, long term CPAP therapy was shown to prevent and, to a certain extent, even reverse OSA-associated cardiac remodelling and pulmonary vascular remodelling in patients with moderate to severe OSA [111]. For all these reasons, one may assume that CPAP therapy has the potential to reduce the risk of ventricular arrhythmia and SCD in patients with OSA, and indeed the majority of studies support a protective effect of CPAP against the occurrence of VA and SCD [106]. However, there is still conflicting evidence on the matter, and a definitive conclusion on whether or not CPAP therapy is effective in reducing the risk of VA and SCD in patients with OSA has yet to be established.

3.10.2 Effect of CPAP on arrhythmia and SCD

Numerous studies have shown that CPAP therapy reduces the frequency of PVCs and other VAs in patients with OSA [78,126]. In a recent (2022) study [121], Domaradzki and colleagues compared a group of patients with OSA treated with CPAP for 3 months to a control group of patients with OSA receiving no treatment. In the CPAP group there was a significative reduction in the number of PVCs and NSVT events, while there was no difference in the control group; in addition, the severity of desaturations at night and the nocturnal dominance of PVCs (expressed as night/day PVC ratio) were found to be correlated with greater reduction of PVCs after 3 months of CPAP, suggesting that patients with severe desaturations at night and nocturnal prevalence of PVCs are those who may benefit the most from the antiarrhythmic effects of CPAP therapy [121].

In a 2018 randomized control trial by Schlatzer et al [128], a significant decrease in QTc interval was seen in patients with OSA after receiving CPAP therapy; the reduction in QTc interval was most prominent at night and in patients with baseline QTc > 430 ms [128]. Furthermore, Roche et al. (2005) [129] reported a significant improvement of QT dynamics with CPAP treatment in patients with severe OSA.

However, in some other studies, patients with moderate to severe OSA did not show any reduction in the risk of arrhythmia and SCD after receiving CPAP therapy. Thus, the evidence is conflicting. [111]

To conclude, Marinheiro and colleagues wrote: “Overall, the duration of CPAP application, compliance with treatment, baseline severity of OSA and cardiac pathology are important confounding factors that influence the effect of CPAP treatment. The small sample sizes that limit extrapolation, as well as the inconsistencies in methodologies for the measurement of outcomes and variables of interest, indicate that larger controlled randomized studies will provide the homogeneity warranted to promote a more useful synthesis of the current evidence”. [106]

4. EXPERIMENTAL STUDY

4.1 Introduction

Obesity is a disease in which excessive fat accumulation and adipose tissue dysfunction pose both a functional limitation and a risk to the health of affected individuals. According to the current guidelines from the World Health Organization (WHO), obesity is defined as a body mass index (BMI) of ≥ 30 kg/m^2, and is further classified as class 1 (moderate, 30 ≤ BMI < 35 kg/m^2), class 2 (severe, 35 ≤ BMI < 40 kg/m^2), and class 3 (morbid, BMI ≥ 40 kg/m^2) obesity. [58] Over the last few decades, obesity has become a "global epidemic" due to the dramatical increase in its prevalence worldwide: in 2016, respectively, 39% and 13% of the global population lived with overweight or obesity, representing almost the triple as compared to 1975 [58,80,86]. Untreated obesity is associated with increased morbidity and mortality, especially due to cardiovascular disease (CVD), musculoskeletal disorders, and certain forms of cancer [58,87,88]. In particular, obesity is a known contributor to the development of CV risk factors, including dyslipidemia, T2DM, hypertension, and obstructive sleep apnoea (OSA), and was also proven to directly contribute to CVD morbidity and mortality, independent of associated CV risk factors [80].

Obesity is a causal factor for Obstructive Sleep Apnoea (OSA) [114]. OSA is characterized by repetitive upper airway collapses during sleep leading to intermittent episodes of hypopnea and/or apnea; this results in intermittent hypoxia and hypercapnia, repetitive intrathoracic pressure swings, and autonomic nervous system fluctuations with sympathovagal imbalance [106,111–116]. Apnoeic episodes are terminated by brief microarousals that result in sleep fragmentation and sleep deprivation [117]. These acute changes result over time in chronic conditions that affect the cardiovascular, pulmonary, and neurocognitive systems [111,114]. Obesity, age, and male gender are the main risk factors for OSA [93,119]. Given the aging population and the global epidemic of obesity, OSA is a growing public health issue, affecting 9-38% of the global adult population [93,106]. OSA is associated with an increased risk of CV morbidity and mortality [118], is well recognized as a major contributor to CVD [111], and its contribution to CVD is additive to that of obesity (when the two conditions coexist). The diagnosis of OSA is based on the Apnea-

Hypopnea Index (AHI), calculated during a polysomnography, and defined as the number of obstructive events per hour of sleep. The diagnosis of OSA is usually made with an AHI ≥ 5 events/h, and is classified as mild (5 ≤ AHI < 15), moderate (15 ≤ AHI < 30), and severe (AHI ≥ 30). Polysomnography is the gold standard procedure for the diagnosis of OSA. [106,111,113,117,118]

Obesity has been associated with a higher risk of ventricular arrhythmia (VA), even in the absence of overt cardiac dysfunction [56,90,92,96]. This association is likely to be mediated by increasing adiposity as well as obesity-related comorbidities, both independent determinants of structural and electrophysiological remodelling of the heart, metabolic dysfunction, and autonomic imbalance, with additive effects [59,78,80,92,96]. Obesity-related structural remodelling of the heart provides the arrhythmogenic substrate for obesity-related VA, while electrical remodelling acts as a direct contributor to VA [92].

Obesity-related cardiac structural remodelling includes cardiac hypertrophy and dilatation, systolic and diastolic dysfunction, myocardial fibrosis, fatty infiltration (at the level of the endocardium, pericardium, and perivascular tissues), and myocardial steatosis [58,80,92]. Obesity-induced cardiac electrical remodelling includes ion channels modulation, delayed ventricular repolarization, increased repolarization heterogeneity, altered intracellular Ca^{2+} homeostasis, and increased generation of premature ventricular complexes (PVCs) [58,59,92].

Delayed ventricular repolarization and increased repolarization heterogeneity are characteristic of obesity-associated electrophysiological abnormalities [92]. Numerous studies reported a close association of obesity, and in particular *central* obesity, with QT/QTc interval prolongation (i.e., BMI, WC, and WHR are positively and significantly correlated with QTc prolongation) [56,58,59,78,80,90,92,96,101–104], and this association is independent of comorbidity and lifestyle factors [90]. Indeed, obesity was demonstrated as a direct and independent cause of QT/QTc prolongation [96,102], and obesity-related comorbidities (such as hypertension, T2DM, metabolic syndrome, NAFLD, and OSA) showed an additive effect on ventricular repolarization abnormalities [80,90,92,96,104].

Obesity-related changes in cardiac ion channels expression and function are the key mediators between obesity, abnormal repolarization, and VA [92]. Various obesity-related factors modulate cardiac ion channels, such as proinflammatory cytokines (IL-1, IL-6, TNF-α), free fatty acids (FFAs), hyperinsulinemia, chronic sympathetic overactivity, leptin, ROS (reactive oxygen species), mitochondrial dysfunction, and structural remodelling (by mechanoelectrical feedback) [59,92,100]. Obesity was shown to affect all major ion channels responsible for the repolarization phase of the cardiac action potential, resulting in increased peak I_{Na} density, increased late I_{Na}, L-type Ca^{2+} channels dysfunction leading to increased I_{CaL}, I_{to} downregulation, and reduced functional expression of both I_{Kr} and I_{Ks} (delayed rectifier K^+ currents) [59]. This is the proposed ionic basis for the repolarization abnormalities seen in obesity.

OSA, as well, has been associated with a higher burden of ventricular arrhythmia (VA), and in patients with OSA (as opposed to those without it) VA is most likely to occur during night-time sleep, with greatest frequency around apneic episodes [106,125]. VA in patients with OSA has been correlated to the severity and the duration of hypoxia (i.e., the degree of oxygen desaturation and the amount of time spent with $SpO_2 < 90\%$), higher AHI, lower total sleep time and sleep efficiency [106,124–126]. May and colleagues (2017) [116] proposed a conceptual model for OSA-related arrhythmogenesis, in which repeated acute pathophysiological stressors (intermittent hypoxia, repetitive intrathoracic pressure swings, and autonomic nervous system fluctuations with sympathovagal imbalance) operate to produce both an arrhythmogenic substrate and arrhythmic triggers through an immediate pathway (i.e., the direct and immediate arrhythmogenic effects of the aforementioned stressors), an intermediate pathway (characterized by systemic inflammation, oxidative stress, and vascular dysfunction), and a chronic pathway (characterized by structural and electrical cardiac remodelling) [106,116,121]. These mechanisms contribute to delayed ventricular repolarization (marked by QT interval prolongation on the ECG) and increased repolarization heterogeneity (marked by increased TpTe interval), which appear to be at the basis of OSA-related propensity for ventricular arrhythmias [93,116,126]. In particular, OSA has been associated with increased I_{CaL} and late I_{Na}, and decreased I_{Ks} and I_{Kr}, with intermittent hypoxia and chronic sympathetic overactivity as the main culprits [35,93,116].

CPAP (continuous positive airway pressure) is the mainstay treatment for moderate to severe OSA, and has been proven to reduce both CV mortality and non-fatal CV events [93,106,111,123,130]. However, an adequate adherence (defined by ≥ 4 h CPAP use per night) is of vital importance for achieving these benefits [93]. CPAP is thought to have a protective effect against the occurrence of VA and SCD in patients with moderate to severe OSA, as exemplified by some recent studies in which a significant reduction in the QTc interval and in the number of PVCs has been observed after CPAP treatment [121,128]. However, there is still conflicting evidence on the matter, and a definitive conclusion on whether or not CPAP therapy is effective in reducing the risk of VA and SCD in patients with OSA has yet to be established.

As seen in patients with congenital long QT syndrome (LQTS), QT/QTc interval may be borderline or even normal at resting conditions despite the presence of major repolarization abnormalities; therefore, provocative manoeuvres such as brisk standing and exercise testing (evaluating QT interval adaptation to sudden heart rate changes or exercise) can be used to "unmask" these repolarization abnormalities, and are widely used in the evaluation of patients with suspected LQTS [1,48,67,68,73–75]. In particular, exaggerated QT stretching (inadequate QT interval shortening in response to the sudden heart rate accelerations provoked by abrupt standing), QT stunning (abnormal persistence of QTc prolongation as the heart rate slows back to baseline following the brief tachycardia induced by abrupt standing), and a maladaptive/paradoxical QTc prolongation during the recovery phase of exercise testing (in particular at 4-minute recovery) are of diagnostic value in patients with congenital LQTS [48,67,68,73,74,77].

Despite the extensive data showing impaired cardiac repolarization and QT interval prolongation in patients with obesity and OSA, we found no studies in the literature evaluating QT interval adaptations to provocative manoeuvres in this specific population. Therefore, the primary aim of this study was to evaluate the QT interval and its adaptations to brisk standing and exercise testing in patients with severe obesity and moderate to severe OSA. We also investigated, as secondary outcomes, (1) the cardiopulmonary function in patients with severe obesity and moderate to severe OSA; (2) the influence of CPAP therapy over the QT interval and the

cardiopulmonary function in this patient population; and (3) the association between OSA and the number of arrhythmic events during exercise testing.

4.2 Materials and methods

4.2.1 Participants and protocol

This observational cross-sectional study was conducted on 126 patients with severe obesity and suspected OSA, who consecutively referred to the Centre for the Study and Integrated Treatment of Obesity at the University Hospital of Padova between January 2014 and January 2020. All patients underwent cardiorespiratory sleep study for suspicion of OSA (based on clinical evaluation and the Epworth Sleepiness Scale questionnaire), spirometry, brisk standing test, and cardiopulmonary exercise testing (CPET). The study was performed in accordance with the Declaration of Helsinki and approved by the local ethics committee; each participant provided written informed consent. Inclusion criteria were age 18-70 years, BMI > 35 kg/m^2, and suspected OSA. Exclusion criteria were active malignancy, chronic inflammatory diseases, active infectious diseases, drugs or alcohol abuse, significant heart/lung/musculoskeletal disease that would prevent maximal exercise testing, atrial fibrillation, permanent ventricular or atrial pacing, assumption of β blockers or other drugs affecting the QT interval, and complete bundle branch blocks. A subgroup of OSA patients was treated with CPAP for at least 8 weeks before functional evaluation, and the rest of OSA patients did not receive CPAP due to intolerance or were waiting to start the treatment. Patients were first divided in two groups (pool 1): patients with obesity but not OSA ("Ob no-OSA") and patients with both obesity and OSA ("Ob OSA"). Then, they were divided in three groups as follows (pool 2): patients with obesity and without OSA ("no OSA"), patients with obesity and OSA but not treated with CPAP ("OSA no CPAP"), and patients with obesity and OSA treated with CPAP ("OSA CPAP"). On note, in our study we considered the presence of OSA for an AHI ≥ 15 events/h (i.e., we considered only moderate and severe OSA).

Table 7 Subgroups used in the study

Pool 1	Number	% of total
Ob no-OSA	51	40.3 %
Ob OSA	75	59.7 %
Pool 2	**Number**	**% of total**
no OSA	51	40.3 %
OSA CPAP	42	33.3 %
OSA no CPAP	33	26.4 %

Ob, obesity; OSA, obstructive sleep apnoea; CPAP, continuous positive airway pressure. Ob no-OSA, patients with obesity but not OSA; Ob OSA, patients with obesity and OSA; no OSA, patients with obesity and without OSA; OSA CPAP, patients with obesity and OSA treated with CPAP; OSA no CPAP, patients with obesity and OSA but not treated with CPAP.

4.2.2 Cardiorespiratory sleep study

The cardiorespiratory sleep study was performed using the SOMNOtouchTM® NIBP device (SOMNOmedics Italia) for ≥ 8 h/night. The following data were recorded: peripheral oxygen saturation, respiratory flow in the upper airways, respiratory movements of chest and abdomen, snoring phases, sleeping position, blood pressure, and ECG. These data were automatically analysed with the DOMINO® software and then validated by an expert operator, according to current guidelines from the American Academy of Sleep Medicine.

4.2.3 Brisk standing test

We used a brisk standing test protocol similar to that proposed by Adler, Viskin, and colleagues. Subjects rested supine for at least 5 minutes in a quiet room, as a baseline ECG was recorded; then they were asked to stand up quickly and remain standing still for 3-5 minutes during continuous ECG recording. The QT interval and the preceding R-R interval were measured at 4 points in time: (1) baseline (QT_{rest}), choosing the interval with less R-R variability; (2) point of maximal tachycardia (QT_{maxHR}); (3) point of maximal "QT stretching" ($QT_{stretch}$) (defined as the time when the end of the T wave gets nearest to the next P wave due to R-R–interval shortening without sufficient QT interval shortening); and (4) upon return

of the heart rate to its baseline value (QT_{return}) (defined as the first R-R interval within 40 ms of the baseline R-R interval) [68,73].

4.2.4 Cardiopulmonary exercise testing (CPET)

Each patient underwent maximal, incremental, ECG-monitored CPET. The test was performed on the treadmill or, in a small percentage of the subjects (10.3%), on the cycle ergometer (depending on clinical characteristics and/or physical limitations). The modified Bruce protocol was used for treadmill testing, whereas a 15 Watts/min ramp protocol was used for cycle ergometer testing. All tests were performed until exhaustion, defined as a respiratory exchange ratio (RER) > 1.10, and/or a rate of perceived exertion (RPE) ≥ 18/20 on the Borg scale, and/or a peak heart rate ≥ 85% of predicted HR max, and/or the achievement of a plateau of oxygen uptake (VO_2) [130]. Ventilatory parameters were sampled breath by breath with the Jaeger-Masterscreen-CPX system (Carefusion). ECG, systemic blood pressure, and peripheral oxygen saturation were continuously monitored.

4.2.5 QT interval measurement

All QT interval and R-R interval measurements were performed manually, consistent with previous studies. At all points the QT interval was measured using the tangent method and was corrected for heart rate, using Bazett's formula for heart rates < 100 bpm and Fridericia's formula for heart rates ≥ 100 bpm [52]. All QT intervals were measured preferably in leads II and V5 or, when the signal in those leads was not optimal, leads I and V6 were used instead. According to the recent literature, when the U wave was present, it was omitted from the measurement of the QT interval when small and included when large [48].

4.2.6 Statistical analysis

Mean ± standard deviation (SD) or median and interquartile range (IQR) were used to describe continuous variables, and percentages were used to describe dichotomous clinical parameters. All variables were tested for normality using the Shapiro-Wilk test. For normally distributed variables, differences between groups

were evaluated by a T test for independent samples; to assess differences between more than two groups, ANOVA with Bonferroni's consecutive post-hoc test was used. For non-normally distributed variables, differences between groups were evaluated by a non-parametric test, i.e. Mann-Whitney test for difference between two groups, and Kruskal-Wallis test with related post-hoc analyses for more than two groups. Chi-squared test was used to compare dichotomous variables, and Pearson's correlation analysis was performed to assess the relationship between continuous variables. Two-sided p values <0,.05 was considered statistically significant. Statistical analyses were performed using Statistical Package for Social Science 29.0 (SPSS Inc., Chicago, IL, USA).

4.3 Results

4.3.1 Overall subject population

Demographic and anthropometric characteristics of the study population are shown in *Table 8*. Of note, of 126 subjects, 74 (58.7%) were male, median age was 49 years (± 10.5), median BMI was 44.3 kg/m^2 (IQR 40.1 – 49.9 kg/m^2), median waist circumference (WC) was 135.0 (126.0 – 147.5) cm, median AHI was 19.5 (4.7 – 36.1) events/h, only 28 patients (22.2%) were physically active, and, among the physically active, the average amount of physical activity was 2 h/week (in the low-to-moderate range of intensity). Major comorbidities were arterial hypertension (55.6%), NAFLD (49.2%), and T2DM (24.6%). 10 patients were active smokers (7.9%). 33 patients (26.2%) had an AHI < 5 events/h, 18 patients (14.3%) had an AHI 5-15 events/h, 33 patients (26.2%) had an AHI 15-30 events/h, and 42 patients (33.3%) had an AHI > 30 events/h.

Spirometry and CPET measurements are shown in *Table 9* and *10* respectively. Corrected QT intervals at rest, at the point of maximal tachycardia after brisk standing, at the point of maximal stretching, upon return to baseline, and at the 4th minute of recovery are presented in *Table 11*. It has not been possible to measure QTc max HR, QTc stretch, QTc return, and respective deltas, in 62 patients out of 126.

Table 8 Demographic and anthropometric characteristics in the subject population		
	Number	% of total
Males	74	58.7 %
Active smokers	10	7.9 %
Arterial hypertension	70	55.6 %
NAFLD	62	49.2 %
T2DM	31	24.6 %
Sedentary	98	77.8 %
Physically active	28	22.2 %
AHI < 5	33	26.2 %
AHI 5-15	18	14.3 %
AHI 15-30	33	26.2 %
AHI > 30	42	33.3 %
	Mean (or median)	SD (or IQR)
Age (years)	49.0	± 10.5
BMI (kg/m^2)	44.3	40.1 – 49.9
WC (cm)	135.0	126.0 – 147.5
AHI (events/h)	19.5	4.7 – 36.1

Continuous variables are expressed as mean ± standard deviation (SD) or median and interquartile range (IQR), and categorical variables are expressed as frequencies (% of total). NAFLD, non-alcoholic fatty liver disease; T2DM, type 2 diabetes mellitus; BMI, body mass index; WC, waist circumference; AHI, apnea-hypopnea index.

Table 9 Spirometry measurements in the subject population		
	Median	IQR
FVC%	102.5	91.0 – 114.0
FEV1%	99.0	88.5 – 110.5
FEV1/FVC	81.0	77.2 – 83.2
PEF%	96.0	87.0 – 110.0

Continuous variables are expressed as median and interquartile range (IQR). FVC, forced vital capacity; FEV1, forced expiratory volume in 1 sec; FEV1/FVC, Tiffeneau index; PEF, peak expiratory flow.

Table 10 CPET measurements in the subject population

	Mean (or median)	SD (or IQR)
SBP rest (mmHg)	130	120 – 140
DBP rest (mmHg)	80	70 – 85
SBP peak (mmHg)	170	150 – 190
DBP peak (mmHg)	80	70 – 90
HR rest (bpm)	78.8	± 12.6
HR peak (bpm)	153.3	± 16.7
HR peak (% of predicted)	88.6	± 8.1
HR reserve (bpm)	74.9	± 19.7
HR recovery – 1 minute (bpm)	18.5	± 8.8
SpO_2 rest (%)	99	99 – 100
SpO_2 peak (%)	98	97 – 98
VE/VCO_2 slope	25.7	23.4 – 27.9
OUES (mL/logL)	2693.5	2114.0 – 3195.0
Peak O_2 pulse (mL/bpm)	16.7	± 4.4
Peak O_2 pulse %	86.1	± 21.6
RER peak	1.13	± 0.09
VTex (mL)	2211.4	± 630.2
BF rest (breaths/min)	19	16 – 22
BF peak (breaths/min)	38.1	± 7.2
BR (%)	25.0	± 14.4
Vd/Vt peak	14.5	± 4.3
VO_2 max (mL/min)	2565.3	± 644.6
VO_2 max/kg (mL/min/kg)	19.3	± 4.0
VO_2 max (% of the predicted)	103.2	18.0
$PETCO_2$ rest (mmHg)	34.1	31.4 – 36.8
$PETCO_2$ peak (mmHg)	37.4	34.5 – 41.3

Continuous variables are expressed as mean ± standard deviation (SD) or median and interquartile range (IQR). SBP, systolic blood pressure; DBP, diastolic blood pressure; HR, heart rate; SpO_2, peripheric oxygen saturation; VE, minute ventilation; VCO_2, CO_2 output; OUES, oxygen-uptake efficiency slope; O_2 pulse, ratio between oxygen uptake and heart rate; RER, respiratory exchange ratio; VTex, tidal volume; BF, breathing frequency; BR, breathing reserve; Vd/Vt, ratio between dead space and tidal volume; VO_2, oxygen uptake; $PETCO_2$, partial pressure of end-tidal CO_2.

Table 11 QT interval measurements in the subject population		
	Mean ± SD (ms)	Number of total
QTc rest D2	421.9 ± 24.7	126
QTc rest V5	424.1 ± 24.8	126
QTc max HR D2	446.2 ± 32.2	64
QTc max HR V5	445.9 ± 31.9	64
QTc stretch D2	469.2 ± 30.4	64
QTc stretch V5	468.2 ± 32.1	64
ΔQTc stretch D2	45.2 ± 29.5	64
ΔQTc stretch V5	41.5 ± 31.1	64
QTc return D2	417.4 ± 21.9	64
QTc return V5	411.3 ± 44.7	64
ΔQTc return D2	-6.3 ± 21.6	64
ΔQTc return V5	-9.6 ± 21.9	64
QTc 4min recovery D2	415.8 ± 26.2	126
QTc 4min recovery V5	417.5 ± 26.3	126

Continuous variables are expressed as mean ± standard deviation (SD). QTc, corrected QT interval; QTc rest, QTc at resting conditions; QTc max HR, QTc at the point of maximal tachycardia after brisk standing; QTc stretch, QTc at the point of maximal QT stretching after abrupt standing; QTc return, QTc upon return of the heart rate to baseline values after brisk standing; QTc 4min recovery, QTc at the 4th minute of recovery after exercise; ΔQTc, difference between the QTc interval measured at one point in time and the QTc interval measured at rest.

4.3.2 Comparison between "Ob OSA" and "Ob no-OSA"

Subjects with obesity were divided in two subgroups, "Ob no-OSA" and "Ob OSA" (see *Table 7*), on the basis of the presence of OSA. Subgroup analysis revealed (1) a higher prevalence of male sex and arterial hypertension (p<0.001 and p=0.021), and a higher WC (p=0.019) in the Ob OSA group compared to Ob no-OSA, with no significant difference in the other demographic and anthropometric parameters between the two groups (*Table 12*); (2) lower HR max and HR reserve (p=0.005 and p=0.019), lower SpO_2 at rest (p=0.004), lower VO2 max (% of predicted) (p=0.039), higher peak O_2 pulse (VO_2/HR peak) (p=0.011), higher peak Vd/Vt (p=0.018), higher peak $PETCO_2$ (p=0.017) in the Ob OSA group compared to Ob no-OSA, and no significant difference in the other CPET parameters between the

two groups (*Table 13*); (3) longer QTc interval at rest (p=0.004 in D2 and p=0.018 in V5), longer QTc return (p=0.035 in D2 and p=0.034 in V5), and longer QTc interval at 4-minute recovery (p=0.007 in D2 and p=0.015 in V5) in the Ob OSA group compared to Ob no-OSA, with no significant difference in the other QT interval measurements between the two groups (*Table 14* and *Figure 29*); (4) there was no significant difference in the total number of PSVCs and PVCs between the two groups, as shown in *Table 15*.

Table 12 Demographic and anthropometric characteristics in patients with OSA vs without OSA

	Ob OSA (n=75)	Ob no OSA (n=51)	*p*
Males	53 (70.7%)	21 (41.2%)	**<0.001**
Active smokers	7 (9.3%)	3 (5.9%)	0.775
Arterial hypertension	48 (64.0%)	22 (43.1%)	**0.021**
NAFLD	39 (52.0%)	23 (45.1%)	0.710
T2DM	18 (24.0%)	13 (25.5%)	0.894
Sedentary	57 (76.0%)	41 (80.4%)	0.561
Physically active	18 (24.0%)	10 (19.6%)	0.561
Age (years)	50.2±10.2	47.2±10.8	0.109
BMI (kg/m^2)	46.1±7.1	44.6±6.1	0.268
WC (cm)	140.8±14.7	133.0±16.0	**0.019**
AHI	37.7±19.1	5.4±4.1	**<0.001**

Continuous variables are expressed as mean ± SD and categorical variables are expressed as frequencies (% of total). NAFLD, non-alcoholic fatty liver disease; T2DM, type 2 diabetes mellitus; BMI, body mass index; WC, waist circumference; AHI, apnea-hypopnea index.

Table 13 CPET parameters in patients with OSA vs without OSA			
	Ob OSA (n=75)	Ob no OSA (n=51)	*p*
HR rest (bpm)	79.0±13.5	78.4±11.4	0.786
HR peak (bpm)	149.9±15.7	159.3±17.0	**0.005**
HR peak (% of predicted)	87.2±8.4	90.7±7.3	**0.016**
HR reserve (bpm)	71.5±18.6	78.9±20.5	**0.019**
HR recovery - 1 min (bpm)	18.4±8.6	18.7±9.2	0.872
SpO_2 rest (%)	98.9±1.5	99.5±0.6	**0.004**
SpO_2 peak (%)	97.4±2.2	97.9±1.1	0.167
VE/VCO_2 slope	25.9±3.9	25.9±3.5	0.994
OUES (mL/logL)	2843.2±832	2578.7±705	0.065
Peak O_2 pulse (mL/bpm)	17.5±4.6	15.6±3.9	**0.011**
Peak O_2 pulse %	83.2±21.3	90.3±21.6	**0.045**
RER peak	1.13±0.09	1.14±0.08	0.445
BF peak (breaths/min)	37.5±6.6	39.1±7.9	0.218
BR (%)	24.8±14.7	25.3±14.1	0.867
Vd/Vt peak	15.2±4.1	13.4±4.3	**0.018**
VE peak	83.3±21.0	79.3±23.4	0.323
VO_2 max (mL/min)	2620.5±631	2484.1±662	0.245
VO_2 max/kg (mL/min/kg)	19.1±4.2	19.6±3.8	0.530
VO_2 max (% of predicted)	101.0±19.3	106.6±15.4	**0.039**
$PETCO_2$ rest (mmHg)	34.9±4.9	34.1±3.3	0.287
$PETCO_2$ peak (mmHg)	39.2±6.0	36.9±3.9	**0.017**

Continuous variables are expressed as mean ± SD. HR, heart rate; SpO_2, peripheric oxygen saturation; VE, minute ventilation; VCO_2, CO_2 output; OUES, oxygen-uptake efficiency slope; O_2 pulse, ratio between oxygen uptake and heart rate; RER, respiratory exchange ratio; BF, breathing frequency; BR, breathing reserve; Vd/Vt, ratio between dead space and tidal volume; VO_2, oxygen uptake; $PETCO_2$, partial pressure of end-tidal CO_2.

Table 14 QT interval measurements in patients with OSA vs without OSA			
	Ob OSA (n=75)	Ob no OSA (n=51)	*p*
QTc rest D2	427.1±23.3	414.3±24.9	**0.004**
QTc rest V5	428.4±23.9	417.8±25.1	**0.018**
QTc max HR D2	447.5±33.4	444.0±30.7	0.685
QTc max HR V5	447.2±32.2	443.8±32.1	0.687
QTc stretch D2	471.7±26.1	465.1±36.7	0.407
QTc stretch V5	470.1±29.5	464.7±36.5	0.518
ΔQTc stretch D2	43.3±25.1	48.5±35.9	0.494
ΔQTc stretch V5	45.0±38.0	39.5±26.4	0.490
QTc return D2	421.8±19.3	410.0±24.4	**0.035**
QTc return V5	420.2±19.5	399.2±67.3	**0.034**
ΔQTc return D2	-6.15±19.3	-6.6±25.5	0.933
ΔQTc return V5	-10.5±19.2	-8.0±26.1	0.661
QTc 4min recovery D2	421.0±21.3	408.1±30.7	**0.007**
QTc 4min recovery V5	422.2±22.2	410.5±30.3	**0.015**

Continuous variables are expressed as mean ± SD. QTc rest, QTc at resting conditions; QTc max HR, QTc at the point of maximal tachycardia after brisk standing; QTc stretch, QTc at the point of maximal QT stretching after abrupt standing; QTc return, QTc upon return of the heart rate to baseline values after brisk standing; QTc 4min recovery, QTc at the 4th minute of recovery after exercise; ΔQTc, difference between the QTc interval measured at one point in time and the QTc interval measured at rest.

Table 15 Total number of PSVC and PVC in patients with OSA vs without OSA			
	Ob OSA (n=75)	Ob no OSA (n=51)	*p*
PSVCs (total number)	3.8±15.8	1.5±4.0	0.745
PVCs (total number)	15.6±48.2	7.1±28.0	0.138

Continuous variables are expressed as mean ± SD. PSVCs, premature supraventricular complexes; PVCs, premature ventricular complexes.

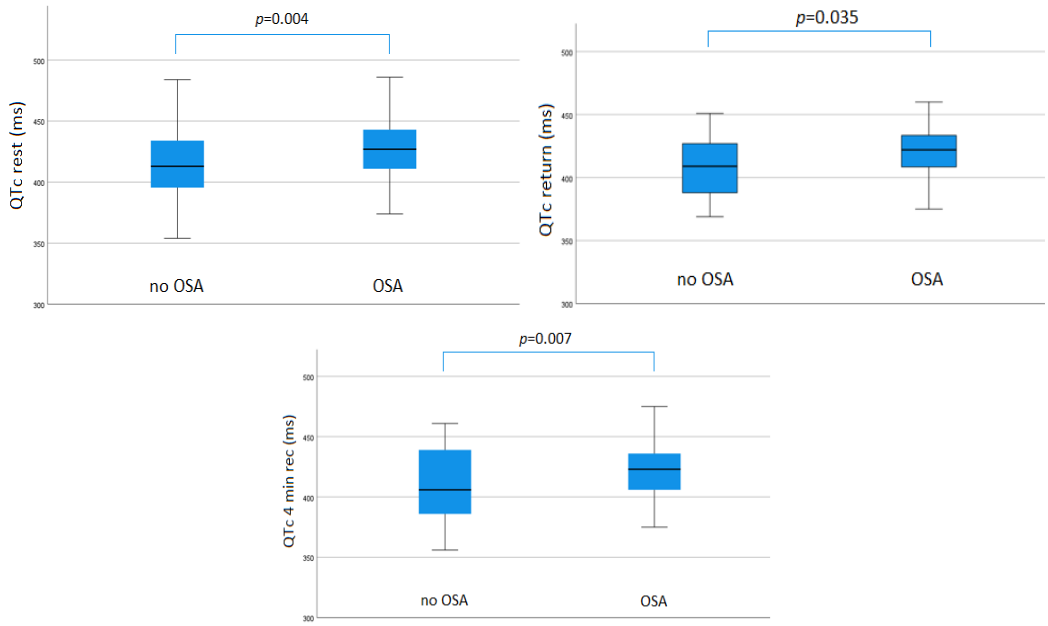

Figure 29 *Box plots representing the distribution of QTc rest, QTc return, and QTc at 4-minute recovery, measured in D2, in the subgroup of patients with OSA and the subgroup of patients without OSA. Blue boxes represent the interquartile range (range between the 25th and the 75th percentile); the thick black line in the box is the 50th percentile, and the bars represent the range of results; outliers are excluded.*

4.3.3 Comparison between "no OSA", "OSA CPAP", and "OSA no CPAP"

Subsequently, we divided the subjects in three subgroups: "no OSA", "OSA CPAP", and "OSA no CPAP" (see *Table 7*), on the basis of the presence of OSA and treatment with CPAP. The subgroup analysis did not reveal any significant difference between OSA patients treated with CPAP and those not treated with CPAP as to demographic and anthropometric parameters (*Table 17*) and QT interval measurements (*Table 18*). Significant difference was found between "OSA CPAP" and "OSA no CPAP" in the following CPET parameters: RER peak, VE peak, and VO_2 max/kg, which were reduced in "OSA no CPAP" compared to "OSA CPAP", p=0.001, p=0.001, and p=0.029, respectively (*Table 16*).

Table 16 CPET parameters in patients with no OSA vs OSA CPAP vs OSA no CPAP

	A: no OSA (n=51)	B: OSA CPAP (n=42)	C: OSA no CPAP (n=33)	*p* AvsB	*p* AvsC	*p* BvsC
HR rest (bpm)	78.4±11.4	78.0±9.8	80.3±17.2	1.000	1.000	1.000
HR peak (bpm)	158.3±17.0	151.1±13.9	148.3±18.0	0.105	**0.021**	1.000
HR peak (% of predicted)	90.7±7.3	87.6±8.0	86.5±9.0	0.205	0.065	1.000
HR reserve (bpm)	79.9±20.5	73.5±15.4	69.0±22.1	0.359	**0.040**	0.946
HR recovery - 1 min (bpm)	18.7±9.2	19.0±8.9	17.7±8.6	1.000	1.000	1.000
SpO_2 rest (%)	99.5±0.6	98.9±1.8	98.9±1.1	**0.019**	**0.040**	1.000
SpO_2 peak (%)	97.92±1.1	97.3±2.5	97.5±1.9	0.397	0.889	1.000
VE/VCO_2 slope	25.9±3.5	25.9±3.4	26.0±4.5	1.000	1.000	1.000
OUES (mL/logL)	2578.7±705.5	2970.8±898.8	2680.8±721.2	0.052	1.000	0.336
Peak O_2 pulse (mL/bpm)	15.6±3.9	17.9±4.7	16.9±4.5	**0.032**	0.523	0.931
Peak O_2 pulse %	90.2±21.6	81.7±21.8	85.1±21.0	**0.029**	0.856	1.000
RER peak	1.14±0.08	1.16±0.08	1.09±0.09	0.842	**0.020**	**0.001**
VE peak	79.3±23.4	91.1±18.4	73.3±20.0	**0.024**	0.611	**0.001**
VO_2 max (mL/min)	2484.1±661	2758.6±551.5	2444.7±688.9	0.120	1.000	0.106
VO_2 max/kg (mL/min/kg)	19.6±3.8	20.2±3.5	17.8±4.7	1.000	0.125	**0.029**
VO_2 max (% of predicted)	106.6±15.4	102.6±19.4	98.9±19.2	0.865	0.169	1.000
$PETCO_2$ rest (mmHg)	34.1±3.3	34.5±3.3	35.5±6.3	1.000	0.455	0.978
$PETCO_2$ peak (mmHg)	36.9±3.9	38.1±4.5	40.7±7.3	0.861	**0.004**	0.097

Continuous variables are expressed as mean ± SD. HR, heart rate; SpO_2, peripheric oxygen saturation; VE, minute ventilation; VCO_2, CO_2 output; OUES, oxygen-uptake efficiency slope; O_2 pulse, ratio VO_2 and HR; RER, respiratory exchange ratio; BF, breathing frequency; BR, breathing reserve; Vd/Vt, ratio between dead space and tidal volume; VO_2, oxygen uptake; $PETCO_2$, partial pressure of end-tidal CO_2.

Table 17 Anthropometric characteristics in patients with no OSA vs OSA CPAP vs OSA no CPAP

	A: no OSA (n=51)	B: OSA CPAP (n=42)	C: OSA no CPAP (n=33)	*p* AvsB	*p* AvsC	*p* BvsC
Age	47.2±10.8	49.4±9.2	51.4±11.4	0.959	0.229	1.000
BMI	44.6±6.1	45.3±6.3	47.2±8.2	1.000	0.298	0.702
WC	133.0±16.0	141.7±14.3	139.9±15.5	0.198	0.447	1.000
AHI	5.41±4.2	38.8±17.4	36.3±21.3	**<0.001**	**<0.001**	1.000

Continuous variables are expressed as mean ± SD. BMI, body mass index; WC, waist circumference; AHI, apnea-hypopnea index.

Table 18 QT interval measurements in patients with no OSA vs OSA CPAP vs OSA no CPAP

	A: no OSA (n=51)	B: OSA CPAP (n=42)	C: OSA no CPAP (n=33)	*p* AvsB	*p* AvsC	*p* BvsC
QTc rest D2	414.3±24.9	428.8±26.2	424,8±19.0	**0.007**	**0.037**	1.000
QTc rest V5	417.8.±25.1	430.8±26.4	425.3±20.2	**0.035**	0.539	0.988
QTc max HR D2	444.0±30.7	446.3±24.2	448.6±41.2	0.972	0.890	0.973
QTc max HR V5	443.8±32.1	445.9±28.3	448.5±36.4	1.000	1.000	1.000
QTc stretch D2	465.1±36.7	468.7±20.4	474.7±31.1	1.000	0.919	1.000
QTc stretch V5	464.7±36.5	465.8±26.4	474.5±32.4	1.000	0.972	1.000
ΔQTc stretch D2	48.5±35.9	41.1±24.7	45.5±25.9	1.000	1.000	1.000
ΔQTc stretch V5	45.0±38.0	36.4±28.7	42.5±24.2	0.638	0.961	0.813
QTc return D2	410.0±24.4	420.1±19.7	423.6±19.3	0.376	0.121	1.000
QTc return V5	399.2±67.3	419.6±21.1	420.9±18.4	0.398	0.330	1.000
ΔQTc return D2	-6.6±25.5	-7.55±20.1	-4.75±18.9	1.000	1.000	1.000
ΔQTc return V5	-8.0±26.1	-9.9±20.1	-11.1±18.7	1.000	1.000	1.000
QTc 4min recovery D2	408.1±30.7	421.5±20.5	421.9±23.2	**0.042**	0.112	1.000
QTc 4min recovery V5	410.5±30.3	422.5±21.7	421.9±23.2	**0.026**	0.159	1.000

Continuous variables are expressed as mean ± SD. QTc rest, QTc at resting conditions; QTc max HR, QTc at the point of maximal tachycardia after brisk standing; QTc stretch, QTc at the point of maximal QT stretching after abrupt standing; QTc return, QTc upon return of the heart rate to baseline values after brisk standing; QTc 4min recovery, QTc at the 4th minute of recovery after exercise; ΔQTc, difference between the QTc interval measured at one point in time and the QTc interval measured at rest.

Lastly, we identified a significant, although weak, direct correlation between QTc at rest and AHI (r=0.251, p=0.018) (*Figure 30*).

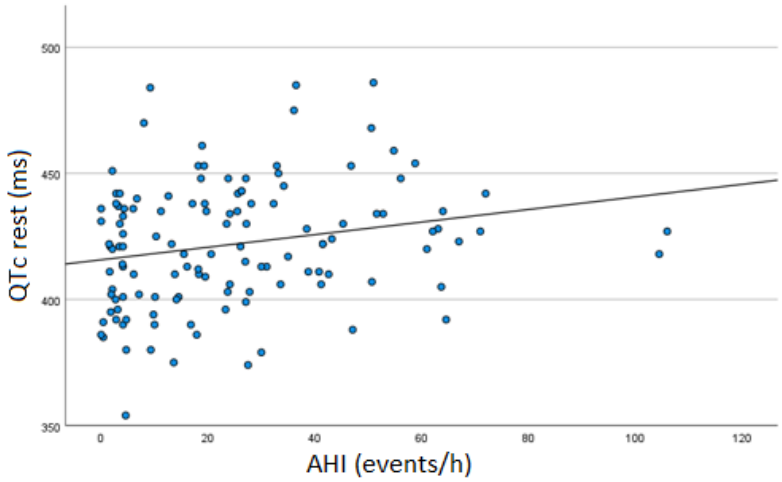

Figure 30 *Positive correlation between resting QTc and AHI. r=0.251, p=0.0018.*

4.4 Discussion

4.4.1 Main findings of the study

- Patients with obesity and moderate to severe OSA had significantly longer QTc rest, QTc return, and QTc 4-min recovery compared to patients with obesity and without OSA, and we observed a significant correlation between QTc at rest and AHI. Among patients with OSA, we did not observe any significant difference in QT interval measurements between those with CPAP therapy and those without it.
- CPET findings are consistent with a lower cardiorespiratory fitness (CRF) in the "OSA no CPAP" group compared to "no OSA" or "OSA CPAP".
- Waist circumference (WC) was significantly higher in patients with obesity and OSA compared to those without OSA, while no significant difference was found in their BMI.
- The difference in the total number of PSVCs and PVCs between obese patients with and without OSA was not statistically significant.

4.4.2 QT interval and provocative manoeuvres

Provocative manoeuvres such as brisk standing and exercise testing are increasingly used in clinical practice for the evaluation of patients with suspected LQTS. While there are many studies evaluating QT interval adaptations to provocative

manoeuvres in patients with congenital LQTS, there are no such studies carried out in patients with obesity and OSA, which are two known conditions associated with QT interval prolongation and altered QT interval dynamics.

In patients with congenital LQTS, exaggerated QT stretching (inadequate QT interval shortening in response to the sudden heart rate accelerations provoked by abrupt standing), QT stunning (abnormal persistence of QTc prolongation as the heart rate slows back to baseline following the brief tachycardia induced by abrupt standing), and a maladaptive/paradoxical QTc prolongation during the recovery phase of exercise testing (in particular at 4-minute recovery) have been validated as of diagnostic value [48,67,68,73,74,77]. The proposed cutoff values of these parameters for the diagnosis of LQTS are the following: QTc stretch ≥ 490 ms [68,73], QTc return ≥ 435 ms or ΔQTc return ≥ 22 ms [68], and QTc 4-min recovery ≥ 480 ms [67].

To the best of our knowledge, this is the first study to evaluate QT interval adaptations to brisk standing and exercise testing in patients with severe obesity and moderate to severe OSA. In our study, patients with obesity and moderate to severe OSA had significantly longer QTc rest, QTc return, and QTc 4-min recovery compared to patients with obesity and without OSA (*Figure 29*). In addition, we found a significant (although weak) direct correlation between QTc at rest and AHI (*Figure 30*). Put together, these results suggest a contribution of OSA to QT interval prolongation and altered QT interval adaptation to changes in the autonomic tone.

However, none of these QT interval parameters were prolonged enough to reach the cutoff value for the diagnosis of LQTS. Hence, we speculate that OSA may not lead to a frank pathologic prolongation of the QT interval, but rather to a reduced repolarization reserve. This is clinically relevant because an impaired repolarization reserve increases the susceptibility to the QT-prolonging effects of agents such as drugs, heart failure, and hypokalaemia (which, by the way, are frequently associated with obesity and OSA).

On note, repolarization reserve is a safeguard mechanism against the loss of repolarizing power, according to which repolarization is provided by multiple redundant ionic currents that can compensate for each other's loss of function [1]. In

this way, the impairment of one of the ion channels involved in the repolarization phase does not necessarily result in excessive repolarization changes (and, thus, QT interval prolongation) because other repolarizing currents can take over and compensate [32].

Lastly, among patients with OSA, we did not observe any significant difference in QT interval measurements between those with CPAP therapy and those without it, despite one would expect otherwise. The only differences that reached statistical significance were between Ob no OSA and Ob OSA CPAP. This finding can be attributed to the fact that patients who did CPAP had a higher AHI on average. Indeed, there is still controversy in the literature on this matter because of conflicting results between different studies. Some considerations should be made on the matter: (1) in our study, we included in the CPAP group patients treated with CPAP for ≥ 8 weeks, without checking for optimal compliance; (2) previous studies demonstrated that the beneficial effects of CPAP are strongly dependent on patients' compliance (defined as ≥ 4 h of CPAP use per night) and long-term adherence, which are not easy to achieve and are the main problems faced by clinicians [106,120]; (3) chronic – i.e., long term – modifications induced by OSA, including structural and electrical cardiac remodelling, play an important role in OSA-associated arrhythmogenesis, and it takes a long time to obtain an improvement over these changes; therefore, it may be possible that our patients were treated with CPAP for too little time to appreciate significant changes on the QT interval.

4.4.3 Anthropometric characteristics

Interestingly, we did not observe a significant difference in BMI between obese patients with and without OSA, while waist circumference (WC) was significantly higher in obese patients with OSA compared to those without it. This is consistent with previous evidence in the literature, indicating WC (reflective of central adiposity) as a better predictor of obesity-related comorbidities, including OSA, than BMI (i.e., overall adiposity). Indeed, central obesity is characterized by an abnormally high deposition of visceral adipose tissue (VAT) [131], which differs from subcutaneous adipose tissue (SAT) in genetic origins, cellular composition,

physiology, endocrinology, immunology, innervation, blood flow, and metabolic activity [132]. VAT accumulation is characteristic of adipose tissue dysfunction [132], which has a central role in the pathophysiology of inflammation, endothelial dysfunction, metabolic disorders, and abnormal neuroendocrine activation that characterize obesity [58]; this is the reason why VAT is considered the fat depot best correlated with adverse health consequences [132].

4.4.4 Cardiorespiratory fitness

According to our data, "OSA no CPAP" patients had lower cardiorespiratory fitness (CRF) compared to "no OSA" or "OSA CPAP". In particular, "OSA no CPAP" had lower VO_2 max (suggestive of reduced aerobic capacity), lower HR response to exercise (suggesting chronotropic impairment at peak exercise), and higher peak $PETCO_2$ (suggesting a reduced ventilatory response at high exercise intensities) compared to the other two groups. Proposed mechanisms for these alterations are chronic intermittent hypoxia and hypercapnia, chronic sympathetic overactivity, sleep deprivation, structural and bio-energetic changes in skeletal muscle fibers, and a low level of physical activity. See the study by Vecchiato et al. (2022) [130] for a more thorough discussion of CRF in OSA patients. Lastly, we observed that CPAP therapy for ≥ 8 weeks was predominantly associated with a significant improvement in CRF.

4.4.5 Total number of PSVCs and PVCs

The difference in the total number of PSVCs and PVCs between obese patients with and without OSA was not statistically significant. This may seem in contrast with the majority of studies in the literature, which observed a higher frequency of cardiac arrhythmia in patients with OSA [106,124–126]; however, we should consider that (1) the majority of studies reported a higher frequency of arrhythmia in OSA patients during sleep (especially around apneic periods) and between midnight to 6 am [106,116,121,124,125], while we counted the number of arrhythmic events occurring during the exercise test only, which was performed in the morning or early afternoon; thus, we cannot exclude a higher occurrence of arrhythmia during nighttime sleep in our patients as well; and (2) the exercise test lasts about 20 min,

i.e. a very limited amount of time; thus, we cannot exclude a higher occurrence of arrhythmia in our patients during the rest of the day.

4.5 Limitations and perspectives

(1) Further research is needed to corroborate our findings on QT interval and the effects of provocative manoeuvres in patients with obesity and OSA; (2) there is growing evidence that other ECG parameters of repolarization are affected by obesity and OSA, such as TpTe interval; it may be worth exploring their association; (3) more research is needed to verify the potential effects of CPAP on cardiac repolarization and arrhythmogenesis in patients with OSA, in particular long-term studies with regards to optimal compliance to the treatment (i.e., ≥ 4 h of CPAP use per night); (4) there is still conflicting evidence on the effects of weight loss on OSA and QT interval, hence more research in this topic is needed as well. The data presented in our study may be further explored (1) by adding a healthy control group to our subject population, and (2) by evaluating the QT interval and the CPET parameters after bariatric surgery.

4.6 Conclusions

Patients with severe obesity and moderate to severe OSA presented longer QTc at rest, QTc return, and QTc at 4-min recovery compared to patients with obesity and without OSA, and we observed a significant correlation between QTc at rest and AHI. However, none of these QT interval parameters were prolonged enough to reach the cutoff value for the diagnosis of LQTS; hence, we speculate that OSA may not lead to a frank prolongation of the QT interval, but rather to a reduced repolarization reserve, which is clinically relevant as it increases the susceptibility to QT interval-prolonging agents. Furthermore, there was no significant difference in the total number of PSVCs and PVCs between obese patients with and without OSA during exercise testing.

Waist circumference (WC) was significantly higher in obese patients with OSA compared to those without OSA, while no significant difference was found in their BMI, suggesting that central adiposity is a better predictor of obesity-related comorbidities than BMI.

Moreover, patients with severe obesity and moderate to severe OSA showed reduced aerobic capacity, exercise tolerance, and ventilatory response to exercise compared to those without OSA.

Finally, we observed beneficial effects of CPAP therapy on cardiorespiratory fitness but not on QT interval; however this may be due to intrinsic limitations of the present study.

REFERENCES

1. Issa ZF, Miller JM, Zipes DP. *Clinical Arrhythmology and Electrophysiology: A Companion to Braunwald's Heart Disease*. Second. Saunders; 2012.
2. Varró A, Tomek J, Nagy N, et al. Cardiac transmembrane ion channels and action potentials: cellular physiology and arrhythmogenic behavior. *Physiol Rev*. 2021;101(3):1083-1176. doi:10.1152/physrev.00024.2019
3. Saenen JB, Vrints CJ. Molecular aspects of the congenital and acquired Long QT Syndrome: Clinical implications. *J Mol Cell Cardiol*. 2008;44(4):633-646. doi:10.1016/j.yjmcc.2008.01.006
4. Chen L, Sampson KJ, Kass RS. Cardiac Delayed Rectifier Potassium Channels in Health and Disease. *Card Electrophysiol Clin*. 2016;8(2):307-322. doi:10.1016/j.ccep.2016.01.004
5. Tristani-Firouzi M, Chen J, Mitcheson JS, Sanguinetti MC. Molecular biology of K+ channels and their role in cardiac arrhythmias11Am J Med. 2001;110-50-59. *Am J Med*. 2001;110(1):50-59. doi:10.1016/S0002-9343(00)00623-9
6. Prenner SB, Shah SJ, Goldberger JJ, Sauer AJ. Repolarization Heterogeneity: Beyond the QT Interval. *J Am Heart Assoc*. 2016;5(5). doi:10.1161/JAHA.116.003607
7. Yan GX, Antzelevitch C. Cellular Basis for the Normal T Wave and the Electrocardiographic Manifestations of the Long-QT Syndrome. *Circulation*. 1998;98(18):1928-1936. doi:10.1161/01.CIR.98.18.1928
8. Ardashev A V., Snezhitskiy VA, Kalatsei L V. Non-Invasive Electrophysiological Markers Associated With Long QT Syndrome. *Cardiac Arrhythmias*. 2022;2(1):13-22. doi:10.17816/cardar100224
9. de Bruyne MC, Hoes AW, Kors JA, Hofman A, van Bemmel JH, Grobbee DE. QTc Dispersion Predicts Cardiac Mortality in the Elderly. *Circulation*. 1998;97(5):467-472. doi:10.1161/01.CIR.97.5.467
10. Panikkath R, Reinier K, Uy-Evanado A, et al. Prolonged Tpeak-to-Tend Interval on the Resting ECG Is Associated With Increased Risk of Sudden Cardiac Death. *Circ Arrhythm Electrophysiol*. 2011;4(4):441-447. doi:10.1161/CIRCEP.110.960658

11. Porthan K, Viitasalo M, Jula A, et al. Predictive value of electrocardiographic QT interval and T-wave morphology parameters for all-cause and cardiovascular mortality in a general population sample. *Heart Rhythm*. 2009;6(8):1202-1208.e1. doi:10.1016/j.hrthm.2009.05.006
12. Okin PM, Malik M, Hnatkova K, et al. Repolarization abnormality for prediction of all-cause and cardiovascular mortality in American Indians: the Strong Heart Study. *J Cardiovasc Electrophysiol*. 2005;16(9):945-951. doi:10.1111/j.1540-8167.2005.40808.x
13. Okin PM, Devereux RB, Fabsitz RR, Lee ET, Galloway JM, Howard B V. Principal Component Analysis of the T Wave and Prediction of Cardiovascular Mortality in American Indians. *Circulation*. 2002;105(6):714-719. doi:10.1161/hc0602.103585
14. Kardys I, Kors JA, van der Meer IM, Hofman A, van der Kuip DAM, Witteman JCM. Spatial QRS-T angle predicts cardiac death in a general population. *Eur Heart J*. 2003;24(14):1357-1364. doi:10.1016/s0195-668x(03)00203-3
15. Shenthar J, Deora S, Rai M, Nanjappa Manjunath C. Prolonged T peak-end and T peak-end /QT ratio as predictors of malignant ventricular arrhythmias in the acute phase of ST-segment elevation myocardial infarction: A prospective case-control study. *Heart Rhythm*. 2015;12(3):484-489. doi:10.1016/j.hrthm.2014.11.034
16. Eslami V, Safi M, Taherkhani M, Adibi A, Movahed MR. Evaluation of QT, QT dispersion, and T-wave peak to end time changes after primary percutaneous coronary intervention in patients presenting with acute ST-elevation myocardial infarction. *J Invasive Cardiol*. 2013;25(5):232-234.
17. Bonnemeier H, Hartmann F, Wiegand UKH, Bode F, Katus HA, Richardt G. Course and prognostic implications of QT interval and QT interval variability after primary coronary angioplasty in acute myocardial infarction. *J Am Coll Cardiol*. 2001;37(1):44-50. doi:10.1016/S0735-1097(00)01061-5
18. Oikarinen L, Viitasalo M, Korhonen P, et al. Postmyocardial infarction patients susceptible to ventricular tachycardia show increased T wave dispersion independent of delayed ventricular conduction. *J Cardiovasc Electrophysiol*. 2001;12(10):1115-1120. doi:10.1046/j.1540-8167.2001.01115.x

19. Erikssen G, Liestøl K, Gullestad L, Haugaa KH, Bendz B, Amlie JP. The Terminal Part of the QT Interval (T peak to T end): A Predictor of Mortality after Acute Myocardial Infarction. *Annals of Noninvasive Electrocardiology*. 2012;17(2):85-94. doi:10.1111/j.1542-474X.2012.00493.x

20. Tatlisu MA, Özcan KS, Güngör B, et al. Can the T-peak to T-end interval be a predictor of mortality in patients with ST-elevation myocardial infarction? *Coron Artery Dis*. 2014;25(5):399-404. doi:10.1097/MCA.0000000000000101

21. Haarmark C, Hansen PR, Vedel-Larsen E, et al. The prognostic value of the Tpeak-Tend interval in patients undergoing primary percutaneous coronary intervention for ST-segment elevation myocardial infarction. *J Electrocardiol*. 2009;42(6):555-560. doi:10.1016/j.jelectrocard.2009.06.009

22. Batchvarov VN, Hnatkova K, Poloniecki J, Camm AJ, Malik M. Prognostic value of heterogeneity of ventricular repolarization in survivors of acute myocardial infarction. *Clin Cardiol*. 2004;27(11):653-659. doi:10.1002/clc.4960271115

23. Morin DP, Saad MN, Shams OF, et al. Relationships between the T-peak to T-end interval, ventricular tachyarrhythmia, and death in left ventricular systolic dysfunction. *Europace*. 2012;14(8):1172-1179. doi:10.1093/europace/eur426

24. Sarubbi B, Pacileo G, Ducceschi V, et al. Arrhythmogenic substrate in young patients with repaired tetralogy of Fallot: Role of an abnormal ventricular repolarization. *Int J Cardiol*. 1999;72(1):73-82. doi:10.1016/S0167-5273(99)00166-7

25. Yi G, Elliott P, McKenna WJ, et al. QT dispersion and risk factors for sudden cardiac death in patients with hypertrophic cardiomyopathy. *Am J Cardiol*. 1998;82(12):1514-1519. doi:10.1016/S0002-9149(98)00696-1

26. Yi G, Prasad K, Elliott P, et al. T wave complexity in patients with hypertrophic cardiomyopathy. *Pacing Clin Electrophysiol*. 1998;21(11 Pt 2):2382-2386. doi:10.1111/j.1540-8159.1998.tb01186.x

27. Ducceschi V, Sarubbi B, D'Andrea A, et al. Increased QT dispersion and other repolarization abnormalities as a possible cause of electrical instability

in isolated aortic stenosis. *Int J Cardiol*. 1998;64(1):57-62. doi:10.1016/S0167-5273(97)00334-3

28. Tun A, Khan IA, Wattanasauwan N, et al. Increased regional and transmyocardial dispersion of ventricular repolarization in end-stage renal disease. *Can J Cardiol*. 1999;15(1):53-56.
29. Saba MM, Arain SA, Lavie CJ, et al. Relation Between Left Ventricular Geometry and Transmural Dispersion of Repolarization. *Am J Cardiol*. 2005;96(7):952-955. doi:10.1016/j.amjcard.2005.05.053
30. Ferrucci A, Canichella F, Battistoni A, et al. A Novel Electrocardiographic T-Wave Measurement (Tp-Te Interval) as a Predictor of Heart Abnormalities in Hypertension: A New Opportunity for First-Line Electrocardiographic Evaluation. *The Journal of Clinical Hypertension*. 2015;17(6):441-449. doi:10.1111/jch.12522
31. Xue C, Hua W, Cai C, et al. Predictive value of Tpeak-Tend interval for ventricular arrhythmia and mortality in heart failure patients with an implantable cardioverter-defibrillator. *Medicine*. 2019;98(49):e18080. doi:10.1097/MD.0000000000018080
32. Varró A, Baczkó I. Cardiac ventricular repolarization reserve: a principle for understanding drug-related proarrhythmic risk. *Br J Pharmacol*. 2011;164(1):14-36. doi:10.1111/j.1476-5381.2011.01367.x
33. He Q, Feng Y, Wang Y. Transient outward potassium channel: a heart failure mediator. *Heart Fail Rev*. 2015;20(3):349-362. doi:10.1007/s10741-015-9474-y
34. Panama BK, Korogyi AS, Aschar-Sobbi R, et al. Reductions in the Cardiac Transient Outward K+ Current Ito Caused by Chronic β-Adrenergic Receptor Stimulation Are Partly Rescued by Inhibition of Nuclear Factor κB. *Journal of Biological Chemistry*. 2016;291(8):4156-4165. doi:10.1074/jbc.M115.694984
35. Jiang N, Zhou A, Prasad B, et al. Obstructive Sleep Apnea and Circulating Potassium Channel Levels. *J Am Heart Assoc*. 2016;5(8). doi:10.1161/JAHA.116.003666
36. Suto F, Zhu W, Chan A, Gross GJ. IKr and IKs remodeling differentially affects QT interval prolongation and dynamic adaptation to heart rate

acceleration in bradycardic rabbits. *Am J Physiol Heart Circ Physiol*. 2007;292(4):H1782-8. doi:10.1152/ajpheart.00932.2006

37. Issa ZF, Miller JM, Zipes DP. *Clinical Arrhythmology and Electrophysiology: A Companion to Braunwald's Heart Disease*. Third. Elsevier; 2018.
38. Van Petegem F. Ryanodine Receptors: Structure and Function. *Journal of Biological Chemistry*. 2012;287(38):31624-31632. doi:10.1074/jbc.R112.349068
39. Antzelevitch C, Burashnikov A. Overview of Basic Mechanisms of Cardiac Arrhythmia. *Card Electrophysiol Clin*. 2011;3(1):23-45. doi:10.1016/j.ccep.2010.10.012
40. Murphy C, Lazzara R. Current concepts of anatomy and electrophysiology of the sinus node. *Journal of Interventional Cardiac Electrophysiology*. 2016;46(1):9-18. doi:10.1007/s10840-016-0137-2
41. Tse G. Mechanisms of cardiac arrhythmias. *J Arrhythm*. 2016;32(2):75-81. doi:10.1016/j.joa.2015.11.003
42. Lerman BB. Mechanism of outflow tract tachycardia. *Heart Rhythm*. 2007;4(7):973-976. doi:10.1016/j.hrthm.2007.03.007
43. Weiss JN, Garfinkel A, Karagueuzian HS, Chen PS, Qu Z. Early afterdepolarizations and cardiac arrhythmias. *Heart Rhythm*. 2010;7(12):1891-1899. doi:10.1016/j.hrthm.2010.09.017
44. Varró A, Baczkó I. Possible mechanisms of sudden cardiac death in top athletes: a basic cardiac electrophysiological point of view. *Pflugers Arch*. 2010;460(1):31-40. doi:10.1007/s00424-010-0798-0
45. Pandit S V., Jalife J. Rotors and the Dynamics of Cardiac Fibrillation. *Circ Res*. 2013;112(5):849-862. doi:10.1161/CIRCRESAHA.111.300158
46. Stevenson WG. Ventricular Arrhythmias. In: Goldman L, Schafer AI, eds. *Goldman's Cecil Medicine*. Twenty Fourth. Saunders; 2012:359-368.
47. Lepeschkin E, Surawicz B. The Measurement of the Q-T Interval of the Electrocardiogram. *Circulation*. 1952;6(3):378-388. doi:10.1161/01.CIR.6.3.378
48. Chan CH, Hu YF, Chen PF, Wu IC, Chen SA. Exercise Test for Patients with Long QT Syndrome. *Acta Cardiol Sin*. 2022;38(2):124-133. doi:10.6515/ACS.202203_38(2).20211101A

49. Panicker GK, Karnad DR, Natekar M, Kothari S, Narula D, Lokhandwala Y. Intra- and interreader variability in QT interval measurement by tangent and threshold methods in a central electrocardiogram laboratory. *J Electrocardiol*. 2009;42(4):348-352. doi:10.1016/j.jelectrocard.2009.01.003
50. Pérez Riera AR, Ferreira C, Filho CF, et al. The enigmatic sixth wave of the electrocardiogram: the U wave. *Cardiol J*. 2008;15(5):408-421.
51. Wu R, Patwardhan A. Restitution of Action Potential Duration During Sequential Changes in Diastolic Intervals Shows Multimodal Behavior. *Circ Res*. 2004;94(5):634-641. doi:10.1161/01.RES.0000119322.87051.A9
52. Goldenberg I, Moss AJ, Zareba W. QT interval: how to measure it and what is "normal". *J Cardiovasc Electrophysiol*. 2006;17(3):333-336. doi:10.1111/j.1540-8167.2006.00408.x
53. Antoniou CK, Dilaveris P, Manolakou P, et al. QT Prolongation and Malignant Arrhythmia: How Serious a Problem? *European Cardiology Review*. 2017;12(2):112. doi:10.15420/ecr.2017:16:1
54. Wilde AAM, Amin AS, Postema PG. Diagnosis, management and therapeutic strategies for congenital long QT syndrome. *Heart*. 2022;108(5):332-338. doi:10.1136/heartjnl-2020-318259
55. Giunti S, Gruden G, Fornengo P, et al. Increased QT Interval Dispersion Predicts 15-Year Cardiovascular Mortality in Type 2 Diabetic Subjects. *Diabetes Care*. 2012;35(3):581-583. doi:10.2337/dc11-1397
56. Milovancev A, Edita S, Popovic D, Tomic-Naglic D, Rankov O, Ilinčić B. Body Weight Reduction and QTc Interval in Obesity. *Advances in Weight Loss Management and Medical Devices*. 2016;1:1. doi:10.4172/AWMD.1000102
57. Giudicessi JR, Wilde AAM, Ackerman MJ. The genetic architecture of long QT syndrome: A critical reappraisal. *Trends Cardiovasc Med*. 2018;28(7):453-464. doi:10.1016/j.tcm.2018.03.003
58. Ren J, Wu NN, Wang S, Sowers JR, Zhang Y. Obesity cardiomyopathy: evidence, mechanisms, and therapeutic implications. *Physiol Rev*. 2021;101(4):1745-1807. doi:10.1152/physrev.00030.2020
59. Aromolaran AS, Boutjdir M. Cardiac Ion Channel Regulation in Obesity and the Metabolic Syndrome: Relevance to Long QT Syndrome and Atrial Fibrillation. *Front Physiol*. 2017;8. doi:10.3389/fphys.2017.00431

60. Liu P, Wang L, Han D, Sun C, Xue X, Li G. Acquired long QT syndrome in chronic kidney disease patients. *Ren Fail*. 2020;42(1):54-65. doi:10.1080/0886022X.2019.1707098

61. Klimas J, Kruzliak P, Rabkin SW. Modulation of the QT interval duration in hypertension with antihypertensive treatment. *Hypertension Research*. 2015;38(7):447-454. doi:10.1038/hr.2015.30

62. Țieranu E, Donoiu I, Istrătoaie O, et al. Q-T Interval Prolongation in Patients with Liver Cirrhosis. *Curr Health Sci J*. 2018;44(3):274-279. doi:10.12865/CHSJ.44.03.11

63. Harvey A, Curnier D, Dodin P, Abadir S, Jacquemet V, Caru M. The influence of exercise and postural changes on ventricular repolarization in the long QT syndrome: a systematic scoping review. *Eur J Prev Cardiol*. 2022;29(12):1633-1677. doi:10.1093/eurjpc/zwac081

64. Crotti L, Celano G, Dagradi F, Schwartz PJ. Congenital long QT syndrome. *Orphanet J Rare Dis*. 2008;3(1):18. doi:10.1186/1750-1172-3-18

65. Tisdale JE, Wroblewski HA, Overholser BR, Kingery JR, Trujillo TN, Kovacs RJ. Prevalence of QT Interval Prolongation in Patients Admitted to Cardiac Care Units and Frequency of Subsequent Administration of QT Interval-Prolonging Drugs. *Drug Saf*. 2012;35(6):459-470. doi:10.2165/11598160-000000000-00000

66. Tester DJ, Will ML, Haglund CM, Ackerman MJ. Effect of Clinical Phenotype on Yield of Long QT Syndrome Genetic Testing. *J Am Coll Cardiol*. 2006;47(4):764-768. doi:10.1016/j.jacc.2005.09.056

67. Sy RW, van der Werf C, Chattha IS, et al. Derivation and Validation of a Simple Exercise-Based Algorithm for Prediction of Genetic Testing in Relatives of LQTS Probands. *Circulation*. 2011;124(20):2187-2194. doi:10.1161/CIRCULATIONAHA.111.028258

68. Adler A, van der Werf C, Postema PG, et al. The phenomenon of "QT stunning": The abnormal QT prolongation provoked by standing persists even as the heart rate returns to normal in patients with long QT syndrome. *Heart Rhythm*. 2012;9(6):901-908. doi:10.1016/j.hrthm.2012.01.026

69. Waddell-Smith KE, Skinner JR. Update on the Diagnosis and Management of Familial Long QT Syndrome. *Heart Lung Circ*. 2016;25(8):769-776. doi:10.1016/j.hlc.2016.01.020

70. Priori SG, Wilde AA, Horie M, et al. Executive summary: HRS/EHRA/APHRS expert consensus statement on the diagnosis and management of patients with inherited primary arrhythmia syndromes. *Europace*. 2013;15(10):1389-1406. doi:10.1093/europace/eut272

71. Priori SG, Blomström-Lundqvist C, Mazzanti A, et al. 2015 ESC Guidelines for the management of patients with ventricular arrhythmias and the prevention of sudden cardiac death: The Task Force for the Management of Patients with Ventricular Arrhythmias and the Prevention of Sudden Cardiac Death of the European Society of Cardiology (ESC)Endorsed by: Association for European Paediatric and Congenital Cardiology (AEPC). *Europace*. 2015;17(11):1601-1687. doi:10.1093/europace/euv319

72. Schwartz PJ, Ackerman MJ. The long QT syndrome: a transatlantic clinical approach to diagnosis and therapy. *Eur Heart J*. 2013;34(40):3109-3116. doi:10.1093/eurheartj/eht089

73. Viskin S, Postema PG, Bhuiyan ZA, et al. The Response of the QT Interval to the Brief Tachycardia Provoked by Standing. *J Am Coll Cardiol*. 2010;55(18):1955-1961. doi:10.1016/j.jacc.2009.12.015

74. Mazzanti A, Priori SG. Diagnosis of Long QT Syndrome: Time to Stand Up! *Rev Esp Cardiol (Engl Ed)*. 2017;70(11):898-900. doi:10.1016/j.rec.2017.05.004

75. Horner JM, Horner MM, Ackerman MJ. The diagnostic utility of recovery phase QTc during treadmill exercise stress testing in the evaluation of long QT syndrome. *Heart Rhythm*. 2011;8(11):1698-1704. doi:10.1016/j.hrthm.2011.05.018

76. Vink AS, Hermans BJM, Pimenta J, et al. Diagnostic accuracy of the response to the brief tachycardia provoked by standing in children suspected for long QT syndrome. *Heart Rhythm O2*. 2021;2(2):149-159. doi:10.1016/j.hroo.2021.03.005

77. Obeyesekere MN, Klein GJ, Modi S, et al. How to Perform and Interpret Provocative Testing for the Diagnosis of Brugada Syndrome, Long-QT Syndrome, and Catecholaminergic Polymorphic Ventricular Tachycardia. *Circ Arrhythm Electrophysiol*. 2011;4(6):958-964. doi:10.1161/CIRCEP.111.965947

78. Patel KHK, Reddy RK, Sau A, Sivanandarajah P, Ardissino M, Ng FS. Obesity as a risk factor for cardiac arrhythmias. *BMJ Medicine*. 2022;1(1):e000308. doi:10.1136/bmjmed-2022-000308

79. Butt JH, Petrie MC, Jhund PS, et al. Anthropometric measures and adverse outcomes in heart failure with reduced ejection fraction: revisiting the obesity paradox. *Eur Heart J*. 2023;44(13):1136-1153. doi:10.1093/eurheartj/ehad083

80. Powell-Wiley TM, Poirier P, Burke LE, et al. Obesity and Cardiovascular Disease: A Scientific Statement From the American Heart Association. *Circulation*. 2021;143(21). doi:10.1161/CIR.0000000000000973

81. Andreacchi AT, Griffith LE, Guindon GE, et al. Body mass index, waist circumference, waist-to-hip ratio, and body fat in relation to health care use in the Canadian Longitudinal Study on Aging. *Int J Obes*. 2021;45(3):666-676. doi:10.1038/s41366-020-00731-z

82. Bosomworth NJ. Normal-weight central obesity: Unique hazard of the toxic waist. *Can Fam Physician*. 2019;65(6):399-408.

83. Kawaji LD, Fontanilla JA. Accuracy of Waist Circumference Measurement Using the WHO versus NIH Protocol in Predicting Visceral Adiposity Using Bioelectrical Impedance Analysis among Overweight and Obese Adult Filipinos in a Tertiary Hospital. *J ASEAN Fed Endocr Soc*. 2021;36(2). doi:10.15605/jafes.036.02.13

84. Ross R, Neeland IJ, Yamashita S, et al. Waist circumference as a vital sign in clinical practice: a Consensus Statement from the IAS and ICCR Working Group on Visceral Obesity. *Nat Rev Endocrinol*. 2020;16(3):177-189. doi:10.1038/s41574-019-0310-7

85. Abarca-Gómez L, Abdeen ZA, Hamid ZA, et al. Worldwide trends in body-mass index, underweight, overweight, and obesity from 1975 to 2016: a pooled analysis of 2416 population-based measurement studies in 128·9 million children, adolescents, and adults. *The Lancet*. 2017;390(10113):2627-2642. doi:10.1016/S0140-6736(17)32129-3

86. Chooi YC, Ding C, Magkos F. The epidemiology of obesity. *Metabolism*. 2019;92:6-10. doi:10.1016/j.metabol.2018.09.005

87. GBD 2015 Obesity Collaborators, Afshin A, Forouzanfar MH, et al. Health Effects of Overweight and Obesity in 195 Countries over 25 Years. *N Engl J Med*. 2017;377(1):13-27. doi:10.1056/NEJMoa1614362

88. Aune D, Sen A, Prasad M, et al. BMI and all cause mortality: systematic review and non-linear dose-response meta-analysis of 230 cohort studies with 3.74 million deaths among 30.3 million participants. *BMJ*. Published online May 4, 2016:i2156. doi:10.1136/bmj.i2156

89. Tremmel M, Gerdtham UG, Nilsson P, Saha S. Economic Burden of Obesity: A Systematic Literature Review. *Int J Environ Res Public Health*. 2017;14(4):435. doi:10.3390/ijerph14040435

90. Patel KHK, Li X, Xu X, et al. Increasing Adiposity Is Associated With QTc Interval Prolongation and Increased Ventricular Arrhythmic Risk in the Context of Metabolic Dysfunction: Results From the UK Biobank. *Front Cardiovasc Med*. 2022;9. doi:10.3389/fcvm.2022.939156

91. Strüven A, Holzapfel C, Stremmel C, Brunner S. Obesity, Nutrition and Heart Rate Variability. *Int J Mol Sci*. 2021;22(8):4215. doi:10.3390/ijms22084215

92. Yao Y, Xue J, Li B. Obesity and sudden cardiac death: Prevalence, pathogenesis, prevention and intervention. *Front Cell Dev Biol*. 2022;10. doi:10.3389/fcell.2022.1044923

93. Blackwell JN, Walker M, Stafford P, Estrada S, Adabag S, Kwon Y. Sleep Apnea and Sudden Cardiac Death. *Circ Rep*. 2019;1(12):568-574. doi:10.1253/circrep.CR-19-0085

94. Hookana E, Junttila MJ, Puurunen VP, et al. Causes of nonischemic sudden cardiac death in the current era. *Heart Rhythm*. 2011;8(10):1570-1575. doi:10.1016/j.hrthm.2011.06.031

95. Hippocrates, Chadwick J, Mann WN. *The Medical Works of Hippocrates: A New Translation from the Original Greek Made Especially for English Readers*. Oxford: Blackwell; 1950.

96. Omran J, Bostick BP, Chan AK, Alpert MA. Obesity and Ventricular Repolarization: a Comprehensive Review. *Prog Cardiovasc Dis*. 2018;61(2):124-135. doi:10.1016/j.pcad.2018.04.004

97. Messerli FH, Nunez BD, Ventura HO, Snyder DW. Overweight and sudden death. Increased ventricular ectopy in cardiopathy of obesity. *Arch Intern Med*. 1987;147(10):1725-1728. doi:10.1001/archinte.147.10.1725

98. Iacobellis G. Epicardial and Pericardial Fat: Close, but Very Different. *Obesity*. 2009;17(4):625-625. doi:10.1038/oby.2008.575

99. Larsen BA, Laughlin GA, Saad SD, Barrett-Connor E, Allison MA, Wassel CL. Pericardial fat is associated with all-cause mortality but not incident CVD: The Rancho Bernardo Study. *Atherosclerosis*. 2015;239(2):470-475. doi:10.1016/j.atherosclerosis.2015.02.022

100. Hoogendijk MG, Géczy T, Yap SC, Szili-Torok T. Pathophysiological Mechanisms of Premature Ventricular Complexes. *Front Physiol*. 2020;11. doi:10.3389/fphys.2020.00406

101. Kumar T, Jha K, Sharan A, Sakshi P, Kumar S, Kumari A. Study of the effect of obesity on QT-interval among adults. *J Family Med Prim Care*. 2019;8(5):1626. doi:10.4103/jfmpc.jfmpc_168_19

102. Divya R, Ashok V. A Comparative Study of QTC in Obese, Non-Obese Hypertensive and Obese Normotensive Males. *Int J Physiol*. 2019;7(2):6. doi:10.5958/2320-608X.2019.00034.9

103. Esposito K, Nicoletti G, Marzano S, et al. Autonomic dysfunction associates with prolongation of QT intervals and blunted night BP in obese women with visceral obesity. *J Endocrinol Invest*. 2002;25(11):RC32-RC35. doi:10.1007/BF03344061

104. Strack C, Fessmann D, Fenk S, et al. QT prolongation is frequently observed in obesity with and without the metabolic syndrome and can be reversed by long term weight reduction. *Eur Heart J*. 2013;34(suppl 1):P4287-P4287. doi:10.1093/eurheartj/eht309.P4287

105. Marcus GM. Evaluation and Management of Premature Ventricular Complexes. *Circulation*. 2020;141(17):1404-1418. doi:10.1161/CIRCULATIONAHA.119.042434

106. Marinheiro R, Parreira L, Amador P, et al. Ventricular Arrhythmias in Patients with Obstructive Sleep Apnea. *Curr Cardiol Rev*. 2018;15(1):64-74. doi:10.2174/1573403X14666181012153252

107. Zhang Z, Liu MB, Huang X, Song Z, Qu Z. Mechanisms of Premature Ventricular Complexes Caused by QT Prolongation. *Biophys J*. 2021;120(2):352-369. doi:10.1016/j.bpj.2020.12.001

108. Xu X, Rials SJ, Wu Y, et al. Left Ventricular Hypertrophy Decreases Slowly but Not Rapidly Activating Delayed Rectifier Potassium Currents of Epicardial and Endocardial Myocytes in Rabbits. *Circulation*. 2001;103(11):1585-1590. doi:10.1161/01.CIR.103.11.1585

109. Vasheghani M, Sarvghadi F, Beyranvand MR, Emami H. The relationship between QT interval indices with cardiac autonomic neuropathy in diabetic patients: a case control study. *Diabetol Metab Syndr*. 2020;12(1):102. doi:10.1186/s13098-020-00609-0

110. Papaioannou A, Michaloudis D, Fraidakis O, et al. Effects of Weight Loss on QT Interval in Morbidly Obese Patients. *Obes Surg*. 2003;13(6):869-873. doi:10.1381/096089203322618687

111. Abbasi A, Gupta SS, Sabharwal N, et al. A comprehensive review of obstructive sleep apnea. *Sleep Sci*. 2021;14(2):142-154. doi:10.5935/1984-0063.20200056

112. Patel SI, Zareba W, Wendel C, et al. A QTc risk score in patients with obstructive sleep apnea. *Sleep Med*. 2023;103:159-164. doi:10.1016/j.sleep.2023.02.005

113. Barta K, Szabó Z, Kun C, et al. The Effect of Sleep Apnea on QT Interval, QT Dispersion, and Arrhythmias. *Clin Cardiol*. 2010;33(6):E35-E39. doi:10.1002/clc.20619

114. Young T, Skatrud J, Peppard PE. Risk factors for obstructive sleep apnea in adults. *JAMA*. 2004;291(16):2013-2016. doi:10.1001/jama.291.16.2013

115. Sakai T, Takemoto M, Koga T, Tsuchihashi T. A case report of an improvement in premature ventricular complex–induced cardiomyopathy following continuous positive airway pressure therapy in a patient with severe obstructive sleep apnoea. *Eur Heart J Case Rep*. 2022;6(9). doi:10.1093/ehjcr/ytac349

116. May AM, Van Wagoner DR, Mehra R. OSA and Cardiac Arrhythmogenesis. *Chest*. 2017;151(1):225-241. doi:10.1016/j.chest.2016.09.014

117. McNicholas WT. Diagnosis of Obstructive Sleep Apnea in Adults. *Proc Am Thorac Soc*. 2008;5(2):154-160. doi:10.1513/pats.200708-118MG

118. Aytemir K, Deniz A, Yavuz B, et al. Increased myocardial vulnerability and autonomic nervous system imbalance in obstructive sleep apnea syndrome. *Respir Med*. 2007;101(6):1277-1282. doi:10.1016/j.rmed.2006.10.016

119. Bilal N, Dikmen N, Bozkus F, et al. Obstructive sleep apnea is associated with increased QT corrected interval dispersion: the effects of continuous positive airway pressure. *Braz J Otorhinolaryngol*. 2018;84(3):298-304. doi:10.1016/j.bjorl.2017.03.005

120. Senaratna C V., Perret JL, Lodge CJ, et al. Prevalence of obstructive sleep apnea in the general population: A systematic review. *Sleep Med Rev*. 2017;34:70-81. doi:10.1016/j.smrv.2016.07.002

121. Domaradzki D, Lelakowski J, Konieczyńska M, Matusik PT. Continuous positive airway pressure treatment reduces ventricular arrhythmias in obstructive sleep apnea patients with nocturnal dominance of arrhythmias and in those with severe desaturations. *Pol Arch Intern Med*. Published online April 1, 2022. doi:10.20452/pamw.16236

122. Peppard PE, Young T, Palta M, Dempsey J, Skatrud J. Longitudinal study of moderate weight change and sleep-disordered breathing. *JAMA*. 2000;284(23):3015-3021. doi:10.1001/jama.284.23.3015

123. Patel N, Donahue C, Shenoy A, Patel A, El-Sherif N. Obstructive sleep apnea and arrhythmia: A systemic review. *Int J Cardiol*. 2017;228:967-970. doi:10.1016/j.ijcard.2016.11.137

124. Koshino Y, Satoh M, Katayose Y, et al. Sleep apnea and ventricular arrhythmias: Clinical outcome, electrophysiologic characteristics, and follow-up after catheter ablation. *J Cardiol*. 2010;55(2):211-216. doi:10.1016/j.jjcc.2009.10.010

125. Almeneessier AS, Alasousi N, Sharif MM, Pandi-Perumal SR, Hersi AS, BaHammam AS. Prevalence and Predictors of Arrhythmia in Patients with Obstructive Sleep Apnea. *Sleep Science*. 2017;10(4):142-146. doi:10.5935/1984-0063.20170025

126. Shamsuzzaman A, Amin RS, van der Walt C, et al. Daytime cardiac repolarization in patients with obstructive sleep apnea. *Sleep and Breathing*. 2015;19(4):1135-1140. doi:10.1007/s11325-015-1119-9

127. Rana S, Prabhu SD, Young ME. Chronobiological Influence Over Cardiovascular Function. *Circ Res*. 2020;126(2):258-279. doi:10.1161/CIRCRESAHA.119.313349

128. Schlatzer C, Bratton DJ, Schwarz EI, et al. Effect of continuous positive airway pressure therapy on circadian patterns of cardiac repolarization in patients with obstructive sleep apnoea: data from a randomized trial. *J Thorac Dis*. 2018;10(8):4940-4948. doi:10.21037/jtd.2018.07.17

129. Roche F, Barthélémy JC, Garet M, Duverney D, Pichot V, Sforza E. Continuous positive airway pressure treatment improves the QT rate dependence adaptation of obstructive sleep apnea patients. *Pacing Clin Electrophysiol*. 2005;28(8):819-825. doi:10.1111/j.1540-8159.2005.00188.x

130. Vecchiato M, Neunhaeuserer D, Quinto G, et al. Cardiopulmonary exercise testing in patients with moderate-severe obesity: a clinical evaluation tool for OSA? *Sleep and Breathing*. 2022;26(3):1115-1123. doi:10.1007/s11325-021-02475-0

131. Shuster A, Patlas M, Pinthus JH, Mourtzakis M. The clinical importance of visceral adiposity: a critical review of methods for visceral adipose tissue analysis. *Br J Radiol*. 2012;85(1009):1-10. doi:10.1259/bjr/38447238

132. Bays H. Central obesity as a clinical marker of adiposopathy; increased visceral adiposity as a surrogate marker for global fat dysfunction. *Curr Opin Endocrinol Diabetes Obes*. 2014;21(5):345-351. doi:10.1097/MED.0000000000000093